leti
cea tech

TECHNOLOGY
RESEARCH
INSTITUTE

2017

Annual research report

SYSTEMS

leti
cea tech

TECHNOLOGY
RESEARCH
INSTITUTE

Committed to Innovation, Leti Creates Differentiating Solutions for its Industrial Partners.

Leti is a research institute of CEA Tech and a recognized global leader in miniaturization technologies. Leti's teams are focused on developing solutions that will enable future information and communication technologies, health and wellness approaches, clean and safe energy production and recovery, sustainable transport, space exploration and cybersecurity.

For 50 years, the institute has built long-term relationships with its industrial partners, tailoring innovative and differentiating solutions to their needs. Its entrepreneurship programs have sparked the creation of 64 start-ups. Leti and its industrial partners work together through bilateral projects, joint laboratories and collaborative research programs.
Leti maintains an excellent scientific level by working with the best research teams worldwide, establishing partnerships with major research technology organizations and academic institutions. Leti is also a member of the Carnot Institutes network*.

*Carnot Institutes network: French network of 34 institutes serving innovation in industry.

DE LA RECHERCHE À L'INDUSTRIE
cea

CEA Tech is the technology research branch of the French Alternative Energies and Atomic Energy Commission (CEA), a key player in research, development and innovation in defense & security, nuclear energy, technological research for industry and fundamental physical and life sciences.

www.cea.fr/english

Leti at a glance

€315
million budget

800
publications per year

ISO 9001
certified since 2000

Founded in
1967

Based in
France (Grenoble)
with offices in the
USA (Silicon Valley)
and **Japan** (Tokyo)

350
industrial partners

1,900
researchers

2,760
patents in portfolio

91,500
sq. ft. cleanroom space, 8" & 12" wafers

64
startups created

2017

Annual research report

SYSTEMS

Based on MINATEC Campus, Systems Integration Division (DSYS) is at the strategic core of Leti's technological solutions, adding a "system perspective" on technological trends. Our research activities focus on the design and integration of innovative solutions based on emerging electronic technologies for a wide panels of applications such as factory of the future, multimedia, smart energy, smart transport, e-health, sports and leisure.

DSYS's expertise is based on four major pillars which are (i) wireless communications, (ii) innovative sensor-system design, (iii) power-management systems and (iv) security solutions for electronics and components. Our teams are using tools and know how inherited from physic, electromagnetism and electronic areas but also from signal and data processing domain ; they also take profit from state of the art facilities for achieving simulation, characterization and prototyping steps.

Thanks to its capability to work on specific application barriers, DSYS Division is particularly attractive for industrial partners who are facing the challenges of IoT , 5G and cybersecurity. It can be either SME or big companies which are looking for a high level expertise in a businesslike environment.

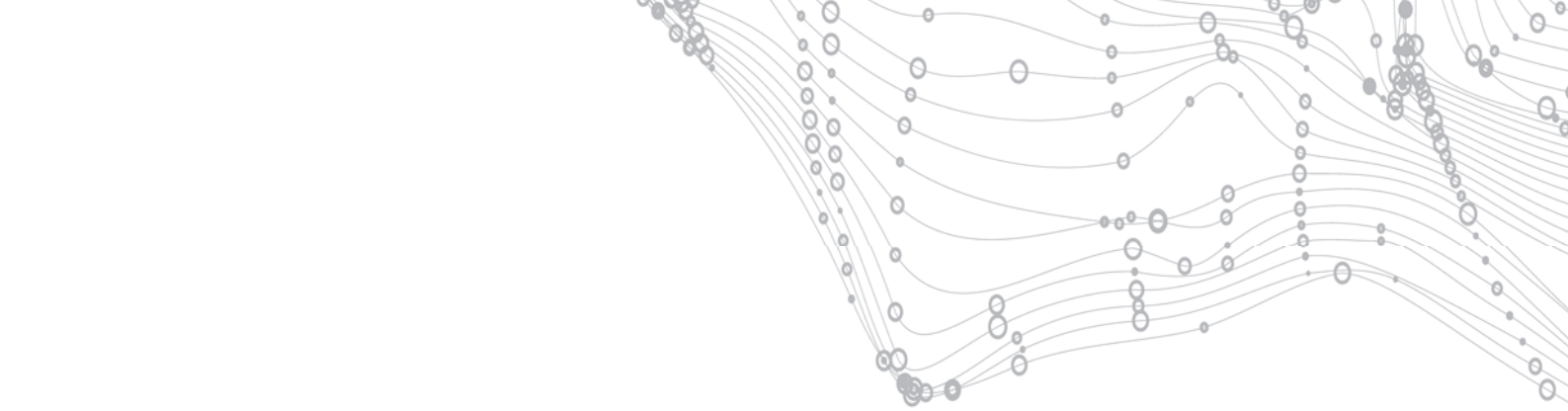

CONTENTS

EDITO 05

KEY FIGURES 07

SCIENTIFIC ACTIVITY 09

01 / WIRELESS HIGH SPEED COMMUNICATIONS 11

02 / LOW DATA RATE AND LOCALIZATION 23

03 / ANTENNAS AND PROPAGATION 32

04 / ENERGY, SENSORS AND SYSTEMS 47

05 / SECURITY 63

06 / PHD Degree awarded 77

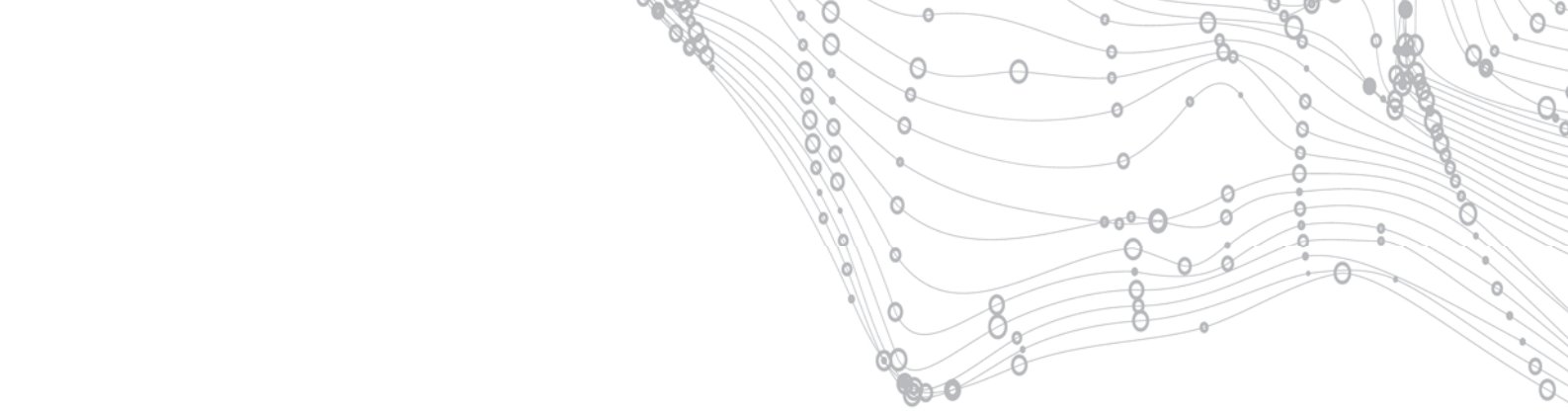

ÉDITO

Sébastien Dauvé,
Head of The System Division

This document publishes our most significant technological and innovation achievements of 2017 selected among a wide variety of scientific results, some of them conducted jointly with external partners who gave their agreement.
2017 has been very fruitful for DSYS, with more than 190 publications, 51 patents and tens of prototypes. In this report, chapter 1 details our scientific finding on both below 6 GHz and millimeter wave wireless communications, advanced coding techniques and advanced spectrum and network management techniques that have today strong relevance for the forthcoming 5G and beyond systems. In addition, in chapter 2 we present our research and results on low data rate communication and localization. In chapter 3 we detail our proposed innovation, its technological implementation and performance measurements on wideband and reconfigurable antennas, including our work on precise propagation characterization. Our continuous efforts on innovative sensors' design and their dedicated signal processing and energy harvesting are detailed in chapter 4 where we propose to exploit either MEMs capabilities for applications where low power or advanced integration present critical constraints or, to explore capabilities of nanotechnology where MEMs do not provide efficient solutions. Target applications are multiple, from multi-modal transport systems, emotional sensing to shape capture. Moreover, in chapter 4 we present our solutions and results for battery energy management. 2017 has been notably marked by a significant increase of our investigations on hardware enabled cyber security and on the identification of countermeasures to threats for the applications related to massive IoT which have a critical impact on vertical industry needs. Our proposed solutions are detailed in chapter 5.

I hope you enjoy reading this report and that it will find inspiration for your future developments and research.

Sébastien Dauvé

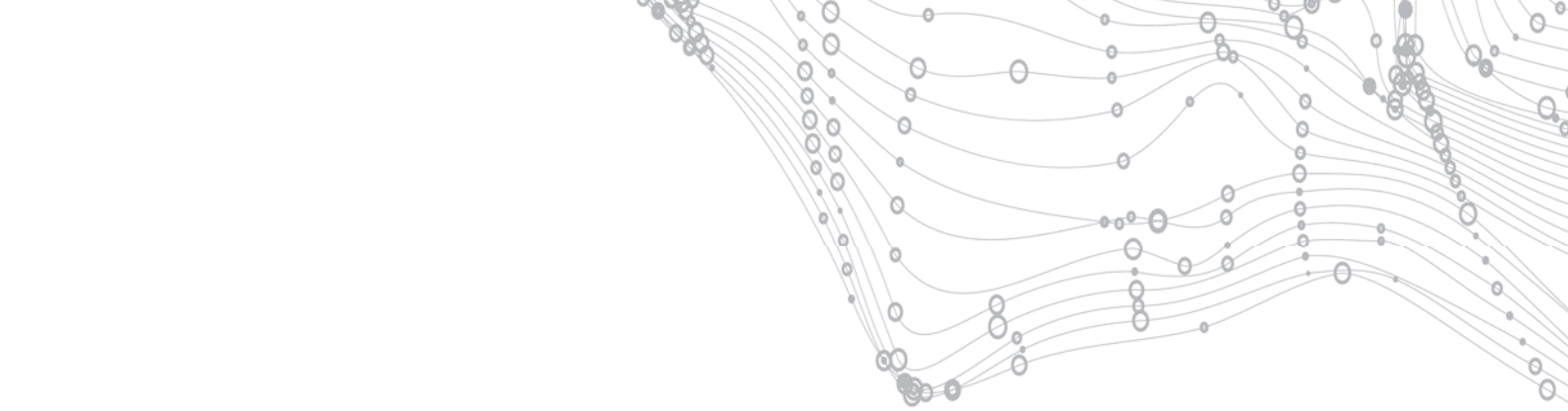

Key figures

164 researchers
44 PhD students and post-docs
43 Temporary employees and interims

27,8 M€ budget
86% external funding

51 patents granted in 2017
445 patents portfolio
45 book chapters and journals
146 communications in conferences and workshops
27 Keynotes and invited talks
7 Organization of internationals conference and workshop

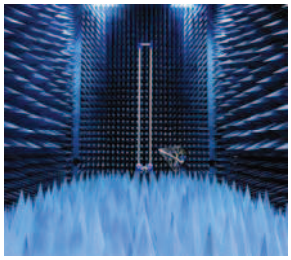

Research facilities:
3 Anechoic chambers
Magnetometer test ground
Information Technology Security Evaluation Facility (ITSEF)
Focus Ion Beam (FIB)
channel analyzer

104 Industrial partners

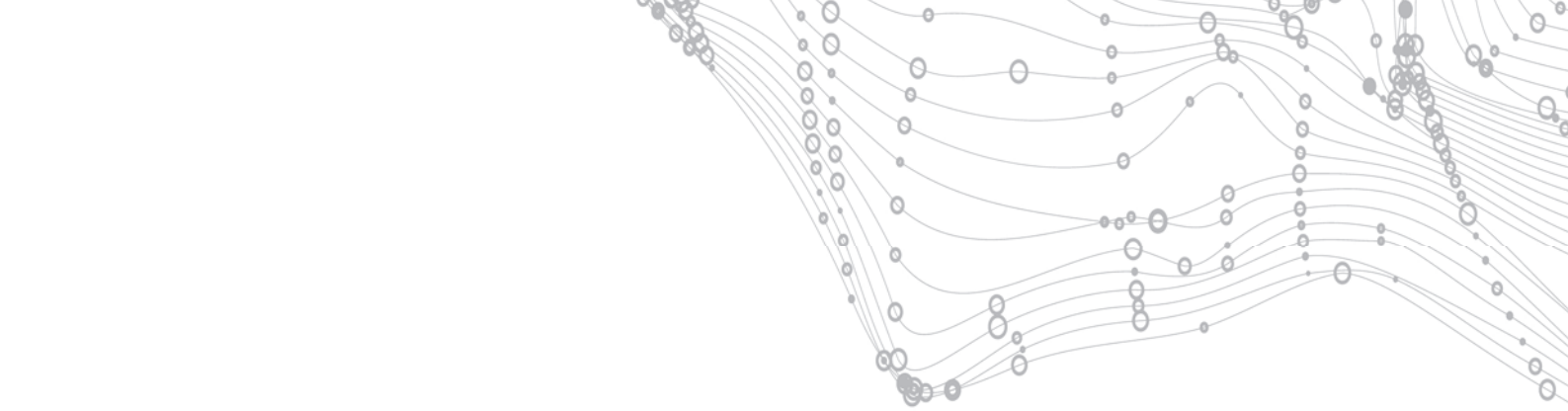

Scientific activity

Publications

191 publications in 2017 including 44 book chapters and top international journals,146 international conference communications. These include IEEE Transactions on Wireless Communications, IEEE Transactions on Antenna and Propagation, IEEE Transactions on Cognitive Communications and Networking, IEEE Transactions on Electromagnetic Compatibility, IEEE Transactions on Communications, IEEE Sensors & Transducers journal, IEEE Transaction on Haptics, IEEE Transactions on Very Large Scale Integration Systems, IEEE Transactions on Vehicular Technology, Smart Materials and Structures journal, IEEE VTC, IEEE ICC, IEEE PIMRC, IEEE WCNC, IEEE GlobeCom, Physiological Computing conference; International Workshop on SHM, PowerMEMS, etc.

Prize and awards

Best paper award: T. Stanko, et al., "Shape from Sensors: Curve Networks on Surfece from 3D Orientations", Shape Modelling International 201, Berkeley, California, USA, June 21-23, 2017.

Best paper award: S. Anceau et al., "Nanofocused X-Ray Beam to Reprogram Secure Cirtuits", Workshop on Cryptographic Hardware and Embedded Systems (CHES) 2017, Taipei, Taiwan, September 25–28, 2017

Best paper award: L. Batel et al., "Réseau d'Antennes Compact, Super Directif et Large-Bande Associé aux Eléments Non-Foster20eme Journée Nationale Micro-Ondes, 16-19 mai 2017, Saint-Malo, France.

Best paper award: R. Gerzaguet et al., "Block-filtered OFDM: A new Promising Waveform for Multi-service Scenarios", IEEE International Conference on Communications (ICC), Paris 21-25 Mai 2017.

Experts

1 International Expert, 17 Senior Experts, 17 Experts, 6 of them holding an HDR.

Scientific committees

- National Research Agency «High performance infrastructures, software technology and science » committee.
- Technical Program committees of: JNM, COST 15104, EurAAP, IEEE EUROCON, IEEE GlobCom, EuCNC, IEEE VTC, IEEE PIMRC, IEEE WCNC, IEEE VTC, IEEE DySPAN, IEEE ICC.

Conferences and Workshops organizations

Conference Organization: ISWCS Conference Organization in Bologna Italy, (general chair)

Workshops, Panels and special sessions organized in the following conferences: EuCAP, EuMW, EuCNC, ISWCS, IEEE ICC, IEEE WCNC, IEEE PIMRC, IEEE WPNC.

International Collaborations

EURECOM (France), University of Rome (Italy) University of Bologna (Italy), University of Calgary (Canada), Université Catholique de Louvain (Belgium), Czech Technical University (Czech Republic), Chalmers Unversity of Technologies (Sweden), Fraunhofer Institute HHI (Germany), ETRI (South Korea), Tokyo Teck University (Japan), Ritsumeikan University (Japan).


WELCOME
to the future of website
About Us
Document
Solution
DOCUMENT Solution
Integrated Solution for
Managing Paperless Document
Learn More...
Home
About Us
Products
Services
Technology is Us

01 WIRELESS HIGH SPEED COMMUNICATIONS

- **Millimeter Waves**
- **Full Duplex**
- **Advanced Coding**
- **Spectrum and Heterogeneous Network Management**

A HIGH DATA RATE LIFI INTEGRATED SYSTEM WITH INTER-CELL INTERFERENCE MANAGEMENT

RESEARCH TOPIC:
LiFi, intercell interference, global controller, resource allocation, spatial reuse

AUTHORS:
L. Maret, D. Miras, M. Maman, M. Laugeois, X. Popon, D. Kténas

ABSTRACT:
This project achieved the first fully integrated Optical Wireless Communication (OWC) network solution with inter-cell interference management. This network uses novel LiFi integrated and real-time modems with advanced physical (PHY), Medium Access Control (MAC) and Logical Link Control (LLC) layers allowing adaptive rates up to 42 Mbit/s at PHY layer and a configurable number of users per lamp. A network layer is designed and implemented to manage inter-cellular interference optimizing the spatial reuse of the resources. Hence, link quality of interfered unserved users is improved and the aggregated network throughput is drastically increased. This whole system eases the deployment of LiFi access points in a dynamic manner (i.e without operator's intervention).

SCIENTIFIC COLLABORATIONS : None

Context and Challenges

Many recent demonstration works have shown LiFi capacities in point-to-point links or in multiuser scenarios but for mono-cellular systems. These recent prototypes are not viable in realistic indoor deployments where a large part of enlightened areas are covered by several lighting fixtures, leading to huge DownLink (DL) inter-cellular interference, as well as for UpLink (UL) often achieved with InfraRed (IR) for Wavelength Division Duplexing (WDD). Without any network coordination, DL and UL inter-cellular interference considerably drops the cell coverage and the overall network capacity. This work presents the first high data rate VLC integrated solution which implements an inter-cellular interference manager using a centralized and dynamic approach, in order to continuously adapt the resource allocations to varying interference.

Main Results

The proposed LiFi network is based on integrated LiFi Access Points (LAP) and User Equipment (UE) modems [1]. The PHY layer is based on an efficient DCO-OFDM waveform in DL close to IEEE 802.15.7r1 mode and a multi-level PAM in IR UL. A complete MAC is implemented for multiuser access. A new software entity called Global Controller (GC) is implemented in the LAP network. Its role is to synchronize all LAP's superframes, to collect all interference detections and to organize the resource allocation with dedicated time slots for interfered receivers. Two different algorithms are run for DL beacon and UL poll separation (coloring graph) and for time-slot allocation (compromise between fair time-sharing and cell rate).

The performance of the interference management is measured by FTP traffic emulation in a real indoor 4.3x6.2m room as shown in Fig.1, with 4 LAPs and 4 UEs randomly distributed.

Figure 1 - Four Light Access Points (left) and one dongle (right)

The performance is assessed by measuring the different data rate of each terminal with a maximum of 4 simultaneous FTP DL and UL requests (traffic queue never empty) using JMeter©. The UEs are fixed (no mobility). In DL, UE1 is not interfered, UE2 and UE3 have 1 interfering LAP, and UE4 is interfered by 2 LAPs. Fig. 2 shows the instantaneous DL data rate of each UE for the case without (top) and with (bottom) interference management [2,3].

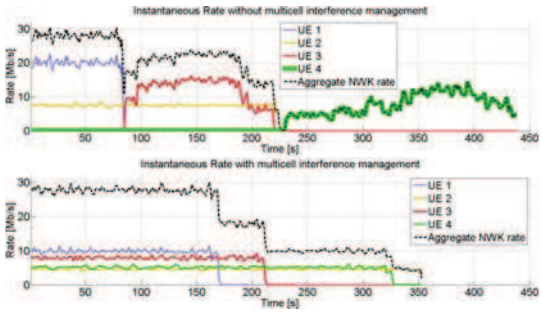

Figure 2 - DL data rates without GC (top) and with GC (bottom)

It reveals that without GC some interfered UEs (e.g. UE4) may never be served. With GC, all users can be simultaneously served. Similar gains can be observed in UL since multicell management is done independently in DL and UL. Moreover this multicell management allows to have spatial reuse of the resource. For a more favorable UE distribution without interference, the aggregated DL and UL network throughputs are considerably increased since proportional to the number of LAPs.

Finally, this novel multicell system has a network self-discovery function and the GC entity can be embedded in a LAP with self-healing feature. This robust and dynamic network solution may avoid any operator's intervention for large scale deployments

Perspectives

Perspectives are twofold. First the studied network could be enlarged (number of LAPs, loads) for complexity studies. Second, one could think to integrate users' mobility in order to study the time convergence of different graph coloring algorithms and the backhaul traffic overhead due to GC control messages.

RELATED PUBLICATIONS:
[1] CEA-Leti Indoor High-Speed LiFi Access, http://www.leti-cea.com/cea-tech/leti/english/Pages/Industrial-Innovation/Demos/LIFI.aspx
[2] D. Miras, L. Maret, M. Maman, M. Laugeois, X. Popon and D. Kténas, "An OWC Network Solution with Intercell Interference Coordination", IEEE Global LiFi Congress, February 8-9, 2018
[3] D. Miras, L. Maret, M. Maman, M. Laugeois, X. Popon and D. Kténas,, "A High Data Rate LiFi Integrated System with Inter-cell Interference Management", IEEE Wireless Communications and Networking Conference, April 2018

BLOCK-FILTERED OFDM: A NOVEL WAVEFORM FOR FUTURE WIRELESS TECHNOLOGIES

RESEARCH TOPIC:
5G, Multi-carrier, OFDM

AUTHORS:
D. Demmer, JB Doré, R. Gerzaguet, D. Demmer, D. Kténas

ABSTRACT:
The forthcoming fifth generation of mobile technology (5G) will be designed to satisfy the demands of 2020 and beyond. A new promising modulation scheme is introduced: Block-Filtered Orthogonal Frequency Division Multiplexing (BF-OFDM). The proposed waveform demonstrates an excellent frequency localization and can straightforwardly be integrated with the OFDM know-how and 4G principles. Besides, the proposed waveform relies on a receiver similar to the one used in OFDM. BF-OFDM systems are also scalable, which is an interesting feature in order to steer the network capabilities on demand.

SCIENTIFIC COLLABORATIONS: None

Context and Challenges

5G does not just promise a huge increase in terms of data rates and capacity but it also targets new kind of use cases like Internet of Things or vehicular communications. The currently deployed 4G technology does not provide enough network capabilities to support this wide diversity of applications which has motivated the research on alternative waveforms. In this context, a new promising modulation scheme is introduced: Block-Filtered OFDM (BF-OFDM). The proposed waveform demonstrates an excellent frequency localization and can straightforwardly be integrated with the OFDM know-how and 4G principles. Besides, the proposed waveform relies on a receiver similar to the one used in CP-OFDM. BF-OFDM systems are also scalable, which is an interesting feature in order to steer the network capabilities on demand.

Main Results

Flexible and efficient use of non-contiguous unused spectrum targeting heterogeneous mobile network deployment scenarios is one of the key challenges that future 5G systems would need to tackle. In this work we propose a new promising waveform called Block-Filtered OFDM that addresses most of the weakness of legacy OFDM in terms of spectral localization and performance in asynchronous scenario, while keeping complex quasi orthogonality and simple Fast Fourier Transform (FFT) based receiver.

The transmitter scheme is depicted in Fig 1. We denote M the number of carriers, and N the number of subcarriers. There are N subcarriers per carrier. To maintain orthogonality, only N/2 subcarriers bear data per carrier. The subcarrier allocation depends on the carrier index parity. For each BF-OFDM symbol, N/2 data are mapped in frequency domain, an IFFT of size N is applied to each carrier, and a CP is appended. A predistortion stage is applied to each subcarrier [1][2].

Performance on several representative criteria have been assessed (spectral efficiency, power spectral density, performance against multipath channel and performance in multi-user asynchronous scenario).

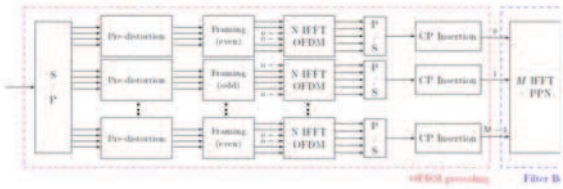

Figure 1 : BF-OFDM transmitter: It is based on precoding and filtering stages

We have compared the performance of BF-OFDM, OFDM, Universal Filtered Multi-Carrier (UFMC) and Filter Bank Multi-Carrier (FBMC) regarding these criteria, showing the potential benefits of the proposed scheme. An example is depicted Fig.2. Besides, a complexity analysis has been provided, showing that the scalability and flexibility of BF-OFDM can be done at the price of a slightly complexity increase.

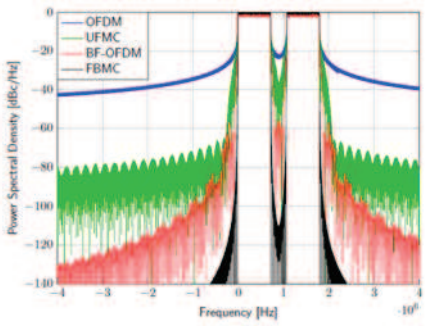

Figure 2 : Power spectral density of OFDM, FBMC, UFMC and BF-OFDM

Perspectives

A complete system is under development (Hardware implementation) to demonstrate through field trials the benefits of the technology.

RELATED PUBLICATIONS:
[1] D. Demmer, R. Gerzaguet, J. B. Doré, D. L. Ruyet, and D. Kténas, "Block-filtered OFDM: A novel waveform for future wireless technologies," in 2017 IEEE International Conference on Communications (ICC), May 2017, pp. 1–6.
[2] R. Gerzaguet, D. Demmer, J. B. Doré, and D. Kténas, "Block-filtered OFDM: A new promising waveform for multi-service scenarios," in 2017 IEEE International Conference on Communications (ICC), May 2017, pp. 1–6...

ASSESSMENT OF MULTICARRIER WAVEFORMS FOR 5G SATELLITE

RESEARCH TOPIC:
5th generation of mobile communications, terrestrial-satellite convergence, physical layer

AUTHORS:
N. Cassiau, B. Chamaillard

ABSTRACT:
It is now certain that satellite systems will play a role in the coming fifth generation of mobile communications (5G). When 5G will be deployed, satellite and terrestrial systems should be able to share the spectrum. In this aim, multicarrier waveforms are good candidates for satellite physical layer. In this study CEA has assessed the performance of several multicarrier waveformsin this context. First, the spectrum localization of the waveforms has been measured by simulation. The peak to average power ratio (PAPR), a key criterion for satellite transmitter, has then be plotted. Bit Error Rate (BER) curves in the presence of a terrestrial interferer were provided and combined with PAPR to propose a fair comparison between the waveforms. Finally, taking into account complexity considerations, implementation recommendations were given. It was shown that the choice of the waveform is highly dependent on the target BER before decoding. These results are used by CNES for arguing in standardization bodies.

SCIENTIFIC COLLABORATIONS: French Space Agency (CNES).

Context and Challenges

For several years, a convergence process of satellite systems towards terrestrial systems can be observed, specifically concerning the physical layer. Standardization bodies are today pushing for a shared spectrum between the two systems. This study assessed the performance of several waveforms in this context. Key Performance Indicators were studied and implementation recommendations based on a synthesis of these results were provided.

Main Results

The study focused on multicarrier modulations, which foster a shared access to the spectrum. Waveforms were compared to the well-known Orthogonal Frequency Division Multiplex (OFDM). More specifically, the Single Carrier (SC) version of OFDM was used. SC allows to decrease the Peak to Average Power Ratio (PAPR) and is therefore an important feature for satellite communications. The studied waveforms were SC versions of Pulse Shaped (PS) OFDM, Extended and Weighted (EW)-OFDM, Precoded OFDM and a waveform designed by CEA-Leti: Block Filtered (BF)-OFDM [2]. The scenario is illustrated by Fig. 1: the satellite is able to create a hole in the bandwidth so that a terrestrial system can transmit in it.

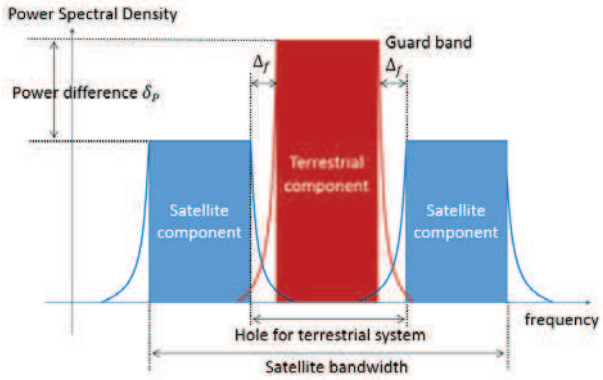

Figure 1. Scenario of the study

The assessed Key Performance Indicators (KPIs) were (i) the Out of Band (OoB) rejections, (ii) the Peak to Average Power Ratio (PAPR) and (iii) the Bit Error Rate (BER). OoB rejections (i) is one of the key factors when dealing with a granular access to the spectrum. This is a waveform intrinsic parameter but additional mechanisms can be used to compensate weak rejections: baseband filtering as for PS-OFDM, introduction of dedicated carriers as in Precoded OFDM, or analog filtering. The temporal fluctuation of the envelope of the signal to be amplified (PAPR) is also a key factor for the satellite downlink considered in this study (ii). A low PAPR indicates a high energy efficiency. BER of the satellite link (iii) was also measured, assuming that a terrestrial system is transmitting in the frequency hole in the satellite bandwidth. This helped evaluating the resistance of the waveforms to a time asynchronous terrestrial interferer.

The best waveforms with respect to OoB rejections, i.e. BF-SC-OFDM and Precoded OFDM were shown to be the worst concerning the PAPR. For this latter KPI, EW-SC-OFDM is the best candidate. When a terrestrial interferer is introduced, the good rejection properties of BF-SC-OFDM and Precoded OFDM allow for better BER performance at high Signal to Noise Ratio (SNR) than EW-SC-OFDM.

A synthesis of the results presented above was realized, in order to provide recommendations. Fig. 2 presents this synthesis, as the throughput of each waveform compared to the throughput of the reference waveform (SC-OFDM), in percent. Three target BER before decoding were chosen (7.10^{-2}, 10^{-2}, 6.10^{-3}) to reflect a wide range of specifications. In particular, a BER before decoding of 7.10^{-2} is a specification that allows almost error-free satellite transmission (after decoding).

It was shown that the choice of the waveform is closely related to the target BER before decoding. In the case where this BER is higher than (around) 2.10^{-2}, such as for a quasi-errorless satellite transmission at SNR=10 dB, EW-SC-OFDM is an excellent candidate. This waveform has average rejection properties but this is not an issue for such high BER. Its excellent PAPR on the other hand allows it to reach higher throughput than the other waveforms. Moreover, the complexity of EW-SC-OFDM is comparable to that of SC-OFDM. If much lower target BER before decoding are required, less than 10^{-2}, or if the interferer is much stronger than the useful signal, then it is recommended to use BF-SC-OFDM.

Target Bit Error Rate (before decoding)	EW-SC-OFDM	PS-SC-OFDM	Precoded SC-OFDM	BF-SC-OFDM
7.10-2	+1,3	-4,3	-6,0	-4,0
10-2	+1,0	-3,3	+5,8	+8,4
6.10-3	-2,2	-1,0	+13,9	+18,3

Figure. 2: Synthesis of the results

Perspectives

A concept note that summarizes the results of this study was provided to CNES. This synthesis is used by the French space agency for defending its position in standardization bodies.

RELATED PUBLICATIONS:
[1] N. Cassiau, B. Chamaillard, "Assessment of Multicarrier Waveforms for 5G Satellite," PIMRC 2017
[2] R. Gerzaguet, D. Demmer, J.-B. Doré, and D. Kténas, "Block-Filtered OFDM: a new promising waveform for multi-service scenarios," in IEEE ICC 2017 (ICC), Paris, France, May 2017.

SDR BASED TESTBENCH TO EVALUATE IN-BAND FULL-DUPLEX TECHNOLOGY

RESEARCH TOPIC:
5G, In-Band Full-Duplex technology, SDR board, low complexity, low cost

AUTHORS:
P. Rosson, D. Dassonville, X. Popon

ABSTRACT:
In-Band Full-Duplex (IBFD) transmissions are promising solutions for wireless 5G small cell communication scenarios. Indeed, transmitting and receiving simultaneously in the same frequency band offers new perspectives: under certain conditions, this new access mode allows to increase the overall capacity or to reduce latency. Usually, this technology requests high performance components with high analog linearity and large range converters (ADC and DAC) which implies expensive solution. Our solution assumes the use of classical wireless broadband components. Based on their characteristics, a simple architecture has been proposed to reduce the undesired self-interference generated by the in-band full-duplex transceiver.

SCIENTIFIC COLLABORATIONS: Intel Deutschland

Context and Challenges

The challenge of In-Band Full-Duplex (IBFD) transceiver is to transmit and receive simultaneously at the same frequency. To be able to listen and decode low power received signal while transmitting powerful signal, it is necessary to mitigate the Self-Interference (SI) signal which is due to leakages between the transmitter (Tx) and the receiver (Rx). Self-Interference Cancellation (SIC) is done in several steps. First, a circulator with only one antenna can provide around 20 dB isolation between Tx and Rx ports. Then, a RF broadband multi-taps analog SIC (RFSIC) is used to mitigate the SI. This RFSIC avoids low noise amplifier saturation and it allows the analog to digital converter (ADC) to convert the useful signal within the adapted power range. Finally, a Digital SIC (DSIC) after the ADC can be applied to remove the remaining nonlinear part of the SI. Small cell scenarios are preferred as there is less difference between transmitted and received power than in large cell scenarios. The SI cancellation performance also depends on the signal bandwidth: the larger the bandwidth, the more difficult the cancellation.

Main Results

To reduce the complexity of the analog broadband filter, a novel architecture has been proposed (see fig 1). An additional Hybrid SIC (HSIC) is inserted between the RFSIC and the DSIC. It combines a second Tx chain (so-called auxiliary chain), with a digital linear filter whose role is to take the effects of the RFSIC, circulator and couplers into account [1].
The broadband analog filter is therefore reduced to a narrow band filter with only 1 complex tap and a fixed delay. Both RFSIC coefficient and HSIC coefficients filter are estimated by digital processing iteratively. The RFSIC has a slow tracking capability while HSIC can track time varying self-interference channel. In [2] it is shown that both RFSIC and HISC can achieve up to 70 dB SI cancellation over 40 MHz in a sub 6 GHz frequency band.

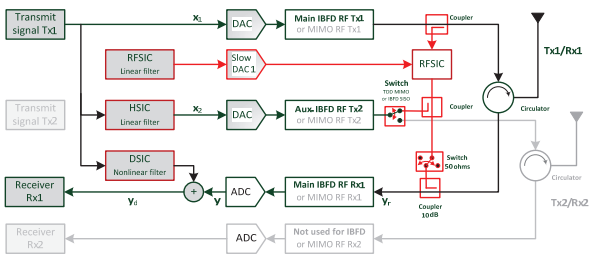

Figure 1. Architecture overview

Figure 2 presents RFSIC and DSIC performance when a signal of interest (SoI) is received while transmitting a powerful signal. To better illustrate the reception of the SoI, the bandwidth of the SoI is set to 10 MHz whereas the bandwidth of the transmitted powerful signal is equal to 20 MHz. The SI is illustrated over the multiple cancellation stages. The first analog canceller reduces by 60 dB the SI (circulator isolation included). The second digital canceller adds 30 dB more. The SoI is visible and can be demodulated if the SINR is greater than the useful threshold. It proves the capability of the system to considerably cancel the SI. Such cancellation performance enables the successful reception of the SoI regardless of the large power difference between the transmitted signal and the SoI. Figure 2 shows that the cancellation reaches a total of 91 dB.

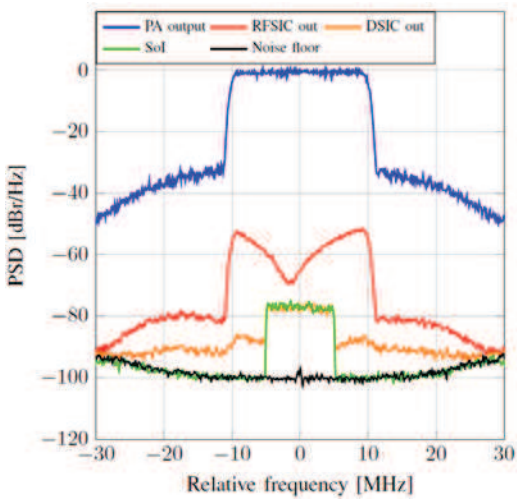

Figure 2: Cancellation performance of RFSIC with DSIC in presence of Signal of Interest

Perspectives

These works allow us to understand the limitations of the SI cancellation in the context of in-band full-duplex wireless transmission. The RF transmitted noise as well as the other RF imperfection of the transceiver are the limiting constraints. A new modelling of the analog components is under study. By taking this new model into account within the DSIC, we expect an overall cancellation greater than 100 dB.

The second main perspective is the evolution to support IBFD MIMO transmission.

RELATED PUBLICATIONS:
[1] A. Debard, P. Rosson, D. Dassonville, V. Berg, “Flexible In-Band Full-Duplex Transceivers Based on a Modified MIMO RF Architecture”, in Proc. of 11th Intern. Conf., CROWNCOM 2016, Grenoble, France, May 30 - June 1, 2016
[2] P. Rosson, D. Dassonville, X. Popon, S Mayrargue, “SDR based test bench to evaluate analog cancellation techniques for In-Band Full-Duplex Transceiver”, 5th International Workshop on Cloud Technologies and Energy Efficiency in Mobile Communication Networks (CLEEN 2017) Torino, Italy - June 22, 2017
[3] M. Emara, P. Rosson, K. Roth, D. Dassonville, “A Full Duplex Transceiver with Reduced Hardware”, Globecom Wireless Communications Symposium, Singapore, Dec. 2017.

5G MULTI-SERVICE FIELD TRIALS WITH BF-OFDM

RESEARCH TOPIC:
5G, BF-OFDM, Field Trials

AUTHORS:
JB Doré, P. Rosson, J. Estavoyer, X. Popon, D. Dassonville, B. Miscopein, M. Pezzin, D. Miras, and D. Kténas

ABSTRACT:
Multi-service transmissions are expected in the upcoming fifth-generation (5G) of cellular networks. These heterogeneous applications lead to many constraints that need to be addressed in a flexible way. We investigate the division of the bandwidth into several subbands, each one having a given physical layer numerology to support a given type of 5G services. This work highlights and demonstrates the possible coexistence of Broadband, Ultra-Reliable Low-Latency and Internet of Things services within the same channel using a flexible waveform. We describe field-test experiments carried out with an implementation of the BF-OFDM (Block-Filtered OFDM) physical layer on custom hardware prototyping boards. Field-trials results confirm the potential of BF-OFDM and the feasibility of the use of mixed numerologies for the next generation of cellular network.

SCIENTIFIC COLLABORATIONS : None

Context and Challenges

Although mobile broadband applications will be one of the important drivers of 5G, pushing for higher data rates and capacity than 4G, there is a wide consensus to consider that 5G networks will also have to accommodate various Quality of Service regimes arising with new fields of applications. In particular, IoT (Internet of Things) and ultra-Reliable and Low Latency Communications (URLLC) may represent a true significant digital transformation with tremendous market speculations for 2020.

Main Results

With regard to the development of 5G orthogonal requirements, many waveforms have been proposed: UFMC (Universal Filtered Multi-Carrier), FBMC (Filter Bank Multi-Carrier), GFDM (Generalized Frequency Division Multiplexing) , f-OFDM etc. Thereupon, a novel waveform, entitled BF-OFDM (Block-Filtered OFDM) [1], was recently proposed and proved to be particularly suitable for 5G requirements, i.e. good spectral confinement, flexible structure as well as simple and transparent receiver. Especially, B-FOFDM frequency localization is greatly improved at the price of a slight complexity increase at the transmitter side. Interestingly the BF-OFDM receiver architecture remains identical to the CP-OFDM one.

This work intends to present field test experiments done with an implementation of the BF-OFDM physical layer on hardware prototyping boards. The frequency band of operation is the 3.5GHz band, for which an experimental license has been granted by ARCEP, the French regulatory body. This experiment is done in an urban-like environment where BF-OFDM is evaluated for representative ranges and propagation conditions covering Line-of-Sight (LOS) and Non Line-of-Sight (NLOS). By collecting quantitative results on SNR and signal demodulation capabilities on various locations, the objective of this study is twofold. It first intends to assess the capability of BF-OFDM to accommodate 5G requirements; secondly it provides feedback from the field on the suitability of the 3.5GHz band in 5G scenarios, in the perspective of its possible designation as a 5G spectrum band

Figure 1 : Picture of the set-up.

For the experimental tests, the transmitter (Tx) antennas and RF units are set on the rooftop of a building, at a height of about 20 meters (see Fig 1). Its behavior is similar to a Base Station (BS). The receiver, that can be considered as a User Equipment (UE) is mobile. Three configurations are considered: broadband, URLLC and IoT ones. Two scenarios are also assessed: a static scenario and a mobile configuration (30 and 50 km/h). The three services coexist in the same band as depicted in Fig 2.

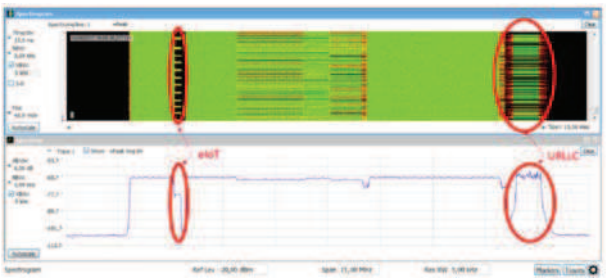

Figure 2 : Snapshot of the frequency allocation acquired by a spectrum analyzer.

The complete set-up has been implemented and initial performance has been assessed. As expected by numerical simulations, field trial results confirm the feasibility of the use of mixed numerologies for the next generation of cellular network.

Perspectives

The presented results are a first milestone, and a new measurement campaign is planned to consolidate the initial results. More precisely, field trials in the 700MHz and 3.5GHz will be realized.

RELATED PUBLICATIONS:
[1] R. Gerzaguet, S. Bicais, P. Rosson, J. Estavoyer, X. Popon, D. Dassonville, J. B. Doré, B. Miscopein, M. Pezzin, D. Miras, and D. Kténas, "5G Multi-Service Field Trials with BF-OFDM," in 2017 IEEE Globecom Workshops (GC Wkshps), Dec 2017, pp. 1–5..

MODELING AND ANALYSIS OF HETNETS WITH MM-WAVE MULTI-RAT SMALL CELLS DEPLOYED ALONG ROADS

RESEARCH TOPIC:
Millimeter-wave communication, Multi-RAT, Heterogeneous Networks

AUTHORS:
Gourab Ghatak, Antonio De Domenico, Marceau Coupechoux (Telecom ParisTech)

ABSTRACT:
We characterize a multi-tier network with macro base stations (MBS), and multi radio access technology (RAT) small cells, which are able to operate in microwave and millimeter-wave (mm-wave) bands. The small cells are assumed to be deployed along roads modeled as a Poisson line process. In this context, we derive the association and RAT selection probabilities of the typical user under various system parameters. Our analysis reveals the need of deploying more small cells per street in cities with more streets to maintain coverage, and highlights that mm-wave RAT in small cells can help to improve the SINR performance of the users.

SCIENTIFIC COLLABORATIONS: Telecom ParisTech

Context and Challenges

With the tremendous increase in demand for data rates, two solutions among others are gaining particular interest: dense deployment of ad-hoc small cell base stations (SBS) and exploitation of higher frequency bands for data transmission. However, most of the work that aim to mathematically model and analyze such systems, do so by considering uniform deployment of base stations. These models are not realistic representations of the network architecture in an urban scenario. On the contrary, our characterization is more realistic as we take into account the randomness in network architecture imposed by the geometry of the roads in a city.

Main Results

First we model the mm-wave interference experienced by an outdoor user. From Figure 1, we see that a user U1 being served by base station B1 experiences interference from B2 if it lies in a serving beam of B2. Accordingly we define 'spillover' as the region of interference generated by a mm-wave SBS to the coverage area of a neighboring SBS, while serving a user near its cell edge. Accordingly, we calculate the probability that a user will lie in such a spillover region.

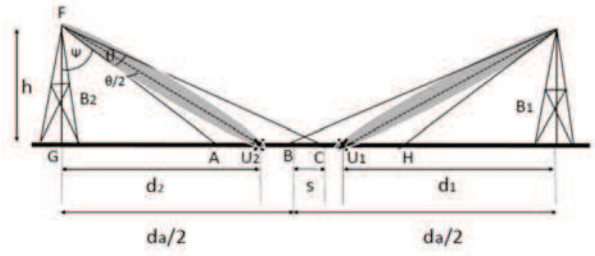

Figure 1: Model for characterization of mm-wave interference.

Furthermore, we assume that the base stations (BSs) send their control signals in the sub-6GHz band, due to the higher reliability of sub-6GHz signals as compared to the mm-wave signals. For the association, a user compares the sub-6GHz signals from the macro and small cell base stations. In case the user is associated with a MBS, it is served in the sub-6GHz band. Whereas, in case it is associated to an SBS, the user compares the power received in the sub-6GHz and mm-wave band, and selects the RAT providing the highest power.

Using the model of the mm-wave interference, and under our tier and RAT selection scheme, we derive the association probabilities of the users to the various tiers and RATs and subsequently, use it to derive the SINR coverage probabilities of the typical outdoor user.

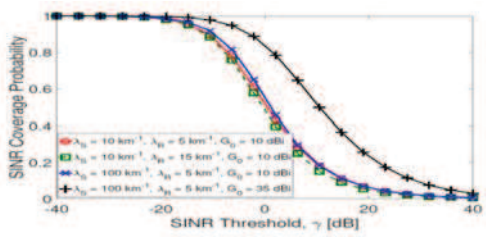

Figure 2: SINR coverage probability of outdoor users with respect to base station deployment and road densities.

First, we observe from Figure 2 that mm-wave (with antenna gain of 35 dB) provides better SINR performance, precisely due to the large directional antenna gain and the fact that mm-wave transmissions suffer from minimal interference. Furthermore, going from a sparser to denser urban scenario with more roads, decreases the SINR performance of the user, because the interfering sub-6GHz signals increase.

Perspectives

We have analytically characterized a multi-tier heterogeneous network, where small cells are deployed along the roads and employ both sub-6GHz and mm-wave RAT. In denser urban scenarios, the operator should necessarily deploy more SBS per road, to maintain the SINR performance of the user. Increasing the SBS deployment in a street efficiently improves the SINR coverage in sub-6GHz operation. However, for mm-wave operation, too large SBS deployment leads to a saturation in the gain in SINR performance

RELATED PUBLICATIONS:
[1] G. Ghatak, A. De Domenico, M. Coupechoux, Modeling and Analysis of HetNets with mm-Wave Multi-RAT Small Cells Deployed Along Roads. IEEE Globecom 2017.
[2] G. Ghatak, A. De Domenico, M. Coupechoux, Small Cell Deployment Along Roads: Coverage Analysis and Slice-Aware RAT Selection (Submitted to IEEE Transactions on Wireless Communications, January 2018)

QOS-DRIVEN SCHEDULING IN 5G RADIO ACCESS NETWORKS - A REINFORCEMENT LEARNING APPROACH

RESEARCH TOPIC:
5G, Artificial Intelligence, Radio Resource Management, Neural Network, Reinforcement Leaning

AUTHORS:
A. De Domenico, I.S Comsa and D. Kténas

ABSTRACT:
Classical scheduling strategies have been designed to deal with some particular Quality of Service (QoS) requirements for specific traffic types. To improve the system performance, this paper proposes an innovative framework, which selects at each interval, the appropriate strategy capable to maximize the user satisfaction in terms of distinct QoS requirements. Neural networks and Reinforcement Learning are jointly used to learn the best scheduling decision based on the past experiences. The simulation results show very good convergence properties and notable improvements with respect to the baseline scheduling solutions.

SCIENTIFIC COLLABORATIONS: None

Context and Challenges

The expected diversity of services and the variety of use cases in 5G networks will require a flexible Radio Resource Management (RRM) able to satisfy the heterogeneous Quality of Service (QoS) requirements. However, due to the multitude of services and requirements, none of the state-of-the-art packet schedulers can be considered as an appropriate option for all network conditions. This paper proposes an innovative downlink scheduling framework that improves the QoS satisfaction in terms of delay, Packet Loss Rate and Guaranteed Bit Rate requirements by selecting at each TTI, the best scheduling strategy based on the momentary system state. To achieve this goal, we use an actor-critic (AC) Reinforcement Learning (RL) scheme that takes advantage of Neural Networks flexibility to learn the appropriate scheduler mechanism that maximizes the QoS satisfaction. In the RRM context, RL algorithms have been proposed to e.g., optimize the network energy saving [1] and minimize the interference [2].

Main Results

Figure 1 shows the mean errors for both the learning functions in the case of a traffic with variable bit rate. We can observe how this errors decrease and become stable after around 1000 seconds, when the learning phase can be concluded successfully.

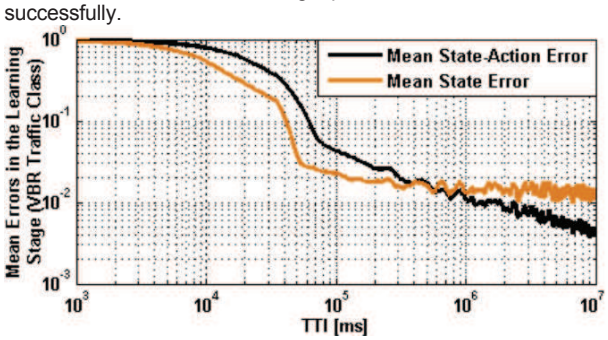

Figure 1. Learning Function Errors Evolution in the Learning Stage.

To validate our solution, we measure the percentage of Transmission Time Interval, where the three QoS requirements are satisfied for each active user. We compare our approach with three baseline algorithms from the literature: Proportional Fair based EXPonential (PF-EXP), PF based Barrier Function (PF-BF), and the PF based Opportunistic Packet Loss Fair (PF-OPLF), focusing on the packet delay reduction, Guaranteed Bit Rate (GBR) satisfaction, and Packet Loss Rates (PLRs) minimization, respectively. We can observe how our approach is capable to adapt the scheduler behavior and dynamically select the policy capable to obtain the best results, thus achieving up to 30% of gain with respect to the existing schemes.

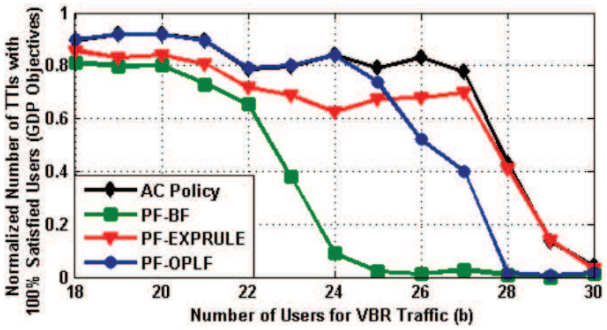

Figure 2. Performance of the proposed AC Policy with respect to baseline algorithms.

Perspectives

In future studies, we aim to investigate how to realize an even further flexible scheme, capable to dynamically prioritize across the active traffic class and users, and then jointly select the appropriate scheduling rule. Furthermore, we target to demonstrate the advantage of our artificial intelligence tools in a realistic proof of concept.

RELATED PUBLICATIONS:
[1] A. De Domenico, V. Savin, D. Ktenas, and A. Maeder, "Backhaul-Aware Small Cell DTX based on Fuzzy Q-Learning in Heterogeneous Cellular Networks,» in IEEE International Conference on Communications (ICC), 2016, pp. 1 – 6
[2] A. De Domenico and D. Ktenas "Reinforcement Learning for Interference-Aware Cell DTX in Heterogeneous Networks," in IEEE Wireless Communications and Networking Conference (WCNC), 2018.

MAC design for 5G dense networks

RESEARCH TOPIC:
5th generation of mobile communications, unlicensed spectrum, medium access control, MAC, 5 GHz band

AUTHORS:
Benoit Miscopein, Rida El Chall, Dimitri Kténas

ABSTRACT:
Fifth generation (5G) networks are expected to provide a massive increase of the network capacity which leads to consider i) spectrally efficient physical layer (PHY) solutions, ii) the use of additional license-exempt spectrum where traffic can be offloaded and iii) the deployment of dense heterogeneous network. All of this may lead to a possibly high and unpredictable interference level in time and space. In order to ensure an efficient use of unlicensed spectrum, CEA has developed a TDD MAC protocol on top of an advanced PHY, which is capable of supporting different quality of services (QoS) and provides fair coexistence with neighboring systems. Based on listen-before-talk procedure, this MAC shows in system level simulations that it outperforms IEEE 802.11.ac solutions in very dense scenarios.

SCIENTIFIC COLLABORATIONS: University of Surrey (UK), Intel-Germany (DE)

Context and Challenges

In order to successfully tackle the well-known challenge of high capacity demands of 5G networks, ultra-densification, efficient use of spectrum and advanced filtered modulation techniques are considered as key enablers for 5G systems [1] [2]. To comply with these requirements, it is mandatory to rely on unlicensed spectrum where traffic can be offloaded, either for interference management or capacity boosting purposes. Given the heterogeneous nature of 5G traffic, the channel access on unlicensed spectrum shall support various QoS. Due to the shared nature of unlicensed spectrum, it also shall support dynamic channel switching to avoid inter-cell interference. An efficient MAC protocol has to be designed to enable these requirements while taking advantage of post-LTE waveforms which are characterised by an excellent spectral confinement brought by advanced filtering process.

Main Results

A novel MAC protocol for 5G small cells operating at 5 GHz has been designed assuming FBMC PHY, knowing it can be extended to any 5G waveform. The proposed design is based on a "Listen-Before-Talk (LBT) procedure to comply with ETSI regulations; it enables a TDD broadband transmission via a flexible frame structure mixing scheduled and contention access modes (cf. Fig.1). The physical layer is exploited to enable the relaxed synchronicity constraint of uplink multiple access. It also dramatically reduces the inter-channel leakage which may cause severe performance reduction in dense scenarios.

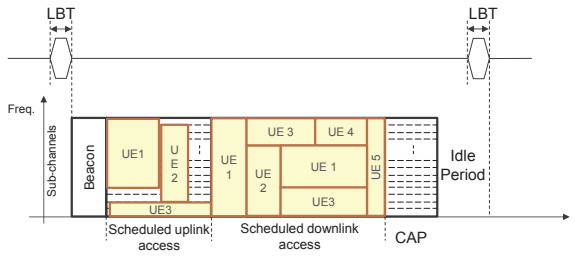

Figure 1: MAC Superframe structure and multiple access

This MAC design has been evaluated through simulations on indoor and outdoor deployment assuming typical traffic patterns; it has been compared to IEEE 802.11ac. Simulations show that our design outperforms WiFi for various inter-site distances (ISD) [4].

ISD [m]	30	50	100
WiFi (802.11ac)	111.33	44.21	19.49
Leti design	240.82	125.90	60.40

Table1: Area spectral efficiency (b/s/Hz/km²)

When considering the coexistence with a WiFi network deployed in the same area, this MAC design exhibits a very good fairness as it provides the same impact on the Wifi network than another WiFi network. This is mainly due to the LBT nature of the protocol.

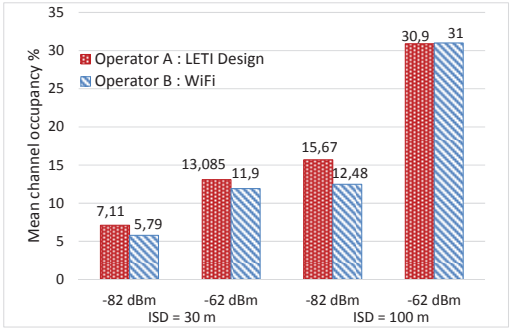

Figure 2: Coexistence fairness with WiFi

In terms of performance when considering dense deployments with cells using adjacent channels (hexagonal grid with frequency reuse factor of 3), the very low out-of-band emissions coming along with the spectral confinement of FBMC allows a better mitigation of inter-cells interference compared to LTE waveform, like shown in Fig.3 [3] [4].

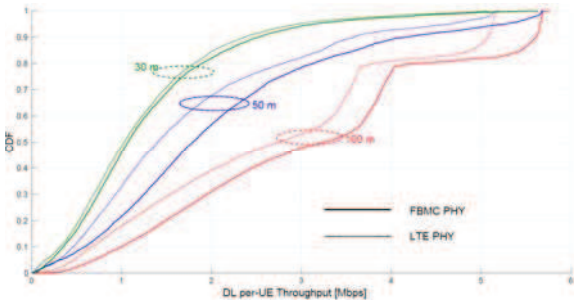

Figure 3: UE-throughput for FBMC and LTE physical layers

Perspectives

This MAC protocol has been implemented on custom HW/SW board, in order to perform field-trial evaluations. It will be further demonstrated with a Machine-Learning based channel selection algorithm to show how it can coexist with neighbouring systems like WiFi. This work can be extended to any frequency band or any physical layer, provided the latter can exhibit the same time-frequency characteristics than FBMC.

RELATED PUBLICATIONS:
[1] NGMN 5G white paper: https://www.ngmn.org/fileadmin/ngmn/content/downloads/Technical/2015/NGMN_5G_White_Paper_V1_0.pdf,
[2] Huawei 5G white paper: http://www.huawei.com/minisite/hwmbbf16/insights/5G-Nework-Architecture-Whitepaper-en.pdf
[3] R. E. Chall, B. Miscopein, D. Kténas, MAC design for 5G dense networks based on FBMC modulation, EAI CROWNCOM conference, Lisbon, 2017
[4] B. Miscopein, R. El Chall, M. Filo, B. Okyere H2020 SPEED-5G project, D5.2 deliverable "MAC approaches with FBMC (final), June 2017".

DYNAMIC SCFLIP FOR POLAR CODES

RESEARCH TOPIC:
Polar codes, 5G, Successive Cancellation-Flip decoding

AUTHORS:
L.Chandesris, V. Savin, D. Declercq (ENSEA / UCP / CNRS)

ABSTRACT:
In this work, we propose a generalization of the Successive Cancellation Flip (SCFlip) decoding of polar codes, characterized by a number of extra decoding attempts, where one or several positions are flipped from the standard SC decoding. To do so, a dynamic process is used to determine the bit-flips that are more likely to correct the trajectory of the SC decoding. We show that the proposed decoder, called Dynamic SCFlip, is an effective alternative to list decoding of polar codes, with an average computation complexity close to the one of the SC decoder.

SCIENTIFIC COLLABORATIONS: D. Declercq (ENSEA / UCP / CNRS)

Context and Challenges

Polar codes recently emerged as the first construction that probably achieves the capacity of any binary-input memoryless symmetric channel, with log-linear encoding and decoding complexity. Their construction relies on a specific recursive encoding procedure, which can be reversed at the receiver end by applying a Successive Cancellation (SC) decoder. Besides their theoretical importance, the particularity of their construction makes them very attractive for practical applications, mainly due to the flexibility it provides in accommodating multiple coding rates or different transmission channels. This also explains the ongoing research effort, by both academia and industry, to investigate their use in 5G systems. Recently, 3GPP selected Polar codes as the official coding method for the control channel in the 5G enhanced mobile broadband use case.

Main Results

Despite their capacity-achieving performance, Polar codes under SC decoding are known to provide rather modest error correction performance for short to moderate block-lengths, as compared to the ubiquitous LDPC and Turbo codes.
This work is aimed at improving the error correction performance of Polar codes, especially at finite block-lengths. We introduce a new decoding algorithm, referred to as Dynamic SCFlip (D-SCFlip) [1, 2], characterized by a number of extra decoding attempts, where one or several positions are flipped from the standard SC decoding. D-SCFlip is based on a Cyclic Redundancy Check (CRC)-Polar concatenated scheme, where the CRC code is used to determine the success of a decoding attempt. Starting with the initial SC decoding, the D-SCFlip performs additional decoding attempts, until one of them passes the CRC test, or a maximum number of allowed attempts is reached. Each new decoding attempt amounts to performing a SC decoding, while flipping one or several hard decision estimates of the data bits. Compared to the State-of-the-art SCFlip, the proposed decoder considers bit-flips of several positions. Moreover, in the proposed scheme, the flipping positions are dynamically determined according to a specific metric, taking into consideration the previous decoding attempts, so that the next attempt is guaranteed to be the one with the best probability of success [1], thus reducing considerably the error rate together with the number of attempts.

Fig. 1 provides a comparison of the SC, SC-Flip, SC-List and the proposed D-SCFlip decoders for Polar codes for a code-length N=256 and various coding rates R = (1/3, 1/2, 2/3), over the binary-input AWGN channel. All three of SC-List, SC-Flip and D-SCFlip decoders have a CRC of 16 bits. SCFlip and D-SCFlip decoders have a maximum number of additional decoding attempts fixed to T = 50, while the list-size for SC-List is set to $L = 8$. It can be seen that the proposed D-SCFlip decoder clearly outperforms the state-of-the-art SCFlip and competes with the SC-List decoding for all of the coding rates considered. Meanwhile, compared to the high complexity SC-List decoding, the proposed D-SCFlip offers an interesting trade-off between complexity and performance, as it keeps both the space and the computational complexity close to the one of the SC decoding.

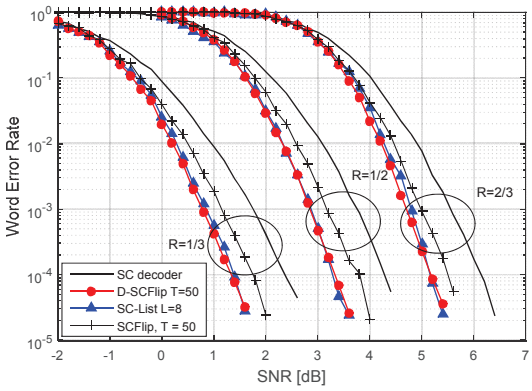

Figure 1: Performance of polar decoders for a code-length N=256 and various coding rates.

Perspectives

Future work will investigate the advantage of using advanced decoders, including D-SCFlip decoder, to decode non-binary polar codes for BPSK modulation as well as higher order modulations.

RELATED PUBLICATIONS
[1] L.Chandesris, V. Savin, D. Declercq "Dynamic SCFlip for polar codes", IEEE Transaction on Communications, 2018
[2] L.Chandesris, V. Savin, D. Declercq " Un décodeur à inversion dynamique pour les Codes Polaires", Gretsi, 2017

ANALYSIS AND DESIGN OF COST-EFFECTIVE, LOW-POWER, HIGH-THROUGHPUT LDPC DECODERS

RESEARCH TOPIC:
LDPC, NS-FAID, low-cost, low-power, high-throughput decoder

AUTHORS:
T. Nguyen-Ly, V. Savin, X. Popon, K. Le (ENSEA), D. Declercq (ENSEA), F. Ghaffari (ENSEA), and O. Boncalo (UPT)

ABSTRACT:
This work introduces a new family of Low Density Parity Check (LDPC) decoders, referred to as Non-Surjective Finite-Alphabet Iterative Decoders (NS-FAIDs). NS-FAIDs are optimized by density evolution for regular and irregular LDPC codes, and are shown to provide different trade-offs between hardware complexity and decoding performance. Two hardware architectures targeting high-throughput applications are also proposed, integrating NS-FAID decoding kernels. ASIC post synthesis implementation results on 65nm CMOS technology show that NS-FAIDs yield significant improvements in both throughput to area ratio, and energy per decoded bit, as compared to state of the art implementations.

SCIENTIFIC COLLABORATIONS: ENSEA (Cergy-Pontoise France) Politehnica University of Timisoara (Romania)

Context and Challenges

This work focuses on cost-effective, high-throughput hardware implementations of LDPC decoders, through exploiting their robustness to approximate computing and storage techniques. The proposed approach, referred to as Non-Surjective Finite-Alphabet Iterative Decoders (NS-FAIDs), allows approximate storage of the exchanged messages, which requires a lower precision than that used by the processing units. We develop specific models and analytic tools, based on density evolution and code-aware quantizers, so as to derive optimal solutions in terms of error correction performance. Our findings have further been validated through low-cost hardware implementations, targeting multi-Gigabit/s applications.

Main Results

NS-FAIDs are Min-Sum-based decoders, integrating techniques of approximate computing and storage at different levels [1]. They may be optimized based on density evolution techniques, such that to achieve the optimal tradeoff between the accuracy of the approximation (which enables cost, throughput, and power improvements) and the error correction performance (Figure 1).

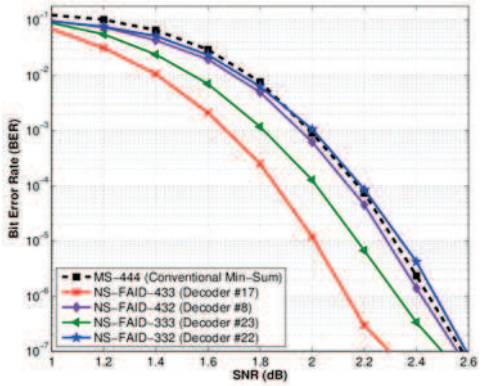

Figure 1: Bit error rate performance of various NS-FAIDs and conventional Min-Sum, for WiMax LDPC code, with length 2304 bits, and rate 1/2 (20 decoding iterations)

To assess the benefits of the NS-FAID approach, two hardware architectures have been proposed, targeting very high throughput applications, by making use of either hazard-free pipelining, or maximum hardware parallelism [2]. Implementation results for both ASIC and FPGA designs have confirmed the low-cost, high-throughput characteristics of the proposed architectures, as compared to state of the art implementations.

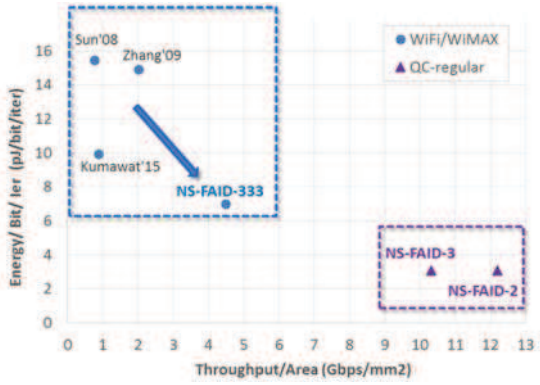

Figure 2: ASIC implementation results for various NS-FAIDs, for WiMax and QC regular LDPC codes

Figure 2 reports ASIC post-synthesis implementation results on 65nm-CMOS technology, in terms of throughput to area ratio (TAR) and energy per decoded bit per iteration. For WiMax LDPC codes, it can be seen that the proposed NS-FAID-333 decoder compares favorably with state of the art implementations. To further emphasize the low-power, high-throughput characteristic of the proposed decoders, Figure 2 also presents implementation results for Quasi-Cyclic (QC) regular LDPC codes, yielding significant improvements in terms of both TAR and Energy/bit/iteration.

Perspectives

Probabilistic bit-flipping based decoders, reducing the storage requirements to only 1 bit per exchanged message, will be investigated in future works.

RELATED PUBLICATIONS:
[1] T. Nguyen-Ly, V. Savin, X. Popon, D. Declercq, "High Throughput FPGA Implementation for Regular Non-Surjective Finite Alphabet Iterative Decoders", IEEE International Conference on Communications (ICC), Workshop on Channel Coding for 5G and Future Networks, Paris, France, May 2017.
[2] T. Nguyen-Ly, V. Savin, K. Le, D. Declercq, F. Ghaffari, and O. Boncalo, "Analysis and design of cost-effective, high-throughput LDPC decoders", IEEE Transactions on Very Large Scale Integration (VLSI) Systems, December 2017..


Navigation
Menu
mobile

02 LOW DATA RATE AND LOCALIZATION

- **Localization and Navigation Techniques**
- **Advanced Coding for LPWA Networks**
- **Body Area Networks**

LOCALIZATION BOUNDS FOR BEAMFORMING OPTIMIZATION IN MULTICARRIER MMWAVE SYSTEMS

RESEARCH TOPIC:
mmWave, 5G, Localization, Beamforming, Theoretical performance bounds, Multicarrier systems.

AUTHORS:
R. Koirala, B. Denis, B. Uguen (Univ. Rennes 1), D. Dardari (Univ. Bologna)

ABSTRACT:
Relying on the unique intrinsic localization capabilities of future 5G mmWave communications, we propose a beamforming (i.e., precoding) optimization scheme suitable to multi-carrier systems, which improves the estimation of delay and/or angle of arrival at the mobile receiver. We first reformulate theoretical location-dependent performance bounds into an optimization problem (per subcarrier), before injecting the obtained optimal beamformer in a power allocation problem (over multiple subcarriers). This two-step solution paves the way to promising tradeoffs with respect to communications, especially in more complex multi-user contexts.

SCIENTIFIC COLLABORATIONS: University of Rennes 1 - IETR, Rennes, France; University of Bologna, Cesena, Italy.

Context and Challenges

In the context of next generation communication networks (5G), the millimeter wave (mmWave) technology has been regularly put forward as a relevant solution to fulfill considerable needs in terms of data rates and channel load, while operating with highly directive antenna arrays in large available bandwidths [3]. Within such mmWave systems, the localization capability is no longer considered as an add-on, but rather as an inherent feature that is useful to communication (e.g., easing beam alignment or users tracking). This is mainly due to the unprecedented possibility of benefitting from network densification and getting spatialized information with high reactivity under device mobility. However, most of the state-of-the-art contributions committed so far in the mmWave field are still strongly focused on communication aspects or at most, they just consider characterizing the theoretical localization performance in simplistic scenarios (typically, in single-user single-carrier cases)..

Main Results

In [1], we have studied and developed an optimal beamforming policy so as to minimize the Cramer Rao Lower Bound (CRLB) of joint angle of arrival (AoA) and time delay estimates in a multicarrier mmWave system.

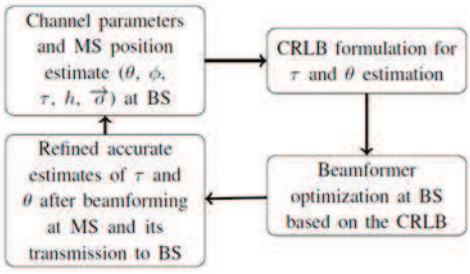

Figure 1: Iterative wireless localization accuracy refinement through bound-based multicarrier mmWave beamforming optimization at the base station (with τ the time delay and the angle of arrival at the mobile receiver).

More specifically, considering one single base station (BS) with rough a priori knowledge of channel coefficients and location information of the mobile station (MS), we have shown that it is possible to Iteratively improve the accuracy of AoA and time delay estimation, and hence of mobile station (MS) positioning, by means of optimized beamforming (in the pre-coding sense) at the base station. For this sake, a mathematical re-formulation of the CRLB has been first introduced. Then, the related optimization problem has been stated and solved for each single subcarrier independently. Finally, we have proposed a global solution optimizing the beamformer jointly over multiple subcarriers, following an original power allocation approach.

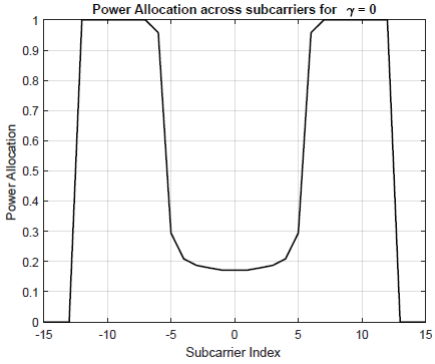

Figure 2: Example of spectrum allocation over multiple subcarriers optimizing only time delay estimation at the mobile receiver over mmWave down links.

In this unified optimization framework, one can arbitrarily chose to favor the estimation of one particular intermediary location-dependent variable (e.g., only time delay and hence, range estimation, See Figure 2), or even the joint estimation of mobile position and orientation (through adequate matrix transformations), thus enabling flexibility at the application level.

Perspectives

Current works have been considering extensions into more complex multi-user contexts (in both unicast and broadcast down link modes) and optimal 5G services differentiation, aiming at practical operating trade-offs between localization performance and communications (in terms of data rates), for instance in case of 1D in-street small cells deployment [2].

RELATED PUBLICATIONS:
[1] R. Koirala, B. Denis, D. Dardari, B. Uguen, "Localization Bound Based Beamforming Optimization for Multicarrier mmWave MIMO", IEEE Workshop on Positioning, Navigation and Communications 2017 (IEEE WPNC'17), Bremen, Oct. 2017.
[2] G. Ghatak, R. Koirala, A. De Domenico, B. Denis, D. Dardari, B. Uguen, M. Coupechoux, "Positioning Data-Rate Trade-off in mm-Wave Small Cells and Service Differentiation for 5G Networks", IEEE Vehicular Technology Conference 2017 – Spring (IEEE VTC-Spring'17), Porto, June 2018

COMPARISON OF DEVICE LIFETIME IN WIRELESS NETWORKS FOR THE INTERNET OF THINGS

RESEARCH TOPIC:
Wireless Sensor Network, Energy consumption, Bluetooth LE, WiFi HaLow, IEEE802.15.4e, Sigfox, LoRa, 6LowPAN

AUTHORS:
E. Morin, M. Maman, R. Guizzetti (STMicroelectronics), A. Duda (CNRS LIG)

ABSTRACT:
The expected lifetime for the Internet of Things (IoT) devices operating in several wireless networks have been compared: IEEE 802.15.4/e, Bluetooth low energy (BLE), IEEE 802.11 power saving mode, IEEE 802.11ah (HaLow), and new emerging long-range technologies, such as LoRa and SIGFOX. Energy constrained nodes that upload data to a sink, are considered analyzing the physical (PHY) layer under medium access control (MAC) constraints, and assuming IPv6 traffic whenever possible. We also consider retransmissions due to corrupted frames and collisions as well as the impact of imperfect clocks. Our analyzer gives all users of IoT technologies indications about the technology that best fits their needs from lifetime point of view and also help IoT network designers to select the right MAC parameters to optimize the energy consumption for a given application.

Context and Challenges

The Internet of Things (IoT) aims at connecting small constrained devices to the Internet via the IP protocol, which enables new communicating applications. Ultra-low energy consumption is critical for IoT devices since they mostly operate on batteries and they need to reach several years' lifetimes without battery replacement. Low power operation becomes even more challenging for nodes that harvest energy from the environment. An estimation of the energy consumption and the device lifetime is thus crucial for choosing the most appropriate technology and finding the optimal settings of configuration parameters..

Main Results

The main contributions of [1] with respect to the state of the art are the extension of a realistic energy model that takes into account the behavior of the PHY and MAC layers to all considered technologies and an open-source lifetime analyzer (Fig. 1), a tool for estimating the lifetime of a given network based on the main hardware and MAC parameters.

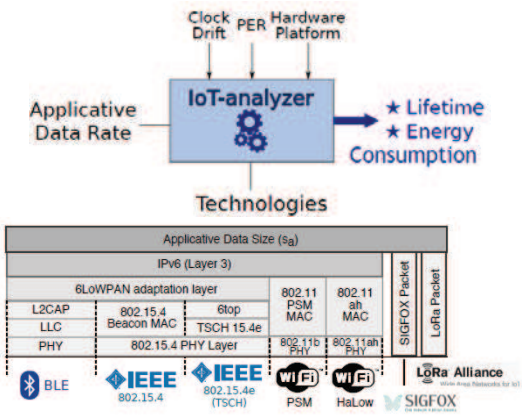

Figure 1: Analyzer computing lifetime for the proposed stack of the considered technologies

This analyzer is used to study the impact of higher layer protocols (fragmentation, protocol overhead), time synchronization, and packet losses on the lifetime. Several new results are revealed:

- The power consumed in Sleep state becomes a determining factor of the device lifetime for very low traffic intensities.
- Due to clock drift, asynchronous LoRa and SIGFOX technologies obtain the best lifetime for low traffic intensity.

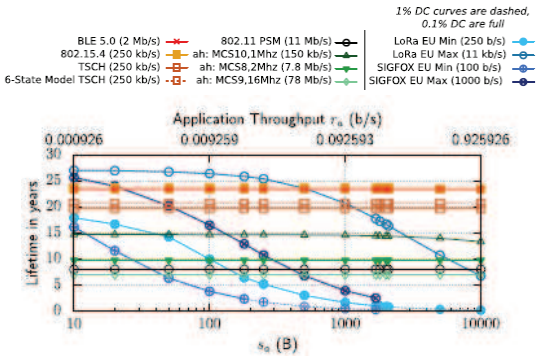

Figure 2: Lifetime of a two-AAA batteries device generating very low intensity traffic (Sa applicative Bytes each Ta= 1 day) with a clock drift of 40 ppm and no packet losses.

- BLE offers the best lifetime for all traffic intensities in its capacity range.
- For low (T_a= 100s) and medium (T_a= 1s) traffic intensity, the relative ranking is: BLE, 802.15.4, TSCH, and 802.11 technologies with the latter becoming interesting solutions for larger data sizes

Other results also show that only BLE and 802.15.4 can operate for medium traffic intensity with an 18 cm² solar panel in typical indoor light intensity of 300 lx and long range technologies are not ready to support energy harvesting for low traffic intensity.

Perspectives

The comparison has raised our interest in interoperability and mixing different technologies. IoT technologies can cooperate in the IoT context to fit the needs of different application traffic requirements. For such cooperation, interoperability between synchronous technologies (e.g., 802.15.4e) and asynchronous (e.g., BLE or Google Thread based on IEEE 802.15.4) is needed.

RELATED PUBLICATIONS:
[1] E. Morin, M. Maman, R. Guizzetti, and A. Duda, "Comparison of the Device Lifetime in Wireless Networks for the Internet of Things", in *IEEE Access journal*, vol. 5, pp. 7097-7114, 2017.

ENERGY EFFICIENT ADVERTISEMENT PROTOCOL FOR COOPERATIVE BODY AREA NETWORKS

RESEARCH TOPIC:

Cooperation, Body Area Network (BAN), Body to Body (B2B) Network, On-Body, Off-Body and Body-to-Body Channel Models

AUTHORS:

L.H. Suraty Filho, M. Maman

ABSTRACT:

One of the current issues on using Wearable Networks is their low-level interoperability among different BANs especially when the Telecom infrastructure is unavailable. Based on an architecture opening BAN to cooperative B2B Networks, we have proposed an energy efficient advertisement protocol for BAN discovery and friendship establishment. On the one hand, the proposed pseudo-random approach allows the MAC layer to pseudo-randomly schedule the communications and to save energy. On the other hand, bringing security based approach directly into the access allows only selected friends to predict next MAC communication attempts. The performance of the proposed scheme is evaluated through an accurate and realistic WSNet-based simulator based on link correlated and time-varying propagation models for On-Body and B2B communications.

Context and Challenges

With the wide adoption of wearable technology and applications, it is foreseen that a massive number of wearable devices will appear in the following years. While fitness and healthcare remain the dominant wearable applications, other applications including entertainment, augmented reality, rescue and emergency management are emerging as well. New requirements imposed by coexistence and collective mobility suggest to revise the old BAN paradigms by exploiting B2B cooperation. Thus we proposed an energy efficient neighbor discovery algorithm for cooperative BANs including a secure based mechanism against selective jamming and for friendship establishment. The main goal of this study was to evaluate the energy consumption of advertisement (ADV) schemes while taking into account the specific context of B2B networks.

Main Results

The main contributions of [1] with respect to the state of the art are: First, the proposed protocol brings the security based mechanism directly into the access thanks to a private pseudo random algorithm shared with friends, thus avoiding selective jamming and establishing friendship.

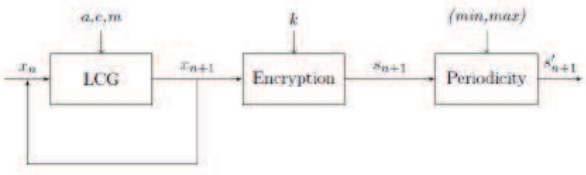

Figure 1: Private pseudo-random sequence block diagram

The pseudo-random access consists of 3 blocks (Fig. 1): a Linear Congruential Generator (LCG), encryption and periodicity. This scheme is responsible for calculating the duration an advertiser must wait before to transmit its next ADV packets and for predicting when to listen to other advertisers.
Secondly, the proposed ADV scheme was evaluated in cooperative BANs context with realistic semi-deterministic propagation models. The semi-deterministic features of WSNet-based Simulator enable to generate link correlated and time varying realistic traces (i.e. with consistent mobility patterns) for On-Body and B2B shadowing and fading including body orientations, rotations and indoor environment effect by means of stochastic channel models.

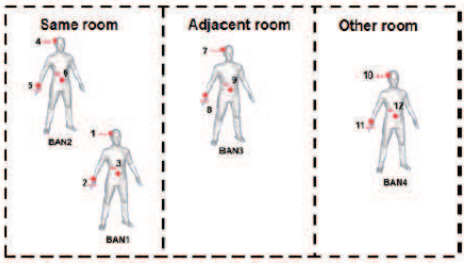

Figure 2: BAN deployment in different rooms

The proposed scheme was compared with different state of the art MAC strategies (Random periodic, scheduled rendez-vous, unslotted CSMA/CA) with/without periodic scanning. First, CSMA/CA scheme has the best Packet Delivery Ratio (PDR) performance but at the expense of energy consumption (i.e. always on receiver). Secondly, the proposed ADV MAC scheme with a periodic scanning provides a significant improvement on the energy consumption while maintaining the average PDR relatively high in comparison to the state of the art solutions. Lastly, augmenting the density of nodes to up to 50 BANs does not degrade the performance of the proposed scheme with scan scheme because the channel occupancy stays low.

Moreover, we have evaluated the impact of sharing the radio between Body-to-Body and Intra-BAN communications. Using a master-slave strategy, the master Intra-BAN performance remains the same while the slave ADV MAC performance is slightly degraded.

Perspectives

In the future, we will demonstrate the feasibility and the effectiveness of the designed cross-layer B2B Networks architecture through prototyping and demonstrations. In particular, we will integrate the designed MAC and Networking functionalities into real hardware sensor nodes and evaluate experimentally the B2B protocols performance.

RELATED PUBLICATIONS:

[1] L. H. Suraty Filho and M. Maman, "Energy efficient advertisement protocol for cooperative body area networks," 2017 IEEE 28th Annual International Symposium on Personal, Indoor, and Mobile Radio Communications (PIMRC), Montreal, QC, Canada, 2017, pp. 1-7

POST-PROCESSING OPTIMIZATION OF PIECEWISE INDOOR TRAJECTORIES BASED ON IMU AND RSS MEASUREMENTS

RESEARCH TOPIC:
Indoor localization, Post-processing, real-time particle filter, Map-matching, sensor fusion

AUTHORS:
Kersane Zoubert-Ousseni, Christophe Villien, François Le Gland

ABSTRACT:

Post-processing indoor navigation has multiple interesting applications, for example to develop crowdsourcing analysis. The post-processing framework allows to provide a better estimation than in a real-time framework. The main contribution of this paper is to present a piecewise parametrization using Inertial Measurement Unit (IMU) and Received Signal Strength (RSS) measurements only. This approach leads to an optimization problem. A Levenberg-Marquardt algorithm improved with simulated annealing and an adjustment of RSS measurements data leads to a good estimation (55% of the error less than 5 meters) of the trajectory.

SCIENTIFIC COLLABORATIONS: INRIA, IRMAR

Context and Challenges

Nowadays, it is possible, in the indoor localization context to provide a coarse trajectory with inertial data from a smart phone using Pedestrian Dead Reckoning (PDR). We also have access to different sources of data, such as Received Signal Strength (RSS) signals (WIFI and Bluetooth Low Energy (BLE)). Many approaches consider the use of a particle filter to fuse this PDR trajectory, with RSS signals or/and a map, to provide a real-time trajectory estimation. However, post-processing is relevant when a real-time estimation of the trajectory is not needed. Indeed, considering a post-processing framework may lead to better performance because of a larger set of information, i.e. the data of the whole trajectory. Moreover, many use cases do not require real-time processing, for example, when trajectories of the users are to feed a database that is then used to compute some statistics (e.g. most visited places, users' behavior) or for automated map maintenance based on crowd-sourced data. We then consider a post-processing of the PDR trajectories and RSS data from a smart phone.

Main Results

Our approach consists in estimating the real trajectory with a parametric transformation of the PDR trajectory computed from RSS measurements, where each piece of the PDR trajectory is associated with a rotation and a scaling parameter that has to be estimated as illustrated in Figure 1. In this example, some breaks are artificially added to increase the degrees of freedom.

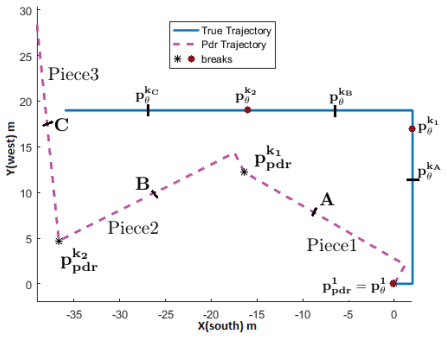

Figure 1: Example of PDR trajectory parametrization

In Figure 2, the PDR trajectory cannot be properly corrected with only two parameters because there is also a drift of the heading caused by the gyro drift, which is not taken into account by our model. However, in this case, it is possible to improve the accuracy using an artificial break at the middle of the trajectory resulting in two segments. We have then one scale parameter and two misalignment angles to estimate, making the model more robust to such drift errors. By adding one break, it is possible to reduce this drift. Still, we have another illustration that the removal of the bias greatly improves the performance of our estimation for both the RMSE, 4.9m to 3.3m, and especially the %D5 (i.e. percent of time when error is less than 5m), 54% to 89%.

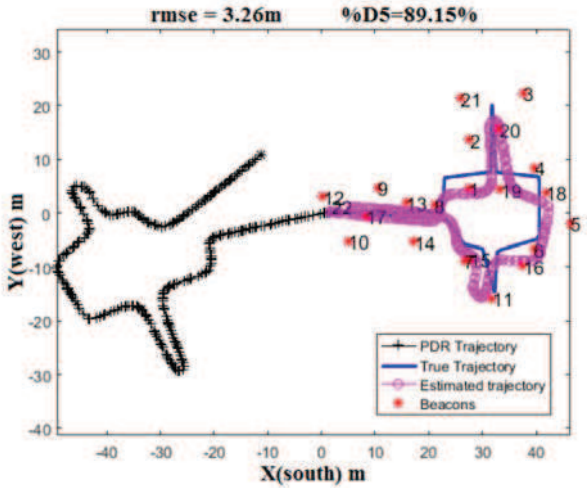

Figure 2 : example of reconstructed trajectory using piecewise optimization

Perspectives

This off-line approach for trajectory estimation based on IMU and RSS measurements has proven superior in terms of performance (reduction of RMSE by 27% computed on 240 real experiments) than real-time approaches. This technique can be useful for many crowdsourcing application, where localization is not constrained by real-time.

RELATED PUBLICATIONS:

[1] K. Zoubert-Ousseni, C. Villien, F. Le Gland, "Comparison of post-processing algorithms for indoor navigation trajectories", 2016 International Conference on Indoor Positioning and Indoor Navigation (IPIN), Alcala de Henares, 2016, pp. 1-6.

TURBO-FSK: A PHYSICAL LAYER FOR LPWA APPLICATIONS

RESEARCH TOPIC:
Low Power Wide Area (LPWA), Internet of Things (IoT), Physical layer, low sensitivity

AUTHORS:
Y. Roth, J.B. Doré, V. Mannoni, F. Dehmas, V. Berg

ABSTRACT:
In the context of Low Power Wide Area (LPWA) networks, terminals are expected to be low cost, to be able to communicate over a long distance, and to operate on battery power for many years. The physical layer needs to be designed highly energy efficient. The combination of M-ary orthogonal Frequency-Shift-Keying (M-FSK) modulation and coding in the same process has shown to be a promising candidate when associated to an iterative receiver (turbo principle). This new digital transmission scheme is then called Turbo-FSK. Comparison in terms of PER, range and also power consumption with LPWA current technologies is performed, showing the potential of this technology. Integration of Turbo-FSK waveform in a new concept of flexible waveform based on frequency domain processing is also proposed to address the large scale of requirements of new LPWA applications.

Context and Challenges

The Internet-of-Things (IoT) has emerged as one of the leading research area for wireless communications as several billions connected devices are forecasted in years to come. A significant part of communication transactions in the IoT is expected to be done through Low Power Wide-Area (LPWA) networks, for which requirements include low cost, low energy consumption and long range. A link budget improvement of 15/20dB in comparison to existing cellular technologies is expected, as reducing the costs to connect the devices to the wide-area network will encourage IoT deployment. To meet these requirements, the current generation of LPWA technologies dramatically extended the sensitivity performance of its receivers. Moreover, future LPWA systems are also expected to provide a higher level of flexibility with a faster data rates and/or lower latency for similar battery lifetime to extend the range of applications the technology can deliver. These new requirements of LPWA have led to reconsider the physical layer for these kinds of system. Turbo-FSK is a new waveform that meets performance close to the Shannon limit for the lower spectral efficiency. This waveform can be combined with another one in order to propose a flexible physical layer required in the new generation of LPWA system.

Main Results

The main parameters of the Turbo-FSK scheme are the size of the orthogonal modulation, M, and the number of repetitions, λ. To each set of parameters correspond a specific spectral efficiency and energy efficiency. With two degrees of freedom, the asymptotic performance of the Turbo-FSK is evaluated using the EXtrinsic Information Transfer (EXIT) chart. The spectral efficiency of each configuration is given versus the energy efficiency in Figure 1. The asymptotic performance of Turbo-FSK approach the minimum achievable Eb/N0 at 0.28dB for parameters M=512 and λ=3. When the information block size is set to 1000, the distance to Shannon's limit is equal to 1.35dB (for a BER of 10^{-5}). This demonstrates the potential of Turbo-FSK to closely approach the theoretical limits.

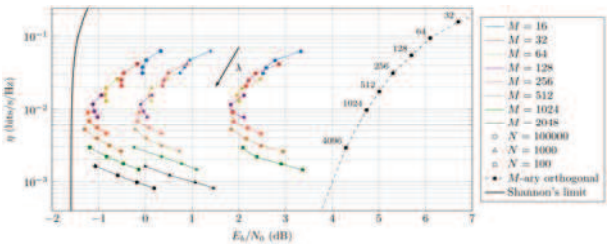

Figure 1: Performance of Turbo-FSK for various values of parameters

A new flexible approach for LPWA has also been introduced to meet the contradictory requirements of long-range, low power consumption and higher throughput. A performance analysis as illustrated in Figure 2 with the power consumption as the function of the throughput for a range of 6 km has concluded that a flexible waveform based on the frequency domain processing (Turbo-FSK, OFDM, SC-FDM) can be parameterized to reach the best performances in a large scale of scenarios (from "low throughput/long range/energy efficiency" to "high throughput").

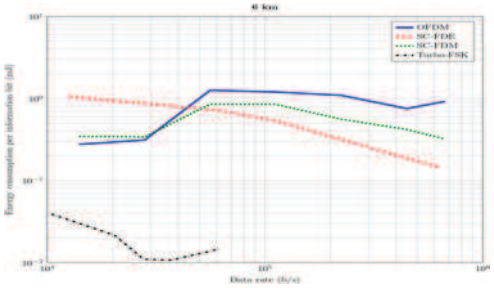

Figure 2: Energy consumption per information bit as the function of the throughput and for a given range of 6 km

Perspectives

Future work should further study common approaches of synchronization mechanisms for the different options of the physical layer. This include timing and frequency synchronization and channel estimation. This should be completed and refined before hardware architecture implementation and its associated complexity evaluation of the flexible concept

RELATED PUBLICATIONS:
[1] Y. Roth, J.-B. Doré, L. Ros, V. Berg, Turbo-FSK, a physical layer for low-power wide-area networks: Analysis and optimization, Comptes Rendus Physique, Volume 18, Issue 2, February 2017, Pages 178–188.
[2] Roth, Y.: The Physical Layer for Low Power Wide Area Networks: A Study of Combined Modulation and Coding Associated with an Iterative Receiver. PhD Thesis, Université Grenoble Alpes (July 2017). https://hal.archives-ouvertes.fr/tel-01568794
[3] V. Mannoni, V. Berg, F. Dehmas, D. Noguet, "A Flexible Physical Layer for LPWA Applications", Cognitive Radio Oriented Wireless Networks and Communications 2017 (CrownCom 2017), Lisbon, Sept. 2017.

RESILIENT VEHICULAR LOCALIZATION IN PATHOLOGICAL ROAD SITUATIONS THROUGH V2X COOPERATION

RESEARCH TOPIC:
Vehicular Localization, V2x Connectivity, Hybrid Data Fusion, Cooperative - Intelligent Transportation Systems.

AUTHORS:
G. M. Hoang, B. Denis, J. Härri (EURECOM)

ABSTRACT:
Intelligent transportation systems (ITS) will require accurate and resilient positioning capabilities regardless of operating conditions. Vehicle-to-vehicle (V2V) communications can hence support novel localization schemes that aim at improving nominal GNSS capabilities. In this context, we propose a cooperative data fusion framework based on particle filtering, which claims fine suitability into pathological road situations (typically, in GNSS-denied environments) by combatting fusion filter overconfidence, error propagation between cooperating vehicles, as well as large location errors perpendicular to the road dimension.

SCIENTIFIC COLLABORATIONS: EURECOM, Sophia Antipolis, France.

Context and Challenges

High-precision vehicular localization (i.e., within a few 10s of cm) is seen as a key enabler for future intelligent transport systems (ITS) and their applications (e.g., autonomous driving, vulnerable road users' safety, local dynamic maps). However, most Global Navigation Satellite Systems (GNSS) can neither fulfil such precision requirements, nor guarantee a true continuity of service in harsh environments (e.g., urban canyons). Vehicle-to-x (V2x) communication standards (e.g., ITS-G5) have thus been considered to support new cooperative localization functionalities (Fig.1). Typically, each vehicle fuses its own GNSS readings with the content of Cooperative Awareness Messages (CAMs) emitted by neighboring vehicles, inter-vehicle range measurements (e.g., based on Impulse Radio - Ultra Wideband (IR-UWB)) and other on-board modalities (e.g., odometers). However, major challenges still need to be addressed in case of severely degraded -or missing- GNSS Information, such as filter's sub-optimality under unbalanced ranging and positioning noises, errors propagation, or large cross-track errors..

Main Results

In a global fusion framework based on cooperative particles filtering and ITS-G5 V2V communications, it has been illustrated in [1] that typical disparities between prior GNSS errors and IR-UWB V2V ranging noises could cause particles cloud depletion in high dimensional estimation spaces (i.e., estimating the 2D positions/speeds of both local and neighboring vehicles). This phenomenon leads the fusion filter to be overconfident in biased location estimates, which are subsequently propagated over the vehicular network, polluting other vehicles' fusion results.

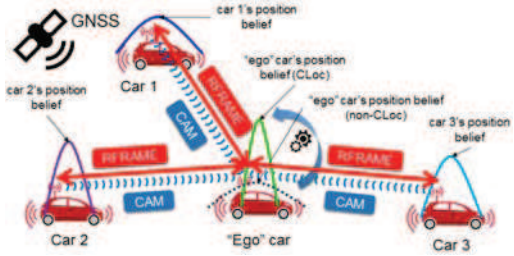

Figure 1: Typical V2X-based cooperative fusion scenario

An adaptive dithering technique has thus been proposed to optimally adjust the assumed observation noise level as a function of expected localization performances (based on Bayesian Cramer Rao Lower Bounds), improving filter's consistency and increasing the probability to reach 20 cm accuracy typically from 50% to 90% (Fig.2).

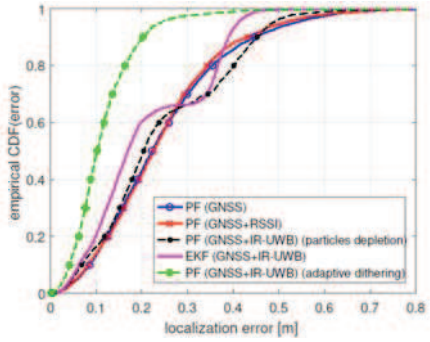

Figure 2: CDF of 2D location errors under adaptive dithering of fusion filter's observation noise (green)

In a similar fusion context, so as to mitigate the poor cross-track Geometric Dilution of Precision (GDoP) observed under typical road constraints [2], we have considered an Inertial Measurement Unit (IMU) to account for the vehicle's heading and/or camera-based lane boundaries detection to truncate the density of posterior state estimates, boosting the probability to reach an accuracy of 0.5 m from 60% to 90% orthogonally to the road.

Finally, addressing GNSS-denied tunnel environments, additional Vehicle-to-Infrastructure (V2I) measurements with respect to Road Side Units (RSUs) have been integrated into the fusion problem with both IR-UWB or ITS-G5 technologies, exploring practical trade-offs between localization accuracy gains and deployment costs (i.e., in terms of RSU density and geometric configuration) in comparison with GNSS repeaters [3].

Perspectives

Current works consider using only LIDARs (through message-passing and decentralized data association) [4], new position awareness messages [5], as well as experimental validations [6].

RELATED PUBLICATIONS:
[1] G.M. Hoang, et al. "Robust and Low Complexity Bayesian Data Fusion for Hybrid Cooperative Vehicular Localization," IEEE ICC'17, Paris, May 2017.
[2] G.M. Hoang, et al. "Mitigating Unbalanced GDoP Effects in Range-Based Vehicular Cooperative Localization", IEEE ICC'17-ANLN Workshop, Paris, May 2017.
[3] G.M. Hoang, et al. "Robust Data Fusion for Cooperative Vehicular Localization in Tunnels", IEEE IV'17, Redondo Beach, June 2017.
[4] G. Soatti, et al. "Enhanced Vehicle Positioning in Cooperative ITS by Joint Sensing of Passive Features", IEEE ITSC'17, Yokohama, Oct. 2017.
[5] I. Khan, et al. "Rethinking Cooperative Awareness for Future V2X Safety-critical Applications", IEEE VNC'17, Torino, Nov. 2017.
[6] S. Severi, et al. "Beyond GNSS: Highly Accurate Localization for Cooperative-Intelligent Transport Systems", IEEE WCNC'18, Barcelona, April 2018.

DIGITAL PROCESSING FOR ULTRA-NARROW BAND RECEIVER

RESEARCH TOPIC:
IoT, LPWA, UNB, DBB, CFO tracking

AUTHORS:
F. Dehmas, D. Lachartre, C. Bernier, E. Mercier, L. Ouvry

ABSTRACT:
Ultra-narrow band (UNB) modulation is a technology enabling low power and wide area (LPWA) communications. Its apparent low complexity hides real difficulties in presence of carrier frequency offset (CFO) since a small offset pushes the signal out of the bandwidth of the receiver. Leti has realized a UNB transceiver chip supporting rates down to 100 b/s in presence of CFO thanks to digital processing to estimate, track and compensate CFO.

SCIENTIFIC COLLABORATIONS: LETI-DACLE

Context and Challenges

The internet of Things (IoT) is rapidly expanding and more than 20 billion devices are expected to be connected before the end of the decade. Low Power Wide Area Networks (LPWA) constitute an important part of the IoT and the leading communication technology is based on Ultra-Narrow Band (UNB) modulation operated by Sigfox. Leti has developed a UNB transceiver semiconductor chip achieving DBPSK modulation with rates down to 100 b/s. In the digital part, to receive the signal with carrier frequency offset (CFO) constitutes the main challenge: frequency shift is superior to the signal bandwidth and the drift during a frame reception has to be compensated.

Main Results

The digital part of the chip [1] is composed (Fig. 1) of a digital front end (DFE) and a digital baseband (DBB).

The three main purposes of the DFE are firstly interference mitigation thanks to filtering (most of the filtering requirements are dealt by the digital part) and secondly signal translation to baseband thanks to a digital mixer based on the CORDIC algorithm. This mixer allows a floating IF and the actuation from the DBB to track the CFO. Thirdly sampling rate reduction thanks to decimation.

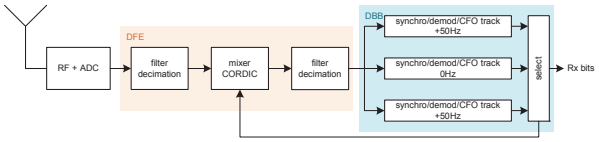

Figure 1: Architecture of the digital part of the receiver

In the DBB part, the detection of the signal in the presence of CFO is done thanks to a 3-fold implementation of the demodulator centered on different frequencies (+50 Hz, 0 Hz and -50 Hz) allowing an initial CFO of up to 75 Hz. This corresponds to the maximum CFO necessary to recover after interference mitigation and thanks to system protocol considerations. One of the three demodulators is selected during the synchronization process thanks to a first CFO estimation. As CFO can shift during a frame reception and push the signal outside the bandwidth of the digital filters, a loop is used to compensate CFO drift thanks to a feedback on the digital mixer. CFO drift leveld of up to 20 Hz/s (maximum drift expected without a TXCO) can be supported. The loss due to CFO is below 1 Hz for initial CFO up to 50 Hz and CFO drift up to 20 Hz/s (Fig. 2).

DBPSK and GFSK modulation are supported with rates from 20 kb/s down to 100 b/s.

Algorithms to digitally estimate and compensate IQ imbalance are also included on the chip.

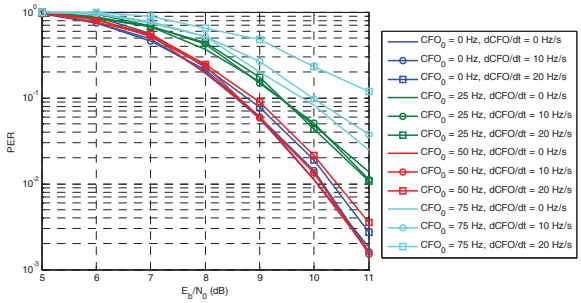

Figure 2: Packet Error Rate (PER) with CFO

Test on the chip have shown results concerning the digital part in total agreement with the expected performance from simulation.

The sensitivity of the circuit is equal to -136dBm in DBPSK at 100 b/s with a power consumption of 14.5 mW.

Perspectives

A part of the work here described has been considered for M2M communications via satellites. As the algorithms dedicated to CFO estimation and tracking are very light, they can also be embedded on a microcontroller in order to be exploited to support multiple radio standards.

RELATED PUBLICATIONS:
[1] D. Lachartre, F. Dehmas, C. Bernier, C. Fourtet, L. Ouvry, F. Lepin, E. Mercier, S. Hamard, L. Zirphile, S. Thuries, F. Chaix, "7.5 A TCXO-less 100Hz-minimum-bandwidth transceiver for ultra-narrow-band sub-GHz IoT cellular networks," 2017 IEEE International Solid-State Circuits Conference (ISSCC), San Francisco, CA, 2017, pp. 134-135.

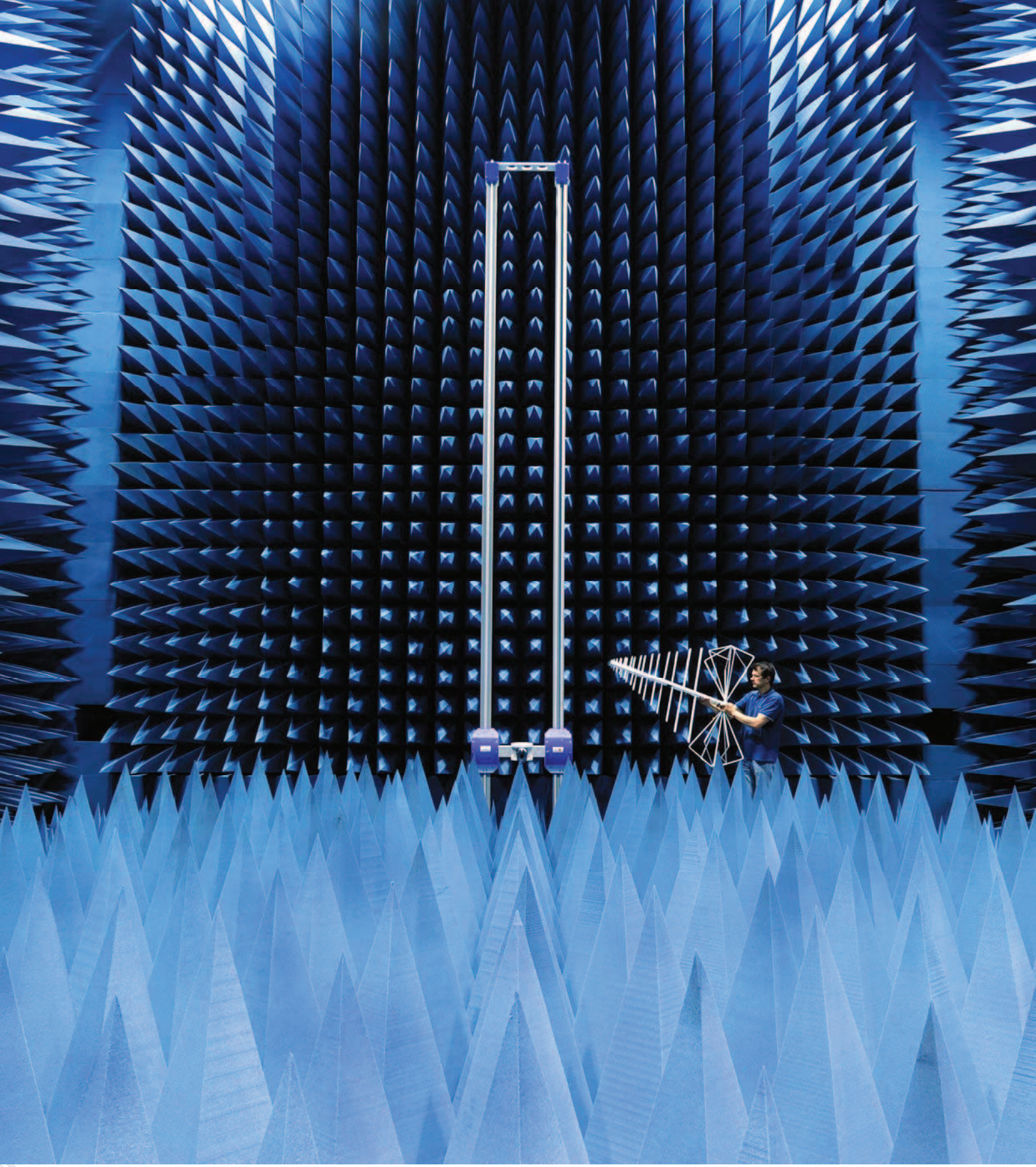

O3

ANTENNAS AND PROPAGATION

- **Antennas Design, Characterization and Experimentation**
- **Reconfigurable Transmit Array**
- **Low Profile Antennas**
- **Channel Modelling**
- **Environment Mapping**

DESIGN AND OPTIMIZATION OF A 2-BIT UNIT-CELL FOR ELECTRONICALLY RECONFIGURABLE TRANSMITARRAY ANTENNAS AT KA-BAND

RESEARCH TOPIC:

Transmitarray antennas, electronically reconfigurable antennas, beamforming, beam steering, 5G, SATCOM

AUTHORS:

F. Diaby, A. Clemente, L. Dussopt, R. Sauleau (IETR, UR1), K. Pham (IETR, UR1), and E. Fourn (IETR, INSA)

ABSTRACT:

This paper presents the design of a linearly-polarized electronically reconfigurable unit-cell for transmitarray antennas with a 2-bit phase resolution in Ka-band. The size of the proposed unit-cell is 5.1×5.1×1.3 mm^3. It is implemented on a dielectric stack-up composed of six metal layers, three dielectric substrates and two bonding films. The radiating elements are printed on both external metallic layers and are loaded by two PIN diodes controlling the transmission phase. This unit-cell is used to design a 196-element transmitarray with 784 PIN diodes. A maximum gain of 22.9 dBi and an aperture efficiency of 32.3% have been obtained at 29 GHz.

SCIENTIFIC COLLABORATIONS: IETR, University of Rennes 1 (UR1), INSA de Rennes 1

Context and Challenges

Transmitarray antennas have been proven to be a promising antenna architecture for a large number of millimeter-wave applications thanks to their high-gain, beam-scanning or beam-forming capability, and relative low-cost. These applications include satellite communications (SATCOM), point-to-point fronthaul/backhaul links, radars, and high data-rate 5th generation (5G) mobile networks. A transmitarray typically consists of a focal source illuminating a first antenna array working in receive mode, and connected (through phase-shifters) to a second array working in transmission mode. Beam-steering and beam-forming can be achieved using electronically reconfigurable unit-cells (which integrate switchable or tunable devices such as PIN diodes [1], microelectromechanical systems (MEMS), micro-fluidic systems or varactors) to control locally the transmission phase on the transmitarray aperture.

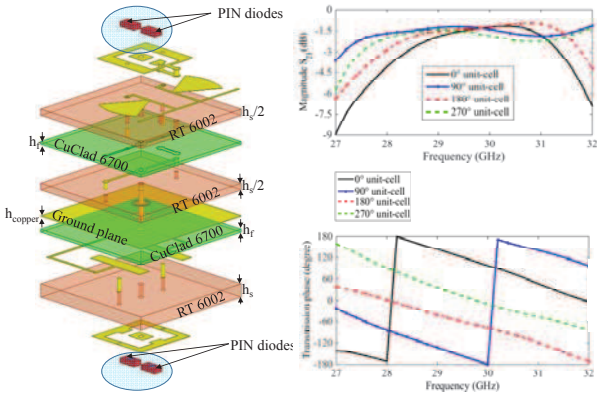

Figure 1: Schematic view of the linearly-polarized 2-bit unit-cell and simulated transmission coefficients (amplitude and phase) computed for each phase state

Main Results

The exploded view of the proposed linearly-polarized unit-cell is shown in Fig. 1. It is composed of six metal layers printed on three Rogers RT/Duroid 6002 substrates (ε_r = 2.94, tanδ = 0.0012) and bonded with two Arlon CuClad 6700 films. The unit-cell size is 5.1×5.1×1.3 mm^3 ($\lambda_0/2\times\lambda_0/2\times\lambda_0/8$ at 29 GHz, where λ_0 is the wavelength in free space at this frequency). The radiating elements consist of center-fed O-slot rectangular patch antennas working in receive (*Rx*) and transmitting (*Tx*) modes, respectively. These two patch antennas are connected by a 200-µm diameter metalized via hole located at their center and are separated by a ground plane. Two PIN diodes MA4GFCP907 are flip-chipped on each patch antenna to tune the transmission phase; they are controlled by two bias lines printed on the opposite side of each patch substrates. More details are presented in [2],[3]. This 2-bit unit-cell has been simulated for its four phase states using the commercial software Ansys HFSS with periodic boundary conditions on the unit-cell lateral faces and Floquet port excitations on both sides of the element. The magnitude and phase of the transmission coefficient (S_{21}) are plotted in Fig. 1. The minimum insertion loss at 29 GHz for the 0°, 90° 180°, and 270° unit-cells equals to 1.0, 1.2, 1.2, and 1.4 dB, respectively. A 14×14-element transmitarray has been simulated by using our *in-house* simulation tool (Fig. 2). These results have also been validated through full-wave simulations [2],[3].

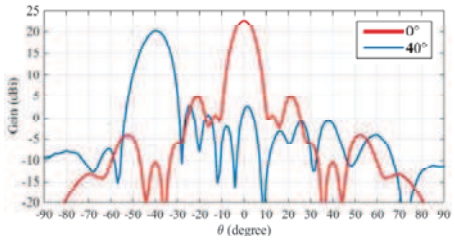

Figure 2: Simulated gain radiation patterns of the 14×14 elements transmitarray compute at the scan angle 0° and 40°

Perspectives

Both 2-bit unit-cell and the electronically reconfigurable transmitarray have been fabricated. The next step is the experimental characterization of the unit-cell in the waveguide simulator based setup and of the full antenna in anechoic chamber.

RELATED PUBLICATIONS:

[1] L. Di Palma, A. Clemente, L. Dussopt, R. Sauleau, P. Potier, and P. Pouliguen, "Circularly-polarized reconfigurable transmitarray in Ka-band with beam scanning and polarization switching capabilities," *IEEE Trans. Antennas Propag.*, vol. 65, no. 2, pp. 529-540, Feb. 2017.

[2] F. Diaby, A. Clemente, L. Di Palma, L. Dussopt, K. Pham, E. Fourn, and R. Sauleau, "Design of a 2-bit unit-cell for electronically reconfigurable transmitarrays at Ka-band," in Proc. *European Radar Conf. (EuRAP 2017)*, Nuremberg, Germany, 11-13 Oct. 2017.

[3] F. Diaby, A. Clemente, L. Di Palma, L. Dussopt, K. Pham, E. Fourn, and R. Sauleau, "Linearly-polarized electronically reconfigurable transmitarray antenna with 2-bit phase resolution in Ka-band," in Proc. *IEEE Topical Conf. Antennas Propag. In Wireless Communications* (*APWC 2017*), Verona, Italy, 11-15 Sep. 2017.

ANALYSIS AND DESIGN OF A FOUR-ELEMENT SUPERDIRECTIVE COMPACT DIPOLE ANTENNA ARRAY

RESEARCH TOPIC:
Directive antennas, superdirectivity, electrically small antennas, parasitic arrays, spherical wave expansion»

AUTHORS:
A. Clemente, C. Jouanlanne, and C. Delaveaud

ABSTRACT:
The design, optimization and experimental characterization of a four-element superdirective array based on a folded meandered dipole element is presented. The proposed array is composed of an active and three parasitic elements. The optimal impedance loads associated to each parasitic elements have been extracted using an *ad-hoc* synthesis method based on spherical wave expansion. To optimize the realized gain, a printed balun has been integrated on the active element. A maximum directivity of 10.0 dBi and a realized gain of 0.82 dBi have been demonstrated at 861 MHz with an element spacing equal to 0.15λ_0.

SCIENTIFIC COLLABORATIONS: None

Context and Challenges

Superdirective electrically small arrays are attractive antenna architectures for the development of emerging technologies in the field of the Internet of Things (IoT), wireless sensor networks, RFID, radiofrequency remote control, and WiFi networks. Harrington derived the expression of the maximum normal directivity ($N^2 + 2N$) of a generic antenna as a function of the maximum degree of spherical wave expansions N (where N depends on the radius of the minimum sphere circumscribing the antenna). Commonly, an antenna could be defined as superdirective if its directivity is higher than the directivity of the uniformly excited (in amplitude and phase) aperture with same physical size or the normal directivity defined by Harrington. In 1946, Uzkov theoretically demonstrated that by opportunely controlling the amplitude and phase of a linear array of P uniformly spaced isotropic radiators it is possible to obtain a maximum directivity in the end-fire direction equal to P^2, when the inter-element spacing tends to zero (e.g. a maximum directivity of 6.0, 9.5, and 12.0 dBi could be obtained in the case of a two-, three-, and four-element array, respectively). As a consequence, the maximum directivity has no theoretical limits. A first experimental demonstration of this theory has been presented in 2005 in the case of a two-element array. Recently, few practical demonstrations of two-, three- and four-element arrays [1] have been presented in the open literature.

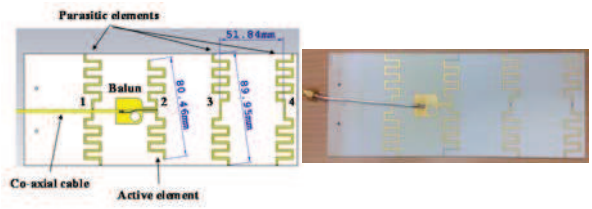

Figure1: Schematic view and photograph of the four-element superdirective array

Main Results

The realized four-element array, with an element spacing equal to 0.15λ_0, is composed of an active (element n. 2) and three parasitic (with identical size) folded meandered dipoles printed on a Rogers RO4003 dielectric substrate (thickness equal to 1.524 mm). A schematic view of the array and the photograph are shown in Fig. 1. A printed balun has been designed, optimized and connected to the active dipole in order to achieve a balanced excitation. The array has been simulated to extract the active element patterns and optimized using our *ad-hoc* synthesis procedure proposed in [1]. The realized prototype radiation performances have been measured in the CEA-Leti anechoic chamber. The measured maximum directivity and realized gain have been plotted as a function of the frequency in Fig. 2. The directivity is equal to 10.0 dBi at 861 MHz and a 1-dB directivity bandwidth in the range 856 – 865.5 MHz has been obtained. The maximum gain measured at 861 MHz is equal to 0.82 dBi. The obtained directivity performances are in good agreement with the simulated ones.

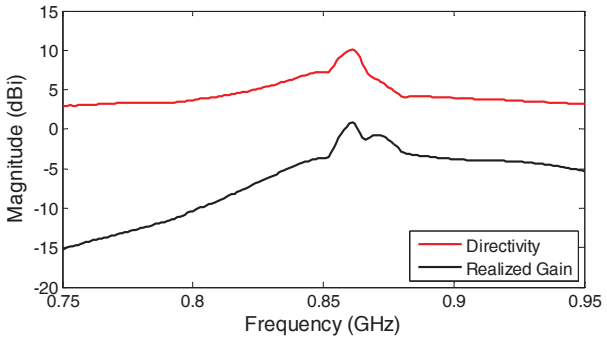

Figure 2: Measured directivity and realized gain of the fabricated four-element array as a function of the frequency

Perspectives

A four-element superdirective array based on parasitic antennas technology has been successfully demonstrated. Future works will explore the possibility to increase the antenna directivity by using Huygens source based elements [3] and the antenna efficiency.

RELATED PUBLICATIONS:
[1] A. Clemente, M. Pigeon, L. Rudant, and C. Delaveaud, "Design of a super directive four-element compact antenna array using spherical wave expansion," *IEEE Trans. Antennas Propag.*, vol. 63, no. 11, pp. 4715-4722, Nov. 2015.
[2] A. Clemente, C. Jouanlanne, and C. Delaveaud, "Analysis and design of a four-element superdirective compact dipole antenna array," in Proc. *European Conf.* Antennas *Propag.* (*EuCAP 2017*), Paris, France, 19-24 Mar. 2017.
[3] A. Debard, A. Clemente, C. Delaveaud, C. Djoma, P. Potier, and P. Pouliguen, "Superdirective Huygens source based end-fire arrays," in Proc. *European Conf.* Antennas *Propag.* (*EuCAP 2017*), Paris, France, 19-24 Mar. 2017.

ANALYSIS OF SUPERDIRECTIVE HUYGENS SOURCE BASED END-FIRE ARRAYS

RESEARCH TOPIC:
Superdirectivity, Huygens source, end-fire arrays, Spherical Wave Expansion, directivity optimization

AUTHORS:
A. Debard, A. Clemente, C. Delaveaud, C. Djoma (DGA), P. Potier (DGA), and P. Pouliguen (DGA),

ABSTRACT:
The directivity limit of end-fire arrays based on Huygens source elements has been numerically investigated. Firstly, the elementary infinitesimal Huygens source behavior is introduced and studied through Spherical Wave Expansion (SWE). Then, the maximum directivity of two-, three- and four-element arrays is calculated as a function of the inter-elements spacing. The optimization has been performed using a synthesis method based on SWE. For an inter-element spacing of a tenth of the wavelength, the obtained directivities are equal to 9.0 dBi, 11.7 dBi and 13.7 dBi for the two-, three and four-element arrays, respectively.

SCIENTIFIC COLLABORATIONS: CEA-LETI and Direction Générale de l'Armement (DGA)

Context and Challenges

An antenna can be defined as superdirective if its directivity is higher than the normal directivity limit defined as $N^2 + 2N$. In the equation N indicates the highest order of spherical waves radiated by the antenna, which can be considered to be proportional to the size of the radiator. Furthermore, it was observed in 2009 that the maximum directivity of a P-Huygens source (crossed electrical and magnetic dipole) array tends to $P^2 + 2P$ when the spacing tends to zero, but this results has not yet been analyzed or theoretically proven. More details are presented in [1],[2].]

Main Results

A physical interpretation based on SWE is proposed in this work. The synthesis method presented in [3] and used to calculate the optimal excitation coefficients α_p of a P element superdirective end-fire array is summarized in Fig. 1.

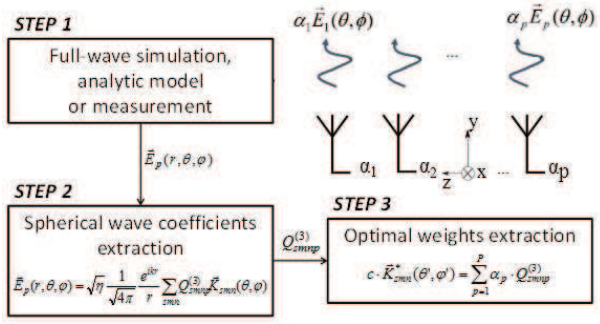

Figure 1: Block diagram of the array synthesis method based on SWE

The principle of this algorithm is based on the spherical modes coefficients $Q^{(3)}_{smn}$ (cf. STEP 2 and 3 of Fig. 1) that give the maximum directivity in a desired direction (θ, ϕ). These coefficients can be calculated by the first term of the equation of STEP 3 in Fig. 1. The α_p coefficients are thus calculated to make the spherical waves radiated by the whole array as close as possible to the ones that maximize directivity in the desired direction. This can be done by calculating the SWE of each individual element of the array (STEP 2 in Fig. 1). In this work, it is demonstrated that the use of Huygens sources is particularly favorable to this optimization. Indeed, the waves radiated by a Huygens source based arrays are naturally of the same kind as the ones that maximize directivity, only with different ponderations. It is then showed that, in the case of inter-element spacing that tends to zero, it is possible to find exact solutions to the arrays' excitation coefficients to match the optimal spherical wave distribution, for a maximum order of modes equal to the number of element in the array ($N = P$).

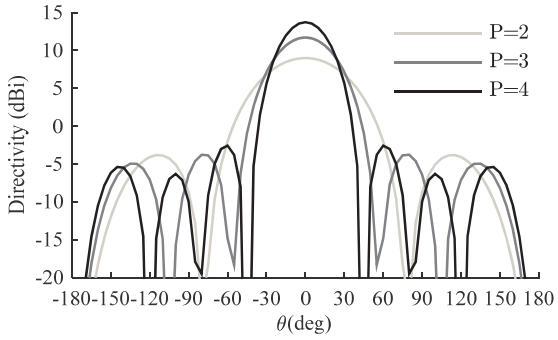

Figure 2: Directivity pattern computed on the E-plane for a P-element Huygens sources based array with an inter-element spacing 0. λ

The directivity pattern of Huygens sources based arrays are displayed in Fig. 2. It was computed using the previously mentioned algorithm and the analytical model of a Huygens source. These results are in agreement with the predicted limit of $10\,log10(P^2 + 2P)$, so 9 dBi, 11.7 dBi and 13.7 dBi, for two-, three- and four-element arrays, respectively.

Perspectives

The realization of Huygens source based arrays is the logical following of this work, which is a technical challenge. The fact that this kind of array can achieve better performance than electrical dipole based dipoles is still to be determined experimentally.

RELATED PUBLICATIONS:
[1] A. Debard, A. Clemente, C. Delaveaud, C. Djoma, P. Potier, and P. Pouliguen, "Analysis of superdirective Huygens source based end-fire arrays," in Proc. *European Conf. Antennas Propag. (EUCAP 2017)*, Paris, France, 19-24 Mar. 2017.
[2] A. Clemente, C. Delaveaud, and L. Rudant, "Analysis of electrical dipole linear array maximum directivity," in Proc. *European Conf. Antennas Propag. (EUCAP 2015)*, Lisbon, Portugal, 12-17 Apr. 2015.
[3] A. Clemente, M. Pigeon, L. Rudant, and C. Delaveaud, "Design of a super directive four-element compact antenna array using spherical wave expansion," *IEEE Trans. Antennas Propag.*, vol. 63, no. 11, pp. 4715-4722, Nov. 2015.

MAXIMIZATION OF MEASUREMENT SENSITIVITY AND READING RANGE OF PASSIVE RF SENSORS FROM COMPLEX IMPEDANCE OPTIMIZATION

RESEARCH TOPIC:

« Electrically small antennas, Radar Cross Section, Sensor, Reading range, Sensitivity »

AUTHORS:

V. Engelhardt, C. Jouvaud, F. Sarrazin, C. Delaveaud and H. Aubert

ABSTRACT:

This paper reports a method to improve the performances of passive Radiofrequency sensors in terms of reading range and measurement sensitivity. More specifically the impedance profile of the sensing device that maximizes the measurement sensitivity and reading range is derived. This profile allows predicting the largest achievable reading range and the highest measurement sensitivity that can be achieved by a given sensor antenna. The proposed original method is illustrated through the design of a wireless and passive temperature sensor. Experimental results are reported for validation purposes.

SCIENTIFIC COLLABORATIONS: CEA-Leti (University of Grenoble Alpes) and LAAS (University of Toulouse)

Context and Challenges

Chipless and passive Radiofrequency sensors present numerous advantages such as unlimited energy autonomy, long-term measurement stability and low cost of fabrication compare to more classical battery assisted sensors. The wireless interrogation of such sensors can be performed from the measurement of the antenna radar signature. An electromagnetic wave is transmitted by the radar reader to the sensor and the energy backscattered by the antenna sensor is function of the measurand, i.e., the physical or chemical quantity of interest. This technique allows the simultaneous wireless interrogation of many sensors, the real-time monitoring of each sensor and provides a simple sensor identification technique. However the well-known limitation of such sensors is the short reading range (typically of few tens meters) and the low measurement sensitivity with respect to the measurand. This work deals with a novel approach for maximizing both the reading range and the measurement sensitivity of passive Radiofrequency sensors.

Main Results

The passive RF sensor is typically composed of an antenna and a sensing device, that is, a load impedance which changes when the measurand varies. The electromagnetic field backscattered by the sensor's antenna can be decomposed into two scattering modes: the so-called structural mode A_s which does not depend on the sensing device impedance and the antenna mode which is related to the impedance mismatch at the antenna's input port.

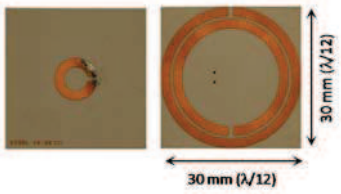

Figure 1: (a) top view of the miniature sensor antenna (b) bottom view showing Split Ring Resonator [1]

For maximizing the reading range by optimizing the sensing device impedance, the developed method requires the knowledge of the key parameter A_s. Several works have been reported on the derivation of this parameter for simple and more complex geometrical antenna shapes. A theoretical and graphic approach to determine A_s has been developed. Consequently, we can calculate the impedance Z_{min} that cancels the backscattering (possible with electrically small antennas) and the impedance Z_{max} that maximizes the RCS. Illustration of Radar Cross Section (RCS) improvement is shown in fig. 2 using the electrically small antenna of fig. 1.

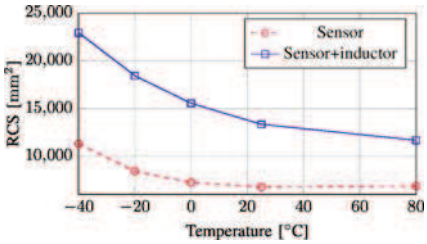

Figure 2: Illustration of sensor RCS improvement. Sensor impedance optimization with inductive part

To maximize the measurement sensitivity, an algorithm was developped to determine how the complex impedance of the sensing device must vary in response to a measurand variation.
The first stage consists of computing the RCS of the antenna loaded by the impedance $Z_0 = Z_{max}$. In the second stage, the impedance Z_0 is replaced by a slightly lower complex impedance (modulus) whose phase is determined by maximization of RCS difference. The process is repeated until RCS becomes minimal ($Z_0 = Z_{min}$). This technique provide an optimal complex impedance for the sensor for maximizing the measurement sensitivity. Applying the described approach to design a miniature temperature sensor antenna operating at 868 MHz (fig. 1), a reading range of 34 m was experimentally obtained in wireless interrogating condition of classical RFID reader

Perspectives

This developed method allows to select the optimal sensing device for a given sensor's antenna. Application to the design of a temperature sensor was reported. Simulations confirm the theory and shows the improvement of the reading range and the sensitivity at high RCS made thanks to the presented algorithm.

RELATED PUBLICATIONS:

[1] V. Engelhardt, C. Jouvaud, F. Sarrazin, C. Delaveaud, H., "Optimisation d'une antenne miniature pour des applications de capteurs sans fil," Journées Nationales Microondes, May 2017, Saint-Malo, France.

[2] V. Engelhardt, C. Jouvaud, F. Sarrazin, C. Delaveaud, H. Aubert, "Maximization of measurement sensitivity and reading range of passive RF sensors from complex impedance optimization" , 2017 IEEE SENSORS, Oct 2017, Glasgow, United Kingdom

PERSONAL EXPOSIMETER TO MONITOR EMF-UPLINK EXPOSURE FROM DAILY USAGE OF MOBILE PHONE

RESEARCH TOPIC:

Radio Frequency (RF) Electro Magnetic Field (EMF) exposure, EM dosimetry, smartphone usage

AUTHORS:

S.Bories, D. Dassonville, S. Brulais, S. Aloui.

ABSTRACT:

Cellular network development and pervasive smartphone usage have brought increased interest in the study of the long-term evolutions of users' EMF exposure. The Up-Link (UL) signal (the signal transmitting from the smartphone to the network base station) is measured by an add-on module on the user's smartphone. This allows the equipment of a sample of users with a non-invasive device, to measure their RF exposure during the real utilization of their smartphone.

SCIENTIFIC COLLABORATIONS: Telecom ParisTech

Context and Challenges

The Up-Link (UL) signal has been identified as the main contributor of mobile phone electromagnetic exposure. For a mobile phone, the specific absorption rate (SAR) is a parameter that measures the RF field absorbed by the human tissues. Manufacturers of smartphones give a value of SAR for a specific case, where the device is used at its maximum allowed RF output power. However the actual value is lower than the normative SAR, and presents a very high variability (frequency, age, propagation conditions, and cellular network instant configuration) which needs to be evaluated by epidemiologists.

As competing solutions (personal dosimeter) don't assess properly the exposure from 'worn' RF source, CEA Leti specifies and develops an add-on module in order to measure the actual SAR of the user during the utilization of his own equipment. To this aim, two questions must be answered: what is the UL RF power transmitted by the smartphone, and what is the position of the smartphone relative to the user, Figure 1.

Main Results

The relative position and orientation of the smartphone are measured by using small beacons (UWB impulse radio) attached to the user's clothes: belt, chest. By measuring the distances between the smartphone and the beacons, it is possible to extract a proxy of the distance from the smartphone to the user's body, and so the actual usage.

The actual UL transmit power is measured by an RF probe that is fitted in an add-on module on the smartphone, Figure 2. The RF probe is able to measure the RF power in pre-defined cellular bands, independently of the radio-access-technology (RAT). It can handle 2G, 3G, and 4G European frequency bands.

The data for the UL power and the distances are instantaneously measured and collected in a memory. At the end of a recording period, the data is post-processed to derive the SAR offline based on numerical power-normalized SAR simulations.

The profile of UL power can be monitored for hours. Each 0.1 second, the maximum, mean and standard deviation are saved. In Figure 2, for a given 'at home' scenario, a 30 dB variation of the mean UL power is observed regarding the usages, the quality of the radio link, and the cell occupation. These analyses allow to identify the Network key parameters (e.g. 4G or small cell deployments), that govern the user exposure.

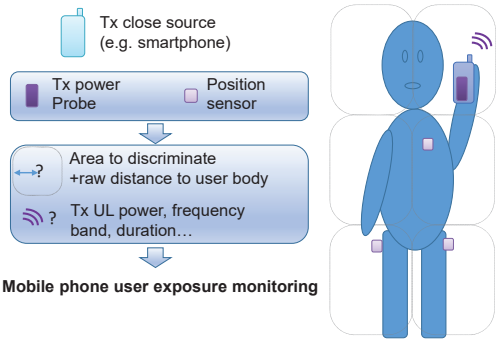

Figure 1: Concept for assessing the daily EM exposure

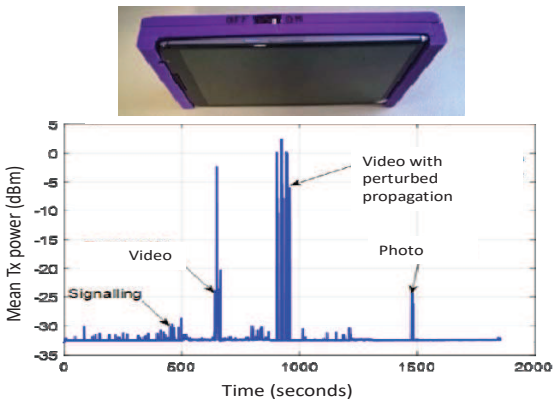

Figure 2: Prototype of the exposimeter placed on the user mobile. Evolution of measured UL power over half an hour for different usages in the 2600 MHz (LTE band)

Perspectives

The second generation of this personal exposimeter has been selected to contribute to a WHO (World Health Organization) epidemiologic campaign in France to monitor public exposure.

RELATED PUBLICATIONS:

[1] S. Bories, J. Wiart, "L'estimation du DAS voie montante : le projet DEVIN", in Anses – Les Cahiers de la Recherche N° 9 - Santé, Environnement, Travail – mai 2017.

SUPER-DIRECTIVE, EFFICIENT, ELECTRICALLY SMALL, LOW-PROFILE ANTENNA BASED ON COMPACT METAMATERIAL

RESEARCH TOPIC:

Low profile, antenna, metasurface, metamaterial, artificial magnetic conductor, electrically small antenna, Super-directivity

AUTHORS:

N. Kristou, J-F. Pintos, K. Mahdjoubi (Institut d'Electronique et de Télécommunications de Rennes)

ABSTRACT:

In this contribution, the behaviour of a modified dipole antenna placed over compact Artificial Magnetic Conductors (AMC) is studied. Simulation and measurement results demonstrate that the Egyptian axe Near-Field-Resonant-Parasitic (NFRP) antenna is miniature (ka_1=0.498) with a low-profile (total height =0.07λ_0) when placed over compact AMC (ka_2=1.29), where λ_0 denotes the free space wavelength at 0.9GHz. It achieves super-directivity (6.5 dBi), high realized gain (5.7 dBi) and high radiation efficiency (83.7%). Both the dipole antenna and the AMC surface are fabricated and measured to demonstrate the potential of this structure.

SCIENTIFIC COLLABORATIONS: Institut d'Electronique et de Télécommunications de Rennes

Context and Challenges

Artificial Magnetic Conductors (AMC) constitutes an attractive reflector for low profile antennas which can take advantage of intrinsic zero reflection phase response to reduce antenna height without the need for thick quarter wave backplane. Main drawback of such structure remains the size of the unit cell which is close to quarter-wavelength in free space. A significant amount of research has been made recently on unit cell miniaturization and several works have been widely proposed in the literature with various miniaturization techniques [1].

In this contribution, a miniature modified NFRP dipole is placed over a compact AMC based on high miniaturized unit cell [2] to demonstrate the potential of the proposed approach.

Main Results

The proposed modified NFRP antenna consists on a driven element printed on the bottom-side of the substrate and a near field resonant parasitic element printed on the top-side. Two lumped capacitors are introduced on both antenna sides to adjust the impedance value once the antenna is placed over the metasurface. The proposed modified NFRP antenna shown in Figure 1 is based on the Rogers Duroid 3003 (ε_r = 3, tan δ =0.0013) substrate with a thickness of 0.75 mm. The dimensions of the NFRP element are specified in [3].

By simulation, at frequency of interest f_0, high peak directivity (6.5 dBi) and peak realized gain (5.7 dBi) more than double the peak realized gain of the NFRP alone (1.9 dBi without AMC) are achieved. The simulated radiation and total efficiencies are 83.7% and 83.5%, respectively. A very good correlation can be observed between simulation and measurement in figure 2(a) on the maximum realized gain.

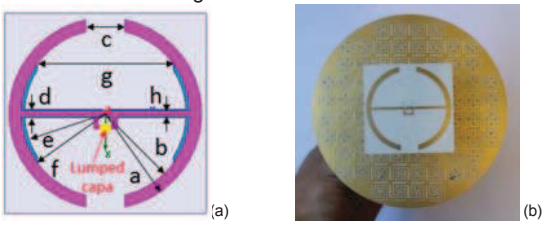

(a) (b)

Figure 1: NFRP dipole antenna alone (a) and over AMC (b)

The proposed system exceeds the Harrington directivity limit shown in [3] and can be considered as a super-directive antenna. The NFRP antenna, with a ka_1 = 0.498, is placed 15 mm (λ_0/20) above the AMC structure as shown in Figure 1(b). The AMC structure has a full diameter equal to 128 mm (λ_0/1.6), which is corresponding to ka_2 = 1.29 at the resonance frequency f_0 = 960 MHz.

The proposed dipole antenna over the AMC structure is simulated, fabricated and measured, as shown in Figure 2(b), in CEA LETI's anechoic chamber. Differential feeding has been used to avoid current flowing back on the cable shield. Experimental results show that, with maintaining low profile and compact size, the antenna system achieves a maximum realized gain measured of 5 dBi in broadside direction. Good agreement are observed between the measured and simulated results.

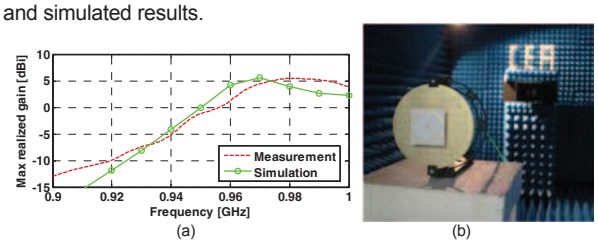

(a) (b)

Figure 2: (a) Measured and Simulated realized gain of the proposed antenna, (b) radiation measurement setup

Perspectives

A super-directive (6.5 dBi), efficient (η_{rad} = 83.7%), electrically small (ka_1 = 0.498), low-profile (total height = 0.07 λ_0) NFRP antenna based on compact Artificial Magnetic Conductor metamaterial (ka_2 = 1.29) have been designed, simulated and measured. Excellent correlation has been observed between simulation and measurement. The final target is to achieve high performances around 700 MHz ($ka_{2\ target}$ = 0.94, size reduction of 27%) with the same device, by using tunability feature.

RELATED PUBLICATIONS:

[1] N. Kristou, J-F. Pintos, K. Mahdjoubi, "Low Profile Dipole Antenna Over Compact AMC Surface," 2017 International Workshop on Antenna Technology (iWAT), Athens, Greece

[2] N. Kristou, J-F. Pintos, K.Mahdjoubi, "Miniaturized Tunable Artificial Magnetic Conductor for Low LTE Band," 2017 IEEE International Symposium on Antennas and Propagation (APSURSI), San Diego, California, USA, 2017

[3] N. Kristou, J-F. Pintos, K.Mahdjoubi, "Super-Directive, Efficient, Electrically Small, Low-Profile Antenna based on Compact Metamaterial," 2017 IEEE International Symposium on Antennas and Propagation (APSURSI), San Diego, California, USA, 2017

PLANAR DISCRETE LENS ANTENNA INTEGRATED ON DIELECTRIC SUBSTRATE FOR MILLIMETER-WAVE TRANSCEIVER MODULE

RESEARCH TOPIC:
Integrated antennas, high gain antennas, millimeter-wave antennas, discrete lenses, transmitarray.

AUTHORS:
K. Medrar, L. Marnat, L. Dussopt

ABSTRACT:
A novel topology suitable for highly integrated and high-gain millimeter-wave antenna is considered. The antenna can be fabricated as a single, robust and compact module using standard low-cost PCB technologies. It is compatible with IC integration such as a transceiver circuit for fully integrated millimeter-wave front-end modules. A compact V-band antenna (32×32×13.2 mm^3) has been designed and fabricated. Promising performances in terms of gain (20.4 dBi), aperture efficiency (26%) and fractional 3-dB gain bandwidth (18%) are obtained experimentally and are aligned with the theoretical results obtained with an *in-house* design tool.

SCIENTIFIC COLLABORATIONS: None

Context and Challenges

The massive expansion of wireless applications and the progress of integrated radio technologies have triggered a strong interest for millimeter-wave frequencies. The large available bandwidths in these frequency bands allow the emergence of high-data rate short- and long-range wireless communications for e.g. wireless networks, high-definition video transmission or point-to-point communications. Discrete lenses have been proven to be attractive at millimeter-wave frequencies by demonstrating good performance [1, 2]. However, classical architecture featured an important drawback as the discrete lens and the transceiver module (with integrated focal source) come as two separate parts which requires a specific assembly and a precise alignment. With the proposed architecture, the complete module can be manufactured as a single component using standard planar technologies. It is composed of a planar discrete lens laid on top of a core dielectric, while the planar focal source is assembled on the bottom side (Figure 1.). It inherently offers good alignment, mechanical robustness and compactness particularly relevant at millimeter-wave frequencies beyond 60 GHz.

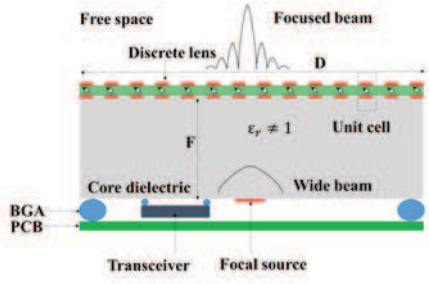

Figure1: Schematic view of a millimeter-wave module with a transceiver chip and a discrete lens antenna fully integrated on low cost organic technology

Main Results

A 60 GHz prototype has been designed with a 3-bit phase quantization using linearly-polarized via-less unit cells and a thick plastic material is used as core dielectric as shown on Figure 2 [3].

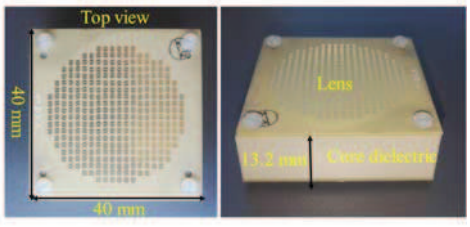

Figure 2: Fabricated prototype operating in V-band

As most plastic are not available at millimeter-wave frequencies, five samples have been characterized in V band. The PEEK material has been selected because it has low dielectric losses (tanδ<0.002) and a relative permittivity of 3. The presence of the core dielectric has an impact on the unit cell design. The cell size must be smaller than the typical 0.5-0.7λ_0 (free-space wavelength) and is set to 0.32λ_0. Our *in-house* design tool has shown that the core substrate does not significantly degrade the radiation performance (0.15 dB loss) but helps improving compactness (0.4 focal ratio). Experimental results are compared with predicted results in Figure 3.

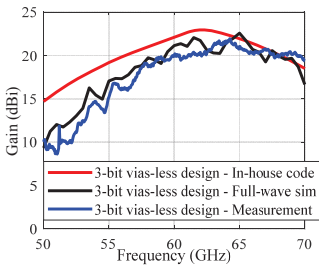

Figure 3: Measured and simulated gain versus frequency

Perspectives

The proposed antenna topology has been validated in V-band with good experimental results. The next step is to show the full potential of this structure at higher frequencies such as 140 and 300 GHz where emergent applications are rising.

RELATED PUBLICATIONS:
[1] H. Kaouach, L. Dussopt, J. Lantéri, T. Koleck, and R. Sauleau, "Wideband Low-Loss Linear and Circular Polarization Transmit-Arrays in V-Band," IEEE Trans. Antennas Propag., vol. 59, no. 7, pp. 2513–2523, Jul. 2011.
[2] L. Dussopt, A. Moknache, J. Säily, A. Lamminen, M. Kaunisto, J. Aurinsalo, T. Bateman, and J. Francey., "A V-Band Switched-Beam Linearly Polarized Transmit-Array Antenna for Wireless Backhaul Applications," IEEE Transactions on Antennas and Propagation, vol. 65, no. 12, pp. 6788–6793, Dec. 2017.
[3] K. Medrar, L. Marnat, and L. Dussopt, "Planar discrete lens antenna integrated on dielectric substrate for millimeter-wave transceiver module," International Journal of Microwave and Wireless Technologies, pp. 1–14, Dec. 2017.

SUPER DIRECTIVE TWO-DIPOLE ARRAY WITH NON-FOSTER ELEMENTS

RESEARCH TOPIC:
Small antennas, directive antennas array, superdirectivity, Non-Foster, Negative Impedance Converters

AUTHORS:
L. Batel, L. Rudant, J-F. Pintos, K. Mahdjoubi

ABSTRACT:
Performances of passive Electrically Small Antennas (ESA) are limited by fundamental physic law. Using active elements into antenna structures appears like an opportunity to overshoot those limits. Non-Foster elements are classically used in matching networks for ESA in order to enlarge their impedance matching bandwidth. In this work, Non-Foster elements are proposed as innovative method to achieve a broadband high directive and compact antenna. The analysis is computed considering a two-dipole compact parasitic array loaded with Non-Foster elements in UHF frequency band near 1.2 GHz.

SCIENTIFIC COLLABORATIONS: CEA-Leti (University of Grenoble Alpes) and IETR (University of Rennes 1)

Context and Challenges

Directive antennas, used to focus the radiation in useful directions, offer new perspectives for wireless applications. Nevertheless, usual techniques to enhance antennas' directivity lead to larger antennas and their integration into small objects would be difficult. Radiation control through directive antennas is being an important issue for the future communications. This kind of antennas allows reducing electromagnetic pollutions which limit wireless systems and communicant objects cohabitation. Recent state of the art has shown new perspectives to establish small antennas with super directive radiation using parasitic antenna arrays. A super directive antenna is a small antenna that exceeds its natural low directivity. Moreover, these last few years, researches on active antennas and associated results could be considered for modern approach to deal with small and directive antennas' issues.

Main Results

This work evaluates the enhancement perspectives brought by the active electronic circuits to solve the small and directive antennas' issues [1]. Typically, special active circuits known as Negative Impedance Converters (NIC) have been designed to achieve reactive Non-Foster behavior. Those sensitive and potentially unstable circuits [2] have been experimentally evaluated to materialize the small and super directive antennas perspectives.

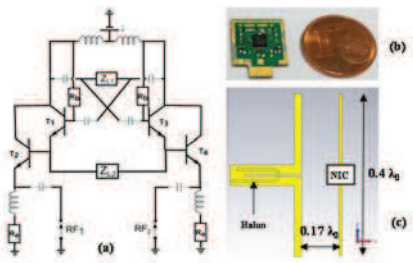

Figure 1: (a) NIC's electrical view (b) NIC's realization (c) Antenna design loaded with NIC device

Figure 2 compares the radiation pattern of two super directive antennas in UHF band between 1 GHz and 1.4 GHz. The passive antenna establishes its maximum directivity in the optimized direction ($\theta = 90°$) at 1 GHz and naturally changes its radiation direction from 1.2 GHz and above. In contrast, the active antenna loaded with Non-Foster elements achieve a directivity higher than 5 dBi in the direction of optimization between 1 GHz to 1.3 GHz. This work has demonstrated for the first time the possibility to establish a super directive radiation pattern within a large frequency bandwidth using a small antenna associated to Non-Foster elements [3]. These innovative and interesting results have received the best paper award of the French JNM conference in 2017.

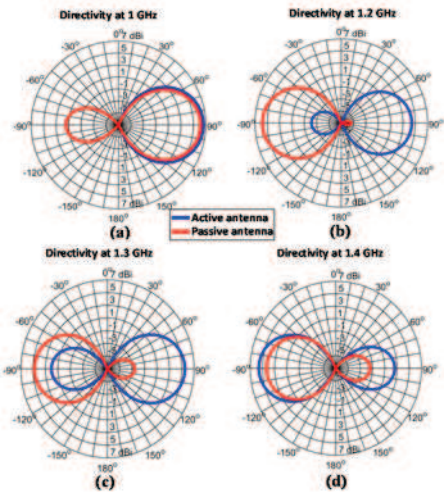

Figure 2: Optimized directivity of active and passive antenna between 1 GHz and 1.4 GHz

Perspectives

This technology opens new compact antenna design opportunities for RFID, IoT, spatial filtering and radars systems.

RELATED PUBLICATIONS:

[1] L. Batel, L. Rudant, J.F. Pintos, K. Mahdjoubi, "High directive compact antenna with non-foster elements," 2015 International Workshop on Antenna Technology (iWAT), 2015, pp. 381-384.

[2] L. Batel , L. Rudant, J.F. Pintos, K. Mahdjoubi, "Sensitivity of negative impedance converter circuit with respect to PCB design effects," 2015 International Workshop on Antenna Technology (iWAT), 2015, pp. 221-224.

[3] L. Batel, L. Rudant, J.F. Pintos, K. Mahdjoubi, "*Réseau d'antennes compact, super directif et large-bande associé aux éléments Non-Foster", 20e Journées Nationales des Microondes ,2017.*

FREQUENCY DEPENDENCE OF 5G MILLIMETER-WAVE CHANNEL CHARACTERISTICS

RESEARCH TOPIC:
Millimeter-wave, channel model, 5G

AUTHORS:
A. Bamba, F. Mani, R. D'Errico

ABSTRACT:
This paper presents wideband channel measurements in indoor environment in different millimeter wave frequency bands for 5G application. Measurements were performed with a VNA and the mechanical steering of directive antennas at both the transmitter and receiver side, allowing a double-directional angular characterization. A comparison of propagation characteristics such as the path loss, multipaths clusters' dispersion properties in the delay and angular domains are provided
.

SCIENTIFIC COLLABORATIONS:

Context and Challenges

The overwhelming demand of resources for broadband communications is motivating the use of millimeter-wave (mmwave) for the next generation of 5G wireless system. The ITU identified a number of mmwave bands to be investigated for a worldwide harmonization of spectrum use. In this context the H2020 mmMagic project has recently provided a new mmwave channel model covering a number of 5G relevant use cases.

Main Results

Measurement campaigns with directive antennas have been conducted in an office and conference room environment at 59-65 GHz and 80.5-86.5 GHz for line-of-sight scenarios. From directive measurements, omnidirectional power delay profiles have been derived. This post-processing was performed to analyze the channel characteristics independently on the antennas used.

A geometric stochastic channel model has been proposed and the related parameters have been determined based on measurement results. Large scale parameters such as the path loss, the delay spread and angular spread have been evaluated. Path loss exponent values range from 1.33 to 1.44 in the investigated bands and environments.

The results show that the delay spread is higher in the V-band than in the E-band. Generally we evidenced a slight decrease of the delay spread as a function of increasing frequency in the investigated indoor environments, although the degree of dependence will depend on the building construction materials and types of furniture inside the rooms (Figure1).

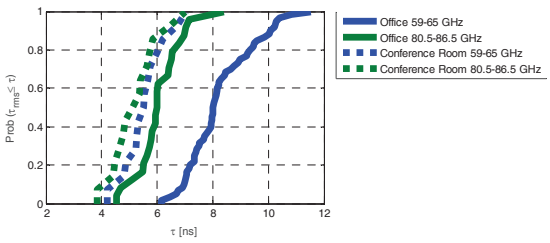

Figure 1: Cumulative distribution function of the rms delay spread

The multipath angle of arrival dispersion analysis reveals that the diffusive nature of multipath at the receiver is more prominent in the lower band and smaller environment. However the frequency dependence was negligible, at least for the investigated bands. It is generally observed that clusters decay faster at higher frequencies which is ascribed to higher path losses. Also, it turns out that clusters decay in time faster than the intra-cluster sub-paths.

Figure 2 shows a representation of multipath components in the space (angle and distance) for a given snapshot. The colors represent the amplitude and the black marker indicates the common paths. Our investigations illustrate that propagation characteristics are similar in the V and E band. The results reveal that frequency-independent common paths can be identified. Theses paths are mainly related with the geometry of the environment, and are scaled with the wavelength. Additional frequency-dependent paths, which are due to frequency-selective phenomena, generally yields a small energy contribution within the power delay profile.

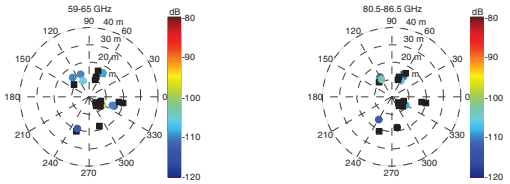

(a) (b)

Figure 2: Example of common multipath at a position in the office room

Perspectives

This work has been included as a part of mmMagic channel model and assessment of frequency dependence of propagation characteristics. This model can be exploited for mmwave beamforming evaluation in 5G communications. Extension of this model to higher frequency, e.g. D-band, as well as the inclusion of elevation angle characteristics are ongoing.

RELATED PUBLICATIONS:

[1] A. Bamba, F. Mani and R. D'Errico, "A comparison of indoor channel properties in V and E bands," 2017 11th European Conference on Antennas and Propagation (EUCAP), Paris, 2017, pp. 3361-3365.
[2] S. L. H. Nguyen, J. Medbo, M. Peter, A. Karttunen, A. Bamba, R. D'Errico, N. Iqbal, C. Diakhate, and J.-M. Conrat, "On the Frequency Dependency of Radio Channel's Delay Spread: Analyses and Findings from mmMAGIC Multi-frequency Channel Sounding" to be presented at EuCAP 2018..

A MILLIMETER-WAVE INDOOR BACKSCATTERING CHANNEL MODEL FOR ENVIRONMENT MAPPING

RESEARCH TOPIC:
Millimeter-wave, channel model, backscattering

AUTHORS:
F. Guidi, A. Guerra (UniBO), D. Dardari (UniBO), A. Clemente, R. D'Errico

ABSTRACT:
In this communication we introduce a channel model for personal radar applications where a millimeter-wave (mm-wave) massive array is required to scan the environment and to reconstruct a map of it. The analysis is based on a measurement campaign, in a corridor and an office room, performed by using mm-waves massive arrays. A two-dimensional technique to extrapolate the multipath components has been proposed and map-oriented channel model has been proposed.

SCIENTIFIC COLLABORATIONS: University of Bologna (UniBO), Italy

Context and Challenges

The joint adoption of massive arrays and mm-wave technology could pave the way for next 5G communications scenarios, especially for those which rely on the integration of a large number of antennas onto mobile devices. In this context, the concept of personal radars has been recently proposed enabling simultaneous localization and mapping (SLAM) features and exploiting the compactness and the beamforming potentialities of mm-wave massive arrays. The performance of the personal radar system depends on the ability of collecting the environmental backscattered response at the radar interrogation signal and, secondly, on the exploitation of such measurements as an input for the mapping algorithm. As a consequence, the characterization of the indoor mm-wave backscattering channel becomes essential to be able to statistically describe the channel properties for mapping applications.

Main Results

Based on mm-wave backscattering channel measurement campaigns using high-directive massive arrays for personal radar applications. Measurements took place in indoor environments, i.e., an office room and a corridor. Based on data collected from different radar positions and steering directions, a multi path components selection mechanism and a clustering algorithm have been proposed [1]. This method discriminate multipath components in joint angular and temporal domain by exploiting the a-priori knowledge of the antennas characteristics into an ad-hoc algorithm for wideband backscattering channels. This allows to reduce undesired effects given by antennas side lobe and solve ambiguity due to the symmetric. An example of multipath and cluster extraction in office environment in two different positions (namely p_1 and p_2) is shown in Figure 1.

The obtained data were used to develop a stochastic channel model of mm-wave backscattering. In this model the multipath are grouped into clusters which are identified in both delay and angular domain. Results have shown that a Laplacian distribution can be used to describe the intra-cluster angle of arrival while an exponential distribution better fits for the intra-cluster time of arrival. Differently from classical one-way channel models presented in the literature, a model related to the environment geometry has been introduced for mapping purposes. For this reason the inter-cluster arrival rate along the environment perimeter and the temporal distance from it have been investigated from a statistical point-of-view. An example of statistics for office environment is shown in Figure 2.

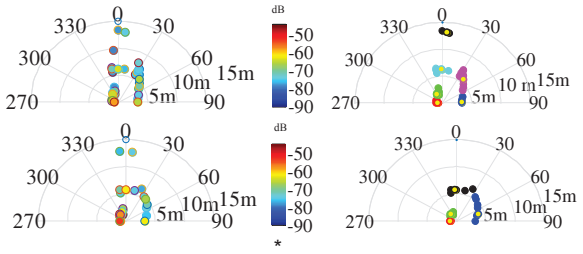

Figure 1: Identified multi path components (left) and cluster (right) for corridor when the radar is in p1 (top) and p2 (bottom)

Thanks to the given channel characterization, we enable the possibility to statistically reproduce the clusters and paths distribution once the environment geometric characteristics are given, as it is required for environment mapping applications [2].

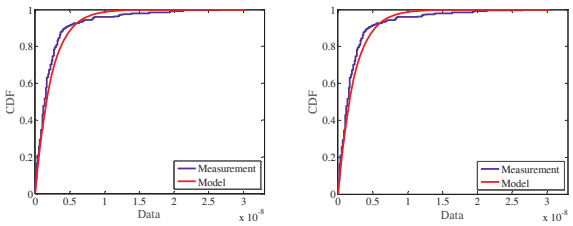

(a) (b)

Figure 2: CDF of intra-cluster ToA (a) and inter-cluster TOA along the environment perimeter

Perspectives

The proposed backscattering channel model is being used for design of mm-wave radar for indoor SLAM applications.

RELATED PUBLICATIONS:
[1] F. Guidi, A. Clemente and R. D'Errico, "Multipath estimation technique for wideband mm-wave backscattering channels," 2017 11th European Conference on Antennas and Propagation (EUCAP), Paris, 2017, pp. 2540-2544
[2] A. Guerra, F. Guidi, D. Dardari, A. Clemente and R. D'Errico, "A Millimeter-Wave Indoor Backscattering Channel Model for Environment Mapping," in IEEE Transactions on Antennas and Propagation, vol. 65, no. 9, pp. 4935-4940, Sept. 2017..

TIME CORRELATION AND DOPPLER MODELING FOR MOBILE-TO-MOBILE FADING CHANNELS

RESEARCH TOPIC:
Channel modeling, mobile-to-mobile communications

AUTHORS:
G. Makhoul, F. Mani, R. D'Errico, C.Oesteges (UCL)

ABSTRACT:
This paper analyzes time correlation and Doppler spectra of mobile-to-mobile (M2M) channels, based on a measurement campaign carried out in an indoor environment. The Doppler spectrum is characterized in line-of-sight (LOS) and non-line-of-sight (NLOS) environments for different types of pedestrian movements. Subsequently, analytical models for correlation and Doppler spectrum are proposed and successfully compared to the measurement data.

SCIENTIFIC COLLABORATIONS: Université catholique de Louvain, Louvain-la-Neuve, Belgium (UCL)

Context and Challenges

Mobile-to-mobile (M2M) communications occur when both transmitter and receiver are moving in the environment. It can take place between moving subjects carrying wireless nodes, as a part of Device-to-Device (D2D) communications eventually exploiting_cooperative approaches to increase coverage and for secure short-range communications with low power consumption. The simulation and performance evaluation of such communication systems and their future enhancements require a deep understanding of propagation channels. In addition, since the mobility of terminals and scatterers surrounding the terminals causes the time variations of the channel, it is important to model the time correlation and Doppler properties.

Main Results

A narrow-band measurement campaign was performed in order to model the time-varying M2M channels. A general time correlation function for M2M fading channels in the presence of moving scatterers was developed in [1]. Analytical time correlation functions for the short-term fading were developed for different types of mobility patterns starting from this general model, considering a uniform distribution of non-isotropic scattering patterns. The isotropic scattering pattern case was derived as a special case.

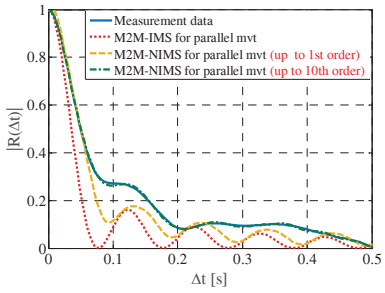

Figure 1: Time correlation function of measurement data vs. analytical formulas for parallel movements (mvt). (IMS: isotropic moving scatterers, NIMS: non-isotropic moving scatterer)

It was shown that the non-isotropic scattering pattern assumption tends to depict the measured correlation function in a more realistic manner while the isotropic scatterers' model can roughly describe it up to the 90% coherence time (Figure 1).

A closed analytical model was also developed in [2] to reproduce the Doppler properties of different indoor M2M scenarios including LOS and NLOS conditions. This model includes the effects of moving scatterers and receiver with respect to transmitter. In fact, taking the transmitter as the observational frame reference, M2M channels can be seen as fixed to mobile channels with moving scatterers. Therefore, the first term in the proposed model is Jakes-like spectrum and it is employed to depict the effects due to the mobility of receiver with respect to transmitter. A second term model accounts for the impact of non-uniform moving scatterers. Finally, a Gauss Doppler spectrum, the third term of the model, is used to include the properties of diffuse scatterers. Figure 2 show an excellent agreement of Doppler spectrum for short-term fading obtained in opposite walking scenario under the LOS condition between the measurement data and the data generated with the proposed method.

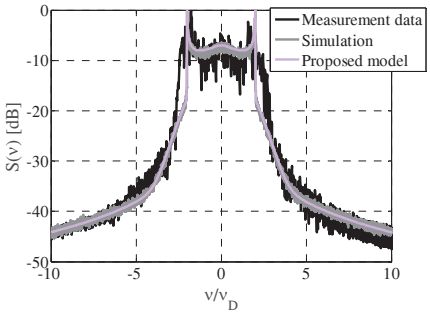

Figure 2: Analytical and measured Doppler spectra versus simulation for opposite movement in LOS condition

Perspectives

Application of the proposed models to other scenarios (including vehicular applications) are now under investigation.

RELATED PUBLICATIONS:
[1] G. Makhoul, F. Mani, R. D'Errico and C. Oestges, "On the Modeling of Time Correlation Functions for Mobile-to-Mobile Fading Channels in Indoor Environments," in IEEE Antennas and Wireless Propagation Letters, vol. 16, no. , pp. 549-552, 2017. doi: 10.1109/LAWP.2017.2682959
[2] G. Makhoul, F. Mani, R. D'Errico and C. Oestges, "Doppler characteristics for indoor mobile-to-mobile channels," 2017 11th European Conference on Antennas and Propagation (EUCAP), Paris, 2017, pp. 2468-2472.

A 3-D WIDE-BAND SET-UP FOR OVER-THE-AIR TEST IN ANECHOIC CHAMBER

RESEARCH TOPIC:
Over-the-Air (OTA) test, radiofrequency channel

AUTHORS:
M. Belhabib, R. D'Errico, B. Uguen (IETR, UR1)

ABSTRACT:
This work introduces a new experimental 3D wide-band measurement bench for Over-the-Air (OTA) tests. The setup is composed of twelve double-polarized antennas, placed around the Zone Under Test (ZUT), on three different elevation planes.

SCIENTIFIC COLLABORATIONS: IETR, University of Rennes 1 (UR1)

Context and Challenges

Multi-probe setup in anechoic chamber, combined with fading emulator, are nowadays considered as an attractive solution for Over-The-Air (OTA) test of mobile communication devices. The multi-probes test methodology employs a number of spatially separated antennas placed in anechoic chamber and combined with a fading emulator, in order to reproduce the channel characteristics in a controlled and repeatable manner. The probes are fed by signals, which are jointly optimized in order to generate a superposed field impinging on the Device Under Test (DUT), as in the real radio environment. Most of contributions in literature focuses on two-dimensional setup by considering a single OTA ring of antennas. However in the real life the radio channel is not limited to one plane and multipath could come at different elevation angles. In this work we present a novel 3D hemispheric OTA test-bed that can be used in a wide span of applications from 2 to 6 GHz.

Main Results

Different 3D probe configurations have been investigated to emulate MIMO channel models. A comparison between different setups as a function of the scenario and angular spreads was presented in [1]. Pre-faded signal techniques for 3D OTA test was used in order to increase the spatial correlation accuracy. It was shown that, when the DUT's antennas are along the z-axis, a cylindrical configuration of probes could be advantageous to emulate higher elevation spread while reducing the number of antennas. However the DUT orientation is generally arbitrary in realistic application.

For this reason it was decided to realize a reconfigurable setup allowing to test different scenarios with a limited number of probes [2]. This set-up is composed by four arcs covered by electromagnetic absorbers, to place the OTA probe antennas at different azimuth and elevation angles. Wide-band two ports dual polarized antennas, designed at CEA LETI and covering the whole 2-6 GHz band, were used as probes. In Figure 1 we show two examples of realizations inside the CEA LETI anechoic chamber: the first aiming the test of omnidirectional channels and the second for directive ones.

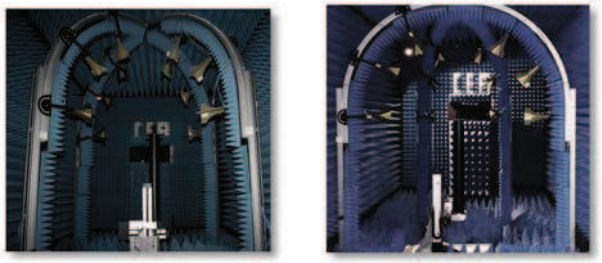

(a) (b)

Figure 1: 3D multi-probes OTA setups in CEA LETI anechoic chamber setup: symmetric (a) and sectorial (b) configurations

If Figure 2 we compare the expected correlation with the measured one. The results show, that despite some imperfections due to the experimental realization and the limited number of probes a good accuracy of the OTA emulated channel is obtained.

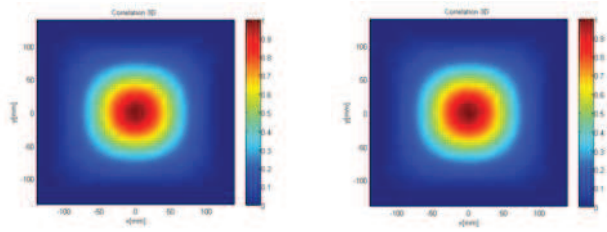

(a) (b)

Figure 2: Simulated (a) and measured (b) autocorrelation in the Zone Under Test

Perspectives

Extension of the OTA setup for large objects testing and scaling to other frequencies is ongoing to address 5G and vehicular applications.

RELATED PUBLICATIONS:
[1] M. Belhabib, R. D'Errico and B. Uguen, "Spatial correlation in spherical and cylindrical 3D MIMO Over-The-Air tests setups," 2016 10th European Conference on Antennas and Propagation (EuCAP), Davos, 2016, pp. 1-4.
[2] M. Belhabib, R. D'Errico and B. Uguen, "A 3-D wide-band set-up for over-the-air test in anechoic chamber," 2017 11th European Conference on Antennas and Propagation (EUCAP), Paris, 2017, pp. 640-643..

WIDEBAND DUAL-POLARIZED MAGNETO-ELECTRIC DIPOLE MINIATURIZATION USING CAPACITIVE LOADING

RESEARCH TOPIC:

Wideband compact antenna, unidirectional antenna, low profile antenna, dual polarization,

AUTHORS:

S. Bories, S. Kaddour, C. Delaveaud, A. Bellion.

ABSTRACT:

An original method to reduce the height of a dual-polarized unidirectional wideband antenna based on two crossed magneto-electric dipoles is proposed. The miniaturization technique consists in loading the magnetic dipole part of the structure with lumped capacitors. Thus the height of the radiating element is reduced to $0.1\lambda_0$, where λ_0 is the wavelength at the lowest operation frequency, which corresponds to a reduction factor of 38% compared to the SotA structure with equivalent performance. Moreover the prototype validates the 64% fractional bandwidth and the high stability of radiation from 1.6 GHz to 3.1 GHz.

SCIENTIFIC COLLABORATIONS: CNES, the French Space Agency, Toulouse

Context and Challenges

From cellular access points to micro-satellites for Earth observation, an increasing number of applications require ultra-wide band, dual polarized, and unidirectional antennas. However covering an octave is a real challenge while the antenna needs to be significantly miniaturized for micro-satellite integration.

A previous work on magneto-electric dipole (MED) antenna focuses on surface miniaturization [1] by reaching a $0.23\ \lambda_0$ x $0.23\ \lambda_0$ dipole surface (45% reduction factor compared to SotA) thanks to 3D folded electrical dipole parts. Here, the height reduction is addressed while maintaining stable radiation on the octave.

Main Results

The MED antenna is based on the concept of Huygens source where an electric and magnetic currents are combined together to form a unidirectional radiation pattern. The magnetic dipole is made with the vertical plates that support the electrical dipole arms (horizontal plates), Fig. 1. Usually MED presents a typical $0.25\ \lambda_0$ height. The proposed design succeeds to reach $0.1\ \lambda_0$ height by virtually enlarge the current path in the magnetic part of the MED, Figure 1. The MED surface ($0.32\ \lambda_0$ x $0.32\ \lambda_0$) is not miniaturized in this development.

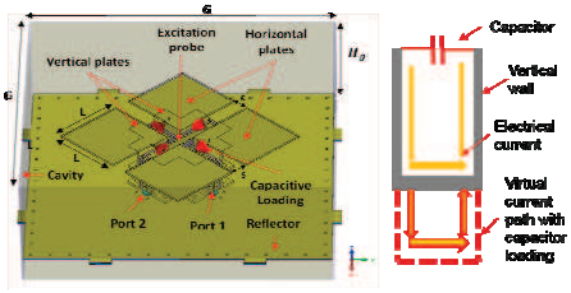

Figure 1: Magneto-Electric Dipole (MED) structure with four lumped capacitors (red cones) to reduce the antenna thickness

The realized prototype (Figure 2) has validated that performance was maintained despite the antenna height reduction. The input impedance fractional bandwidth (SWR<2.5) is 64%. The measured broadside gain is 8.5±1.5 dBi from 1.6 GHz to 3.1 GHz. The symmetry of the radiation structure ensures the same performance for both crossed dipoles and so an excellent circular polarization purity both over the beam width (±30°) and over the octave frequency band, Figure 2. Measured and simulated results are in very good agreement all over the frequency range.

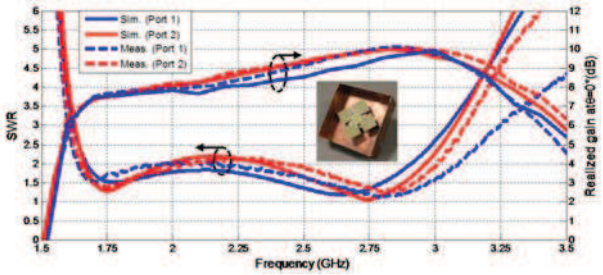

(a)

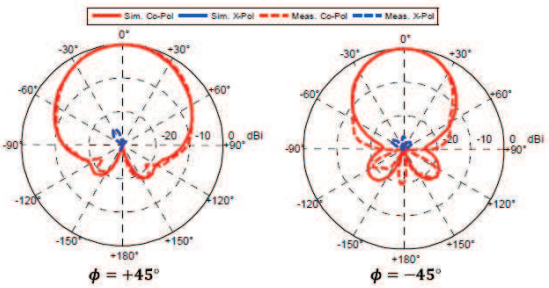

(b)

Figure 2 : Prototype results: SWR and broadside gain regarding frequency (a); Radiation pattern at 2.6 GHz for Circular polarization (b) in two cut-planes

Perspectives

Next work will implement the frequency band commutation in order to cover two octaves with such a low profile magneto-electric antenna. A prototype in VHF band will demonstrate its radiation performance (polarization, aperture) stability over the two octaves for a structure with only $0.1\lambda_0$ height.

RELATED PUBLICATIONS:

[1] S. Kaddour, S. Bories, A. Bellion, C. Delaveaud, "3D printed compact dual-polarized wideband antenna". In Antennas and Propagation (EUCAP), 2017 11th European Conference on (pp. 3441-3443). IEEE.

[2] S. Kaddour, S. Bories, A. Bellion, C. Delaveaud, "Wideband dual-polarized magneto-electric miniaturization using capacitive loading". In Antennas and Propagation & USNC/URSI National Radio Science Meeting, 2017 IEEE International Symposium on (pp. 545-546). IEEE..


2
liten
liten

04 ENERGY, SENSORS AND SYSTEMS

- Nano systems
- Mems Devices
- Energy Harvesting
- Battery Energy Management
- Emotional Sensing
- Shape Capture
- Context Recognition

IMPLEMENTATION OF MONOLITHIC BIDIRECTIONAL SWITCHES IN ZVS AUTO-SWITCHING MODE INTO AN AC/DC DUAL ACTIVE BRIDGE

RESEARCH TOPIC:
« Bidirectional switch », « GaN », « automatic switching », « Zero-Voltage-Switching »

AUTHORS:
L. Sterna, J-P. Ferrieux (G2ELab), O. Ladhari, P. Perichon, D. Frey (G2ELab), P-O. Jeannin (G2ELab)

ABSTRACT:
This paper presents the implementation of single gate bidirectional switches into a Dual Active Bridge topology. The quasi-resonant mode is introduced to operate in full ZVS mode at the primary bridge level. This mode involves automatic turn ON at zero voltage. A theoretical study validates the quasi-resonant full-ZVS automatic switching in AC/DC conversion. The driver circuit, used to guarantee ZVS automatic switching on each bidirectional switch, is then described. Finally, experimental results show the feasibility of the converter.

SCIENTIFIC COLLABORATIONS: G2ELab

Context and Challenges

The AC/AC and AC/DC converters leads the power electronics designers to investigate the interest of a switching device able to support bidirectional voltage in off state [1]. These devices allow to design single stage isolated topologies [2], as the Dual Active Bridge. One of the implementation key features of such a converter is thus the control of the bidirectional switch. Although classical control techniques that involve dual gate control, the proposed solution, using automatic switching [3], allows to have just one gate driver circuit per bidirectional switch.

Main Results

The converter input is directly fed with a sinusoidal voltage. The primary bridge switches are therefore bidirectional. Specific ZVS automatic switching transitions are implemented for the bidirectional switches on the primary bridge. They should be turned-off “classically”, with an external control signal, but the turn-on is automatic when their voltage crosses zero at the end of each resonant switching transition: that point implies no switching losses at all at the primary bridge. Resonant switching mode also induces lower common mode noise than hard switching.

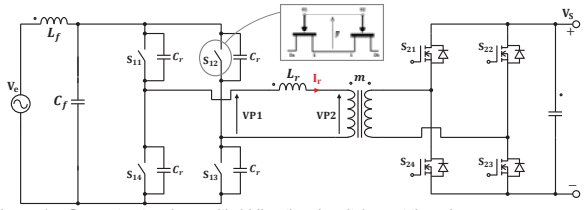

Figure 1 : Converter topology with bidirectional switches at the primary bridge level

The converter control has been designed to ensure both PFC operation and full ZVS switching at the primary bridge. The output bridge duty cycle is modulated in order to perform these two targets:

$$D2 = \pi.\left(1 - \sqrt{1 - \frac{8.Lr.m.Fd.|Ie(\theta)|}{Vs}}\right) \qquad (1)$$

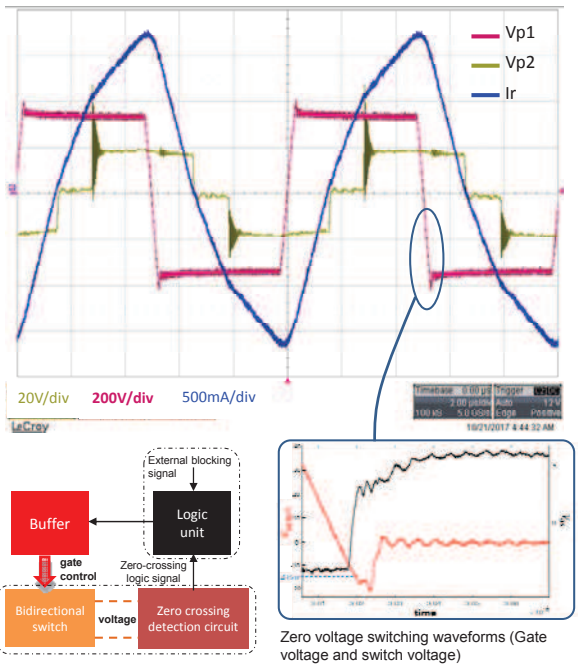

Zero voltage switching waveforms (Gate voltage and switch voltage)

Figure 2 : HF waveforms (up) ; driver principle and auto-switching waveforms (down)

A specific auto-switching driver circuit is designed in order to provide a particular switching behavior: "controlled" turn OFF and automatic turn ON at zero voltage. Two main blocks are needed : a voltage zero-crossing detection and a logic unit. The automatic driver has been validated experimentally (figure 2).

Experimental results validate the whole converter operation.

Perspectives

The first experimental results validate the concept and lead to optimize and integrate the whole system.

RELATED PUBLICATIONS:

[1] D. Bergogne, O. Ladhari, L. Sterna, C. Gillot, R. Escoffier and W. Vandendaele, "The single reference Bi-Directional GaN HEMT AC switch," Power Electronics and Applications (EPE'15 ECCE-Europe), 2015 17th European Conference on, Geneva

[2] O. Ladhari, L. Sterna, P. Perichon and D. Bergogne, "A novel AC/DC converter topology using a bidirectional GaN switch application: Led driver," 2017 IEEE 18th Workshop on Control and Modeling for Power Electronics (COMPEL), Stanford, CA, 2017, pp. 1-7.

[3] D. Siemaszko, P. Barrade, Y. R. De Novaes and A. C. Rufer, "New self-switching mechanisms for active bidirectional switches," 2007 European Conference on Power Electronics and Application

A NOVEL LED DRIVER CONVERTER BASED ON BIDIRECTIONAL GAN HEMT AC SWITCHES

RESEARCH TOPIC:
LED driver », « AC switch », « Gallium nitride (GaN)

AUTHORS:
L. Sterna, D. Bergogne, O. Ladhari, P. Périchon

ABSTRACT:
A novel topology for LED drivers is proposed. The system does not require rectifier input stage nor storage DC bus capacitor. The topology is described and studied by simulation. Experimental results on an AC LED demonstrator using GaN transistors validate the proposed circuit.

SCIENTIFIC COLLABORATIONS:

Context and Challenges

LED devices are now representing one of the most promising technology in lighting systems due to their high potential light output and also an increased lifetime. The common LED power supplies include a diode bridge that limits the efficiency, and also electrolytic capacitors. The whole system lifespan is limited by this capacitor (about 7000h) while LEDs lifetime is higher than 50 000h. Recent works on Monolithic Bidirectional switches [1] offer the opportunity to explore new topologies of conversion [2], taking advantage of Bi-Directional AC switch current-voltage characteristic.The proposed topology implements these particular switches in order to produce a single stage conversion in two versions : AC/AC and AC/DC

Main Results

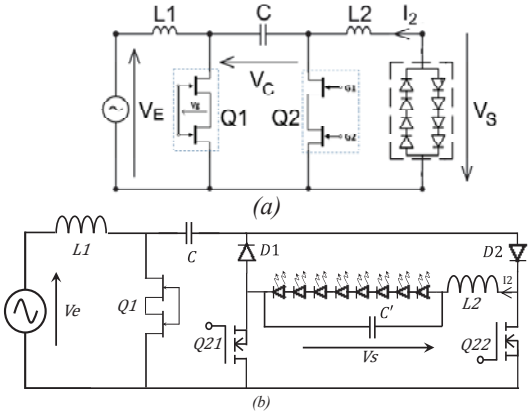

Figure 1: Proposed topologies: (a) AC/AC version ; (b) AC/DC version

The two versions are based on the DC/DC Cuk topology, allowing buck/boost operation. A bidirectional switch is implemented at the input to be able to convert directly the AC mains without any rectifier stage. The first version is AC/AC, including a bidirectional load: two branches in anti-parallel. The second version operates an AC/DC conversion with rectifying function.

In both cases, the bidirectional switches use allows to avoid diode rectifier stage.
A converter prototype has been designed and tested directly plugged into the 230VAC mains. Due to its higher reliability concerning the LED cost, the second version of the converter has been preferentially implemented. The converter has been tested in mains operated conditions, feeding a dedicated LED load. The prototype is composed of two boards and a dedicated LED load with its bulb. The converters board (figure 10) implements the topology, including the switches and the passive elements. The converter topology is implemented on a pcb (see Figure 2). The prototype is not optimized in size and bidirectional switches are not monolithic but based on circuits with discrete HEMT GaN transistors and diodes, visible on the figure. As the mains voltage is not ideal, distortion and slight frequency variations are common, a PLL technique has been implemented in order to synchronize the converter operation with the mains variations. Thus, the mains operation also requires a measure of the alternating input voltage and also a stable zero crossing detection ability to control the different switches.

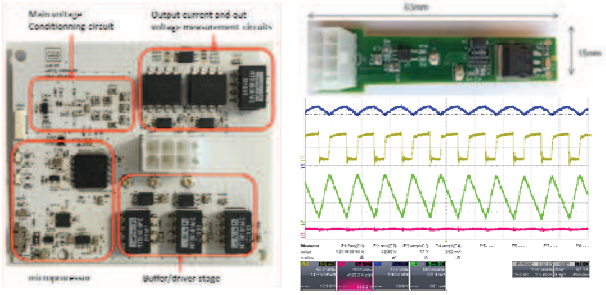

Figure 2: Control board (left), converter board (top right), series capacitor voltage (blue), switched voltage (yellow), input current (green), output voltage magenta)

Perspectives

Current closed-loop control would be required to improve output current waveform for a practical application. Full integration of the different passive elements on pcb is the final perspective.

RELATED PUBLICATIONS:
[1] D. Bergogne O. Ladhari L. S. C. Gillot R. Escoffier W. Vandendaele "The single reference Bi-Directional GaN HEMT AC switch" Power Electronics and Applications (EPE'15 ECCE-Europe) 2015 17th European Conference
[2] J. W. Kolar, T. Friedli, F. Krismer and S. D. Round: The essence of three-phase AC/AC converter systems, 2008 13th International Power Electronics and Motion Control Conference, Poznan, 2008, pp. 27-42. [3] R. Finkel, R. Taylor, R. Bolles, R. Paul, and J. Feldman, “An overview of AL, programming system for automation,” in Proc. Fourth Int. Joint Conf Artif. Intell., pp. 758-765, Sept. 3-7, 1975

INDUCTOR-LESS DC-DC CONVERTER USING A PIEZOELECTRIC TRANSDUCER

RESEARCH TOPIC:
Piezoelectric, conversion, DC/DC, adiabatic

AUTHORS:
B. Pollet, G. Despesse & F. Costa (ENS Cachan)

ABSTRACT:
A new kind of piezoelectric DC-DC converter has been developed. A ceramic is used as an energy storage element to replace the traditional inductance. Once resonating, the system describes a cycle at each resonance period taking energy to the source, storing it and transmitting it to the load with soft switching. A simulation representing the whole system, gives very attracting results with very high efficiency for different output powers. The converter was tested and fully validated by experimental works. An efficiency of 85 percent was reached for a 10-20 volts step up converter with an output power of 500 milliwatts.

SCIENTIFIC COLLABORATIONS: This work is done in collaboration with the SATIE lab of ENS Paris-Saclay, Cachan, France

Context and Challenges

Today, most of the DC/DC converters are using an inductor. This inductor stores an input electrical energy under a first voltage level before restoring it under a second one. In between, the energy is transiently stored in a magnetic form. With piezoelectricity, the energy is transiently stored in mechanical energy in place of magnetic. The interest is to benefit of the high quality factor of some piezoelectric materials (>1000) ensuring theoretically a drastic reduction of power losses (no resistive coil). However, a piezoelectric structure has mainly a capacitive behavior making challenging a voltage to current transduction compare with the classical inductive elements. Nevertheless, a specific cycle applied at piezoelectric resonance was defined and shows the possibility to operate at zero voltage switching avoiding large switching losses knowing the piezoelectric capacitive behavior [1,2].

Main Results

The whole 6-phases cycle is represented in Figure 1 for a 10-20 Volt converter; this cycle is applied thanks to the circuit described in Figure 2 in association with a driving FPGA circuit. The origin of time is chosen when the piezoelectric voltage Vp is equal to Vout and the resonator internal current is null. At this time, all the switches are off and the voltage drops until reaching Vin (phase1). When Vp is equal to Vin, k_{in} is turned on to connect the piezoelectric material to the input voltage with zero voltage switching mode (ZVS) in order to avoid switching losses.

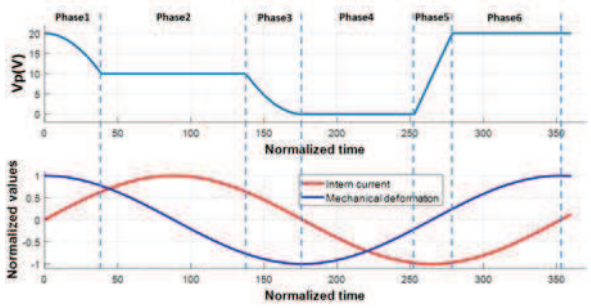

Figure 1: Steady-state piezoelectric waveforms

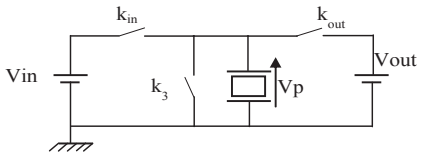

Figure 2: Converter topology

During this phase, Vp is equal to Vin and the resonator takes energy from the source (phase2). Then kin is turned off and Vp drops until reaching zero volt when the piezoelectric deformation is maximum and the intern current generated by the vibration is zero (phase3). When Vp is equal to zero volt, k_3 is turned on to have a ZVS commutation and the voltage remains zero (phase 4). k_3 is turned off and Vp increases until reaching Vout. (phase5). When Vp is equal to Vout, k_{out} is turned on with no switching losses (ZVS mode). In this phase, the material is restituting energy to the load. This constant voltage phase lasts until the transfer current reaches zero (phase6). Then a new cycle begins.

The following figure shows the experimental validation:

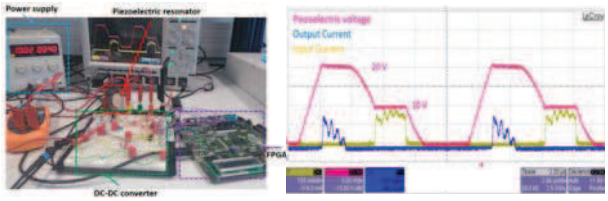

The first experimental results show an efficiency up to 87% for power of few hundreds of mW. Just by using active rectification in place of simple diodes, we expect to reduce by around 2 the losses.

Perspectives

Theoretical analysis lets to expect a promising efficiency higher than 95% up to 1 Watt of output power.
The high voltage capability (>500 V), the high quality factor (>1500) and the low piezoelectric thickness (<700µm) let to expect at same time a good power density, a good efficiency and a good form factor for integration in low thickness devices.

RELATED PUBLICATIONS:
[1] B. Pollet, G. Despesse, F. Costa, "A new inductorless DC-DC piezoelectric flyback converter", The 19th International Conference on Industrial Technology, IEEE ICIT2018, Lyon, February 20-22th
[2] B. Pollet, G. Despesse, F. Costa, "Inductor-less DC-DC converter using a piezoelectric transducer", JNRSE2017, Lyon, May 9th-10th

BATTERY AGING-AWARE ENERGY MANAGEMENT OF GREEN SMALL CELLS POWERED BY THE SMART GRID

RESEARCH TOPIC:

Cognitive energy management, Green communication, Energy harvesting, Small cell, Battery, Smart grid

AUTHORS:

M. Mendil, A. De Domenico, V. Heiries, R. Caire(UGA, G2Elab) and N. Hadjsaid (UGA, G2Elab)

ABSTRACT:

Mobile operators are deploying energy-harvesting networks due to their foreseen advantages such as self-sustainable capability and reduced operating expenditure. However, the used energy storage is subject to irreversible aging mechanisms, requiring intelligent management that considers both the energy cost and battery life cycle. We propose a cognitive energy management strategy for base stations powered by local renewable energy, a battery, and the smart grid to simultaneously minimize electricity expenditures and enhance the life span of the storage device. Results show that a degradation-aware policy significantly improves the battery lifetime, while achieving considerable cost savings

SCIENTIFIC COLLABORATIONS: University Grenoble Alpes, INPG, G2Elab

Context and Challenges

Recently, mobile user density and data traffic volume have exponentially increased. To respond to this trend, the mobile network operators have to find new strategies to enhance their network service capabilities while being more energy efficient. Several concepts have been proposed to improve the energy efficiency in wireless communications. In addition, renewable energy (RE) usage in cellular networks has drawn attention for its numerous benefits such as decreasing carbon emissions, enabling long-term cost savings thanks to reduced operating expenditure, and feeding off-grid base stations where the connection to the power grid is expensive or impossible. The current energy-harvesting technologies require local energy storage to absorb the production fluctuation and ensure a continuous equilibrium between energy offer and demand. However, the typical used energy storage, i.e. electric battery, generates expensive investment cost and is subject to irreversible degradations. The presence of energy storage requires intelligent energy management policies to optimize the energy cost of grid-connected base stations with energy harvesting. We propose here a smart energy controller that uses reinforcement learning techniques to elaborate an optimal energy flow policy without prior knowledge of the environment stochastic behavior. Contrary to previous studies, our controller not only focuses on maximizing the energy saving, but also integrates both calendar and cycle battery aging in the energy management. Indeed, there is a trade-off between pure cost-efficient and battery aging-aware energy management strategies that has not been evaluated so far. This motivated us to investigate the design of a cognitive energy controller that optimizes the operating energy cost while using the battery in the most effective way to avoid accelerated cycle and calendar aging.

Main Results

Our proposed architecture, called Green Small cell Base Station, corresponds to the multiple-sources multiple-loads system represented hereafter. It is composed of three categories of components. The energy sources (the photo-voltaïc panel), the energy sinks (base station), and the hybrid components which can act like both energy sources and sinks(the battery and the smart grid). The cognitive decision architecture is centered around the battery and uses realistic models to capture the non-linear battery behavior and aging mechanisms. The algorithmic architecture, based on Q-learning, jointly optimizes the energy cost and reduce the battery aging effects. System simulations show that the proposed controller achieves considerable cost reduction compared to simpler strategies ([1], [2]). Furthermore, the trade-off between pure energy cost optimization and battery aging-aware policies is explored.

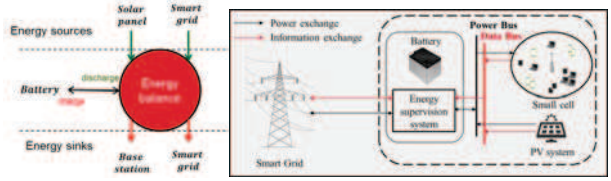

Figure 1: System architecture of the proposed cognitive energy supervisor for small cells

The energy cost and battery aging are evaluated in different configurations. Simulation results show that the proposed energy management, taking into account the battery aging processes, allows considerable battery life extension such that the battery lasts five times longer compared to a pure energy cost optimization strategy ([3]). In exchange, the opex is slightly increased but this additional expense remains negligible with respect to the current battery replacement cost.

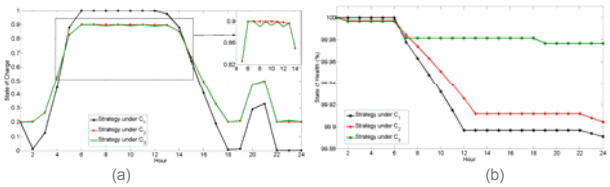

(a) (b)

Figure 2: (a) Daily energy strategy under the constraint sets c_1 (no battery life preservation), c_2 (medium constraints on the battery usage), and c_3 (full constraints on the battery usage); (b) Average battery calendar aging of the ideal strategy under the constraint sets c_1, c_2, and c_3

Perspectives

It is planned to study the proposed cognitive energy supervision framework considering casual information about the environmen energy variable. We also aim to realize a demonstrator of the proposed solution to assess its performances in real-life conditions.

RELATED PUBLICATIONS:

[1] M Mendil, A De Domenico, V Heiries, R Caire, N Hadjsaid, in Personal, Indoor, and Mobile Radio Communications (PIMRC), 2016 IEEE 27th Annual International Symposium on. "Fuzzy Q-learning based energy management of small cells powered by the smart grid", pp. 1–6

[2] M Mendil, A De Domenico, V Heiries, R Caire, N Hadjsaid, in International Conference on Cognitive Radio Oriented Wireless Networks. "Energy management of green small cells powered by the smart grid" (Springer, 2016), pp. 642–653

[3] M Mendil, A De Domenico, V Heiries, R Caire, N Hadjsaid, in EURASIP Journal on Wireless Communications and Networking, Article N°127, Published: JUL 18 2017, "Battery aging-aware energy management of green small cells powered by the smart grid ".

AEROELASTIC FLUTTER ENERGY HARVESTERS SELF-POLARIZED BY TRIBOELECTRIC EFFECTS

RESEARCH TOPIC:
Energy Harvesting, Aeroelasticity, Triboelectricity

AUTHORS:
M. Perez, S. Boisseau, J. Willemin, P. Gasnier, G. Despesse, J.L. Reboud (G2Elab)

ABSTRACT:
Flutter effect is a great opportunity to develop thin airflow energy harvesters. Hereafter are introduced flutter energy harvesters exploiting triboelectricity. The main idea is to use the flutter capability of thin flexible films confined between lateral walls to induce simultaneously the capacitance variations and the electrostatic polarization required by the triboelectric/electrostatic conversion. The prototypes have a quick startup (3 m/s) and an electrical power density up to 40µW/cm². Energy harvesters combined with a Maximum Power Point power management circuit are able to supply 868MHz wireless sensor nodes with temperature and acceleration measurements, validating the complete energy harvesting chain.
SCIENTIFIC COLLABORATIONS: G2Elab

Context and Challenges

Airflow energy harvesting is an area of substantial and growing interest for the energy harvesting community. Airflows exist in various situations and offer a high density of kinetic power. One common option to convert the flow's kinetic power into electricity is to go through an intermediary mechanical power. This mechanical power can take the form of a rotary (turbines) or an oscillatory motion (flutter) of a mechanical element. The exploitation of aeroelastic motion of a flexible film and its contacts with lateral walls enable to develop efficient and low cost energy harvesters by exploiting the electrostatic conversion. Yet, the main issue of the electrostatic conversion, i.e. the polarization source, has to be solved.

Main Results

The flutter motion of flexible films and the contacts with lateral walls can be craftily exploited to simultaneously induce the two necessary conditions for the electrostatic conversion: capacitance variations and self-polarization by using triboelectric effects [1-2]. The airflow energy harvester is made of a flexible membrane in Teflon confined between two walls; electrodes are in copper since Teflon/copper is one of the best triboelectric couple of materials in the triboelectric series (Figure 1). When the FEP membrane starts to oscillate and collides with the lateral copper electrodes, electric charges are exchanged by triboelectric effects. A portion of the negative charges are trapped (<0.25mC/m²) in the dielectric membrane turning the FEP membrane into a triboelectret, and polarizing the variable capacitor.

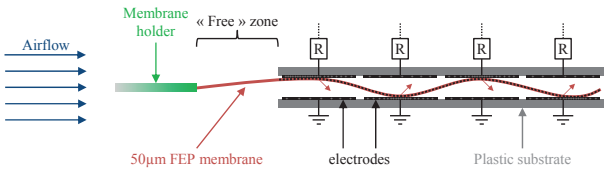

Figure1: Aeroelastic flutter energy harvester exploiting triboelectricity

Various prototypes with various dimensions and parameters have been tested between 0 and 20m/s; typically with lengths, widths and thicknesses comprised respectively between 5 and 8 cm; 2 and 3 cm; and 25 and 125µm. The startup speed is around 3m/s with a power density of 0.35µW/cm². At 20m/s, the power density reaches between 20µW/cm² and 40µW/cm² without pre-polarization of the membrane (triboelectric operation only), and between 60 µW/cm² and 150 µW/cm² by pre-charging the membrane at -650V by corona discharge.

A Maximum Power Point (MPP) circuit has been developed to efficiently use the power provided by the energy harvesters. The power management circuit is able to start from scratch, without battery, by exploiting the two-path approach presented in [3].

Energy harvesters coupled to the MPP circuit have been used to supply a low-power wireless sensor node based on ST's SPIRIT1 RF chip and STM32L0 microcontroller, and embedding a temperature sensor and an accelerometer/magnetometer. This validates the whole energy harvesting chain from ambient energy to autonomous sensor nodes.

The Maximum Power Point strategy turned out to be more efficient than other common strategies such as Synchronous Electric Charge Extraction or the Diode-Bridge-Capacitor passive circuit, enabling to send data more often as presented in Figure 2: a measurement cycle and its RF emission are performed each time the voltage on the storage capacitor drops.

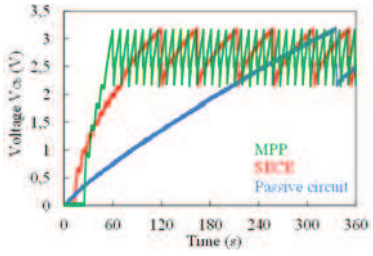

Figure 2: Voltage on the storage capacitor (V_{cb}) as a function of the time

Perspectives

Research is now focused on the size reduction of flutter energy harvesters and on the reduction of the startup speed.

RELATED PUBLICATIONS:
[1] M. Perez et al., "Aeroelastic flutter energy harvesters exploiting triboelectric effects", Smart Materials and Structures (2017)
[2] M. Perez et al., "Triboelectret-based aeroelastic flutter energy harvesters", Proc. PowerMEMS (2016)
[3] S. Boisseau et al. "Self-starting power management circuits for piezoelectric and electret-based electrostatic mechanical energy harvesters, Proc. PowerMEMS (2013)"

HUMAN MOTION ENERGY HARVESTERS

RESEARCH TOPIC:
Energy Harvesting, Electromagnetism, Low-Power Electronics

AUTHORS:
M. Geisler, S. Boisseau, I. Ait-Ali (Cityzen Sciences), J. Willemin, P. Gasnier, G. Despesse, S. Perraud (CEA LITEN)

ABSTRACT:
The development of energy harvesters for smart wearables is a challenging topic, with a difficult combination of ergonomics constraints, lifetime and electrical requirements. Hereafter are presented two inertial energy harvesters concepts developed to supply autonomous Body Area Sensors for sportswear applications, and exploiting an electromagnetic conversion with permanent magnets. Thanks to accurate analytical models and optimizations, output powers in the range of 5mW have been reached; this is among the best output powers achieved in the state of the art for small-scale human motion energy harvesters.

SCIENTIFIC COLLABORATIONS: CEA LITEN, Cityzen Sciences

Context and Challenges

The functionalization of ordinary objects with embedded electronic systems is a fast-growing trend, commonly referred to as the Internet of Things. This phenomenon is especially visible in the nearest human environment where “smart” objects – watches, phones, cars, houses – have become commonplace. The growth of this domain has triggered an interest for energy harvesting solutions to reduce the need to recharge energy storage units, or even to replace them. This is typically the case for smart wearables for sportswear applications. However, the development of energy harvesters for smart wearables is a challenging topic, gathering ergonomics constraints, lifetime issues and electrical requirements.

Main Results

Two types of inertial energy harvesters for smart wearables exploiting an electromagnetic conversion have been developed. Inertial devices offer the great opportunity to develop hermetic devices compatible with clothes' harsh environments, such as washing machines. The first concept is a 1D inertial electromagnetic energy harvester (Figure 1), consisting of a magnetic mass moving freely inside a tube between two repulsive magnets [1]. The mass is made of stacked magnets with alternate polarities and separated with ferromagnetic disks.

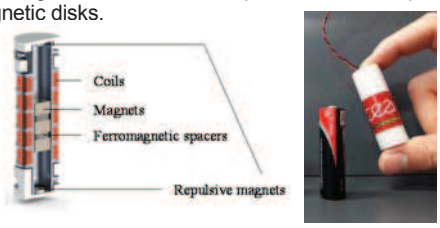

Figure 1: 1D inertial electromagnetic energy harvester

Advanced modeling and optimizations have enabled to maximize the output power and the power density for human motion. An optimized prototype of 14.8mmØ×52mm, weighting 20g, has generated up to 4.95mW in a resistive load when worn at the arm during a run, and 6.57mW when hand-shaken. Among the inertial electromagnetic energy harvesters for human motion reported so far, this one exhibits the highest power density, up to 730µW/cm³. The second structure (Figure 2a) is composed of a magnetic ball circulating inside a closed-loop guide and several coils wrapped around the loop to turn the variation of magnetic flux into electricity [2]. This shape aims at taking advantage of both mechanical energy from the step impacts and the swing of the limbs, while avoiding as much as possible the “containment” effect which limits the performance of resonant generators. The device has been modeled and prototyped. From a 2g moving ball, the 5cm-diameter 21cm³ prototype generated up to 4.8mW when worn by someone running at 8km/h, which is an excellent performance regarding the small size of the moving magnet (Figure 2b).

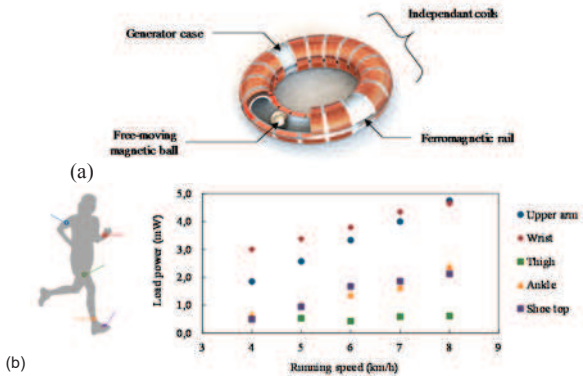

Figure 2: (a) Looped energy harvester and (b) output powers

The two concepts were proven to be application-ready as they were both able to supply a wireless 3-axis acceleration and temperature sensor node measuring and transmitting data by Bluetooth Low Energy at frequencies up to 25Hz

Perspectives

Future work will focus on the size reduction and the integration to clothes of these energy harvesters. .

RELATED PUBLICATIONS:
[1] M. Geisler et al., "Human-motion energy harvester for autonomous body area sensors", Smart Materials and Structures (2017)
[2] M. Geisler et al., "Looped energy harvester for human motion", Smart Materials and Structures (2017).

HIGH-RESOLUTION FINGERPRINT SENSING WITH VERTICAL PIEZOELECTRIC NANOWIRE MATRICES: MAIN ACHIEVEMENTS OF THE PIEZOMAT PROJECT

RESEARCH TOPIC:
Nanosystem, ZnO nanowire, force sensor, microfabrication, microelectronics

AUTHORS:
E. Saoutieff, M. Allain, A. Viana, E. Pauliac-Vaujour

ABSTRACT:
The aim of the project was to implement the proof of concept of a new technology of pressure-based fingerprint sensor based on the integration of piezo-electric ZnO nanowires grown on a silicon wafer. This technology opens the path to ultra-high resolution fingerprint sensors, able to reach resolution higher than 1000 dpi. The fabrication of a demonstrator embedding a silicon chip with 250 pixels, and its associated electronics for signal collection and post-processing was achieved. It was designed to demonstrate the concept and the major technological achievements.

SCIENTIFIC COLLABORATIONS: MTA EK MFA, Fraunhofer IAF, ULEI, Specific Polymers, IDEMIA, KTU, Tyndall

Context and Challenges

Ended in June 2017, the 44 months FP7 European project PiezoMAT brought together 8 partners from academia, R&D centres along with small and medium enterprises as well as large enterprises from across the EU.

Increase the reliability and develop robust fingerprint sensors beyond today's 500dpi international standards is one motivation for designing a new technology of fingerprint sensor.

The work carried out aims at developing and demonstrating a concept based on a matrix of inter-connected piezoelectric NWs grown directly onto a microelectronics chip. The interest of vertically-integrated piezoelectric NWs for high sensitivity sensor applications lies in high densities of integration, which occur through the size diminishing of individual pixels. The high spatial resolutions that it is possible to obtain - 3000 dpi for our proof-of-concept chip - should enable the detection of level 3 minutiae of fingerprints (pores, ridge-edge recognition.

Main Results

Three different sensing architectures have been fabricated with the charge collections at the bottom of single nanowires (A-I / A-II) or with top-bottom contacts (A-III) as described on figure 1.

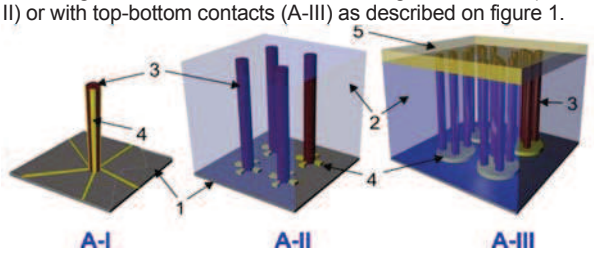

Fig. 1: Schematics of the 3 architectures: 1-patterned silicon chip (carrier) / 2-insulating polymer matrix / 3-ZnO NW / 4–electrodes / 5-top contact

For the architecture 1, we developed a direct write lithography method by using electron beam-induced deposition (EBID) for contacting vertical ZnO facets with electrically isolated lines with sub-micron size.
The second main result is the first experimental demonstration of bottom-bottom contacted 'bending mode' force sensor with a resolution of 5000dpi.

We also demonstrated the feasibility of the third architecture, with the fabrication of a demonstrator embedding a silicon chip with 250 pixels (1000dpi), and its associated electronics for signal collection and post-processing (figure 2).

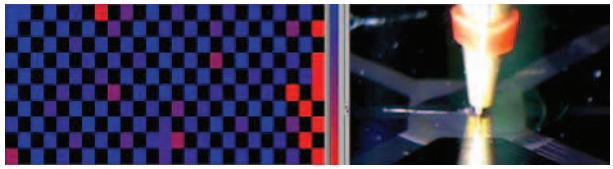

Figure 2: Tactile mapping by wire stamp and set-up device for force sensitivity demonstration of the chip (MTA EK MFA)

All along the project, partners challenges were the integration of ZnO nanowires, onto microelectronics chips, considering process compatibility at the wafer scale of the successive nanowire growth, contacting and encapsulation steps.

Valuable experience and know-how was gained in several areas, such as optimization of seed layers processing, localized growth of well-oriented ZnO nanowires on silicon substrates, mathematical modelling of complex charge generation, and development of multi-functional UV-crosslinkable encapsulating polymers.

Perspectives

Perspectives are long-term developments with full electronics integration for an optimal sensor resolution.

RELATED PUBLICATIONS:
[1] E. Saoutieff et al., "Integration of piezoelectric nanowires matrix onto a microelectronics chip ", Procedia Engineering 168 (2016) pp1638 – 1641
[2] J. Volk et al, "Integrated Piezoelectric Nanowire Arrays for High Resolution, Tactile Mapping", Eurosensors conference, Budapest (2016)
[3] E. Saoutieff et al, "Axially stressed piezoelectric nanowires for high resolution tactile imaging", Eurosensors conference, Paris (2017)
[4] A.Bouvet-Marchand et al., "UV-crosslinked polymeric materials for encapsulation of ZnO nanowires in piezoelectric fingerprint sensors", Procedia Engineering 168 (2016) pp1135 – 1139
[5] E. Saoutieff et al,"PiezoMAT project: high-Resolution Fingerprint Sensing with Vertical Piezoelectric Nanowire MATrices", NanoFIS conference, Graz (2017).

CHALLENGES OF NANOSYSTEM ARCHITECTURES: REALISTIC PATHS TO MULTISCALE, MULTI-MODALITY INTEGRATION

RESEARCH TOPIC:
Nanosystem, flexible sensor, GaN nanowire, piezoelectricity, finite element modeling

AUTHORS:
E. Pauliac-Vaujour, A. El Kacimi, E. Saoutieff, J. Eymery

ABSTRACT:
We investigate complete solutions for the integration of nanotechnologies, and in particular nanosensors, with a view to ultra-low power, fully flexible systems, so called "sensitive surfaces", for applications as varied as automotive, predictive maintenance, wearables, health, sports and wellness, etc. The example of flexible piezoelectric sensors based on GaN wires is given, were developments were carried out from pure model-based design considerations to experimental validation. All our processes and developments are aimed to be scalable and, ultimately, transferable.

SCIENTIFIC COLLABORATIONS: None

Context and Challenges

The paradigm of artificial intelligence conveys multiple challenges in the domains of electronics miniaturization, energy management, communication modes, packaging and assembling, data fusion and participatory sensing and learning. Every day sees the emergence of new smart objects and products which embed more and more electronic intelligence. Considerable research effort is put worldwide towards the integration of new electronic functionalities. In this context, nanotechnologies have an important role to play and, in the first place, novel and evolutionary multi-scale, multi-modality architectures which feature and combine some of the latest technologies in terms of sensing, energy harvesting, communication, etc. [1] Our group investigates several approaches for the efficient integration of nano-electronic devices. One research area is in systems based on piezoelectric nanowires of either ZnO or GaN, which we interconnect either at a single chip level or at a larger scale on varied (flexible) substrates. Application-specific system architecture and electronics are designed, with the help of multi-physics and multi-competence models.

Main Results

We have developed and tested several configurations of GaN wire-based piezoelectric devices for flexible applications cases.

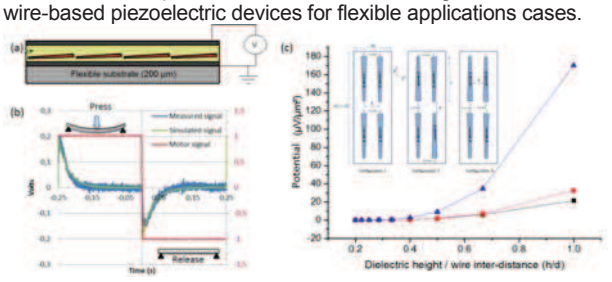

Fig. 1. (a) Flexible capacitive force sensor architecture with horizontal GaN wires; (b) experimental characterization of piezoelectric response of sensor upon deformation [2]; (c) model of sensor response as a function of wire configuration within sensor [3].

Ultra-thin flexible sensors were designed based on state-of-the-art finite element predictive models, which account for the structural characteristics and the physical principle of operation of wires and ensembles of nanowires within the overall sensor environment. For vertical wire devices (Figure 2), we have developed a scalable fabrication process by peeling which provides efficient control of the wire orientation and an additive contribution of the individual piezoelectric signals. Devices integrating 190 µm long wires reproducibly generate 2V signals under manual finger compression. Stability upon several thousand compression and release cycles, carried out at a 900 mm/min deformation rate and a 1.11Hz frequency on a calibrated compression bench, was demonstrated.

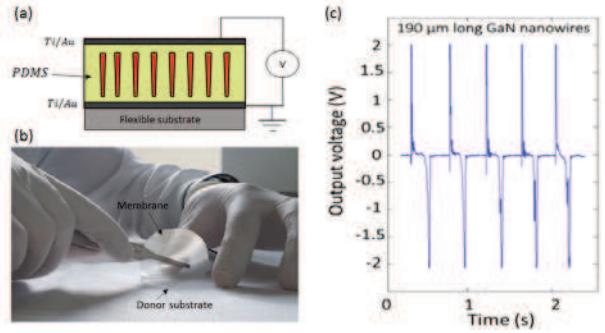

Fig. 2. (a) Flexible capacitive force sensor architecture with vertical GaN wires; (b) Scalable peeling process was developed for the fabrication of sensors; (c) Devices repeatably generate several volt signals upon finger-applied compression. [4]

Perspectives

The patented processes for the fabrication of this sensor were developed so as to be fully compatible with large area manufacturing processes (200 mm wafer size and beyond). Arrays of such "sensitive surfaces and lines" with dedicated electronic interfaces and reading circuits are aimed to be implemented in ultra low-power and fully flexible (including printed active components) systems for force and deformation mapping in a variety of applications.

RELATED PUBLICATIONS:
[1] E. Pauliac-Vaujour, A. El Kacimi, E. Saoutieff, J. Eymery, "Challenges of nanosystem architectures: realistic paths to multi-scale, multi-modality integration", NanoS&T conference (2017), Fukuoka, Japan.
[2] S. Salomon, J. Eymery, E. Pauliac-Vaujour, "GaN wire-based Langmuir-Blodgett films for self-powered flexible strain sensors", Nanotechnology 25, 375502 (2014).
[3] A. El Kacimi, E. Pauliac-Vaujour, J. Eymery, "Flexible capacitive piezoelectric sensor based on vertical GaN wires", Nanowire Week (2017), Lund, Sweden.
[4] A. El Kacimi, E. Pauliac-Vaujour, J. Eymery, "Flexible capacitive piezoelectric sensor with vertically aligned lutralong GaN wires", accepted for publication in ACS Applied Materials & Interfaces, 10 (5), pp 4794-4800 (2018).

DISTORTION EFFECTS ON ASM-V DATA: PRELIMINARY ANALYSIS AND CORRECTION PERSPECTIVES FOR SWARM AND BEYOND

RESEARCH TOPIC:
Optically pumped ^{4}He magnetometers; Swarm; ASM instrument; Vector magnetometers calibration

AUTHORS:
T. Jager, J.M. Léger, G. Hulot (IPGP) and P. Vigneron (IPGP)

ABSTRACT:
The Absolute Scalar Magnetometers (ASM) provide the scalar reference measurements for the calibration of the Vector Field Magnetometers (VFM) onboard ESA Swarm satellites. Vector measurements have also been continuously delivered [1] and the performance of ASM vector data (ASM-V product) has already allowed to build standalone geomagnetic field models of great quality [2] without using VFM data. Additional corrections for distortions effects will further enhance their performance [3] and consolidate the payload performance and capabilities for the next generation of ASM-based magnetic space missions.

SCIENTIFIC COLLABORATIONS: G. Hulot and P. Vigneron, IPGP, Paris, France

Context and Challenges

Improving the accuracy of the already well performing ASM-V data is of major interest in the perspective of building the next generation of magnetic mission using an ASM-like instrument as the only source for magnetic data. Providing high-performance scalar and vector measurements performed at the same time and at the same location with a single instrument would not only enable scientific grade geomagnetic mission to be built on nanosatellite platforms at lower cost but also open the way to multiple constellations configurations and continuous Earth magnetic field monitoring from space. The work described here is directly related to this topic by ensuring that the requested vector performance can be achieved.

Main Results

The current ASM instruments on Swarm provide additional vector measurements through vector modulations applied on ^{4}He atoms thanks to a tri-axial coils system. Well-known sinusoidal modulation signals are thus superimposed onto the ambient magnetic field and their frequency demodulations on the scalar field measurement give the information about the orientation of the field in the vector coils reference frame of the instrument [1]. Besides orthogonality and vector transfer functions corrections, the ASM vector data is also usually corrected for temperature and mechanical imperfections effects: the overall accuracy of this data is of 1.5-2 nT (1 σ), as expected before launch [1]. However ASM-V data exhibit small geographic discrepancies when compared to both geomagnetic models and VFM data (cf Figure 1).

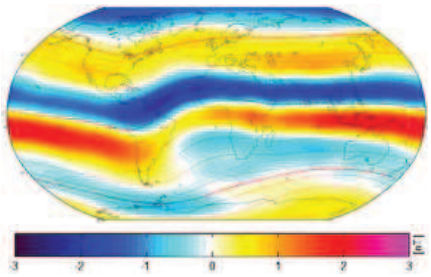

Figure 1: Example of ASM-V vs Geomagnetic model discrepancies (ASM Z-axis)

These discrepancies have been found to be related to small distortions effects of few 10^{-4} w.r.t. to the vector modulation amplitudes. Depending on the orientation of the magnetic field with each of the vector modulations, non-linear effects translate a part of system response from fundamental projections into odd harmonics, essentially 3rd harmonics here. These effects also depend on the ratio of the modulation frequency over the internal scalar bandwidth of the instrument. Preliminary characterizations have been performed on ground on the ASM EQM instrument and corrections parameters have been derived: the in-orbit corresponding correction displayed on the example of Figure 2 fits well with what has been observed so far on Fig. 1.

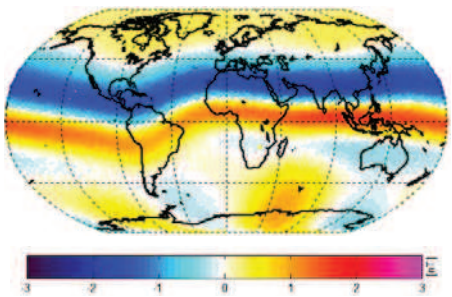

Figure 2: Calculated In-orbit distortion effect derived from ground characterizations (ASM Z-axis).

A complete evaluation process is currently ongoing with IPGP for the entire mission duration with updated ASM-V data corrected for these distortions effects.

Perspectives

Once fully validated, these investigations and corrections for additional distortions disturbances on the ASM-V data will enable the production of updated standalone ASM-based geomagnetic field models of equal quality w.r.t. the ones currently obtained with the full Swarm payload. The ASM vs VFM comparison investigations may also benefit of these updated corrections.

A significant step is also close to be achieved in the validation and the improvement of the next generation of ASM payload currently under development for scientific missions on nanosatellite platforms.

RELATED PUBLICATIONS:
[1] J.-M. Léger et al., "In-flight performance of the Absolute Scalar Magnetometer vector mode on board the Swarm satellites. Earth Planets and Space, 2015, 67, pp.57.
[2] P. Vigneron et al. "A 2015 International Geomagnetic Reference Field (IGRF) candidate model based on Swarm's experimental absolute magnetometer vector mode data". Earth Planets and Space, 2015, 67, pp.95.
[3] T. Jager, J.-M. Léger, G.Hulot and P. Vigneron, "Distortion effects on ASM-V data: preliminary analysis and correction perspectives", Swarm 7th Data Quality Workshop, TU Delft, Netherlands, 24-27/10/2017..

MAGNETOCARDIOGRAPHY MEASUREMENTS WITH ^{4}HE VECTOR OPTICALLY PUMPED MAGNETOMETERS AT ROOM TEMPERATURE

RESEARCH TOPIC:
Optically pumped magnetometers, medical imaging

AUTHORS:
M. Le Prado, A. Palacios-Laloy, S. Morales, W. Fourcault, E. Labyt, F. Bertrand, C. Gobbo, F. Alcouffe.

ABSTRACT:
Leti has been developing high-end magnetometers for more than 50 years. After 10 years of intense developments of optical pumping magnetometers for space applications, its application to medical imaging is considered. We sum-up here the improvements achieved in terms of size 5 x 2 x 2 cm^3 and sensitivity 68 fT/√Hz to adapt the technology for medical applications. The preliminary results of the first application to magnetocardiography are illustrated. Magnetoencephalography can now be considered.

SCIENTIFIC COLLABORATIONS: Pr. G. Vanzetto, Department of Cardiology, University Hospital, Grenoble, France

Context and Challenges
After 10 years of developments of optically pumped magnetometers (OPM) for space applications, Leti is adapting and evaluating its technology of sensors, maintenance free and operated at ambient temperature, for medical magnetic imaging. Medical magnetic imaging is used to detect and localize electrical activity of brain or heart for example. The current technology used for these applications require cryogenics and a budget of 3 M€ over 7 years. The OPM technology could lower the prices of medical imaging so as to democratize them but we have to miniaturize the sensor and improve its sensitivity.

Main Results
The size and the sensitivity had to be improved, with reference to the space version of the OPM, to be compatible with magnetic medical imaging. We have studied and tested various ways to keep a good density and lifetime of helium atoms inside a cell small enough to be placed on an array. Once we reached a sensitivity of 210 fT/√Hz for a size of 20 cm^3, we proceed to the first tests on healthy volunteer, in magnetocardiography (MCG), which is the most accessible magnetic medical imaging application.

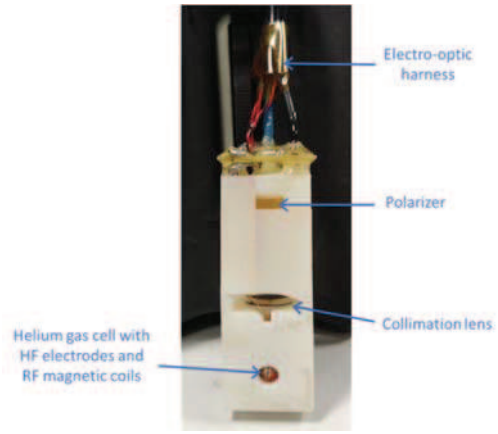

Figure 1:Picture of the OPM, 2 x 2 x 5 cm^3

The MCG recording has been matched to electrocardiograph (ECG) and approved by the professor of cardiology G. Vanzetto.

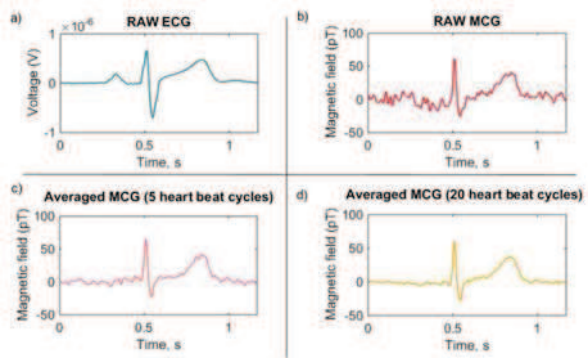

Figure 2: ECG and MCG signals of the healthy 37 years old volunteer. a) Real-time filtered un-averaged ECG signal (one heart beat cycle),b) Real-time filtered un-averaged MCG signal (one heart beat cycle), c) 5 beats averaged MCG signal, d) 20 beats averaged MCG signal

Thanks to the absence of cryogenics or heating technology, the sensors can be directly put onto the skin. Closer to the magnetic sources to be analyzed, this leads to an improvement of at least 5 in the amplitude of the signal versus cryogenics based devices [3].

After these MCG measurements, the sensors sensitivity has been improved to 70 fT/√Hz opening the way to magnetoencephalography (MEG). Leti and Blumorpho received the "best early stage innovation" from the radar prize, H2020 - ICT programs for these results [4].

Perspectives
The sensitivity still has to be improved to serenely address MEG.

Leti will study the possibility to use the OPM technology for MEG and the potential impact of the cost reduction onto the democratization of such medical Imaging devices.

All these works of miniaturization and sensitivity improvements will also be useful for space applications based on nanosatellites.

RELATED PUBLICATIONS:

[1] S. Morales et Al. "Magnetocardiography measurements with 4He vector optically pumped magnetometers at room temperature" Phys Med Biol. 2017 Aug 21;62(18):7267-7279

[2] J.M. Léger et Al. "SWARM absolute scalar and vector magnetometer based on helium 4 optical pumping " Eurosensors XXIII, sept. 2009, Lausanne

[3] H. Koch "SQUID magnetocardiography, status and perspectives" IEEE transactions of applied superconductivity, Vol. 49, March 2001

HIGH FREQUENCY MECHANICAL BEHAVIOR OF NANOMETRIC SUSPENDED MEMBRANES FOR VIBRATING MEMS DEVICES

RESEARCH TOPIC:
MEMS, micro-C-MUTS, carbon, membranes, mechanical properties, resonances, large bandwidth acoustic transducers

AUTHORS:
S. Thibert, M; Delaunay, A Ghis

ABSTRACT:
Resonant behavior of self standing 10nm thick membranes made with amorphous carbon is explored and measured.
Natural and high order resonance modes (until order 3) have been excited and observed in accordance with theory.
Though measurements were taken at room temperature and ambient pressure, displacements as large as 10% of the suspended length have been observed. These membranes exhibit both outstanding flexibility and strength

SCIENTIFIC COLLABORATIONS: None

Context and Challenges

The achievement of new materials now makes it possible to use ultrathin membranes as resonators. Amorphous carbon fabricated with thickness of a few nanometers provides great advantages for MEMS engineering as it combines mechanical strength, chemical inertness and integrability. The question now is : how do such thin membranes behave with frequency, can they store enough energy to resonate in a fluid like air despite the ambient pressure ?

Static and low frequency displacement, under capacitive actuation, of self-standing 10nm thick membranes made with amorphous carbon have been previously reported. Today we report on the observation and measurement of the resonances phenomena, up to 110MHz.

The devices are long trenches 1-2µm large and 50-100µm long., The amplitudes of displacement are measured at ambient pressure and room temperature using an AFM; Frequency spectra are obtained by varying the excitation voltage frequency, thus highlighting the resonances along the scanned range.

Main Results

From these measured spectra, we first consider the fundamental resonance frequency. They range from 20Mhz for 2.3µm large devices, to 110MHz for 0.8µm large devices (fig. 1). Quality factor up to 122 and factor of merit up to 3.10^{10}Hz have been obtained.

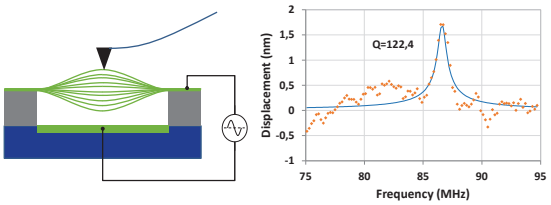

Figure 1: (left) Scheme of the AFM measurement for high frequency vibration; (righ) an example of frequency spectrum.

We analyzed this dependency to depict the mechanical mechanisms involved. They reveal that for the considered set of devices, the mechanical law ruling the vibration behavior is mainly a membrane model, driven by the stress built in the layer, with a notable contribution of a plate model, driven by material properties, namely for the narrowest and thickest devices.

Exploring the frequency spectra above the fundamental, we were able to identify higher modes of resonance, transversal and longitudinal modes in good accordance with theory of vibration. Figure 2 presents the mapping of a third order resonance mode.

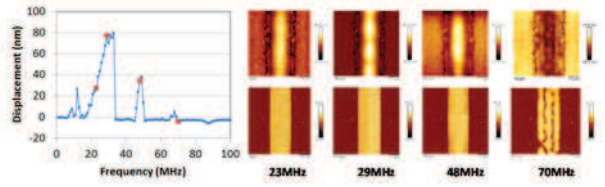

Figure 2: Resonances of a 2,3µm wide device with a A-type membrane (left) spectrum measured for Vdc=10V, Vac=3V. Bullets indicate the frequencies corresponding to the scans shown on the right. (right): scans amplitude (top) and phase (bot) taken when biased with VDC=10V, Vac=4V, at frequencies 23MHz, 29MHz,48MHz, and 70MHz, on a 6µmx6µm area along the trench.

More, Displacements as high as 10% of the suspended length have been observed.

These observations corroborates the flexibility and strength of the material is remarkable.

The realness of significant vibration and resonance in air of ultrathin membranes is now demonstrated.

Perspectives

These membranes exhibit both outstanding flexibility and strength. They appear as good candidates for playing the active part in both high spatial resolution pressure mapping and acoustic engineering.

Two specific advantages of these MEMS are the multiple frequency operability that enlarges the acoustic imaging field, and the inertness of the surface material, for embedding and operating in either fragile (biological) or harsh (SHM) environments.

RELATED PUBLICATIONS:
[1] Thibert, S., Delaunay, M., Ghis, A., 2018. Carbon-metal vibrating nanomembranes for high frequency microresonators. Diamond and Related Materials 81, 138–145. https://doi.org/10.1016/j.diamond.2017.12.005
[2] Thibert, S., Ghis, A., Delaunay, M., 2016. AFM study of 2D resonators based on Diamond-Like-Carbon, in: Nanotechnology (IEEE-NANO), 2016 IEEE 16th International Conference on. IEEE, pp. 479–482. BEST PAPER AWARD.
[3] Ghis, A., Sridi, N., Delaunay, M., Gabriel, J.-C.P., 2015. Implementation and mechanical characterization of 2nm thin diamond like carbon suspended membranes. Diamond and Related Materials 57, 53–57. https://doi.org/10.1016/j.diamond.2015.02.006.

SHAPE RECONSTRUCTION OF MESHED SMOOTH SURFACES EQUIPPED WITH INTERIAL SENSORS

RESEARCH TOPIC:
Shape capture, curve networks, smooth surface, normal vector input, shape monitoring

AUTHORS:
T. Stanko, S. Hahmann (LJK, INRIA), G.-P. Bonneau (LJK, INRIA), L. Jouanet, N. Saguin-Sprynski

ABSTRACT:
We introduce a new method for real-time shape sensing. Using a single inertial measurement unit (IMU), our method enables to scan physical objects and to reconstruct digital 3D models. By moving the IMU along the surface, a network of local orientation data is acquired together with traveled distances and network topology. We then reconstruct a consistent network of curves and fit these curves by a globally smooth surface. To demonstrate the feasibility of our approach, we have constructed a mobile device called the Morphorider, which is a node equipped with 3-axis accelerometer, 3-axis magnetometer and an odometer for distance tracking.

SCIENTIFIC COLLABORATIONS: Université Grenoble Alpes, CNRS (Laboratoire Jean Kuntzmann), INRIA

Context and Challenges

Traditionally, digital models of real-life shapes are acquired with 3D scanners, providing point clouds for surface reconstruction algorithms. However, there are situations when 3D scanners fall short, e.g. in hostile environments, for very large or deforming objects.

In the last decade, alternative approaches to shape acquisition using data from microsensors have been developed. Small size and low cost of these sensors facilitate their integration in numerous manufacturing areas; the sensors are used to obtain information about the "scanned" structure, such as spatial data or deformation behavior. We consider a new setup: a device with a single IMU is moved along a virtual network of curves on the scanned surface, and the data is acquired interactively. Previous works focused on the resulting problem of surface reconstruction from a well-connected mesh curves; we here focus on producing a network of smooth curves on the scanned surface with our device, enabling the surface reconstructing process.

Main Results

Morphorider (figure1) is a novel MEMS based dynamic device, which is used for data acquisition. The key idea is to provide a device which can trace an unconstrained virtual network of curves on the scanned surface. This enables acquisition and reconstruction of a broader family of shapes than existing fixed-topology devices. It is equipped with one node of sensors (3-axis accelerometer and 3-axis magnetometer) providing its orientation in space, and an odometer, giving its displacement. A microcontroller sends data in real time via a serial bus.

Figure 1: Morphorider demosntrator

Any smooth surface can be scanned with this device by an operator, the additional constraint being to number the intersections of the different curves acquired on it. Our method ic composed of four stages:

- we first filter raw data in removing outliers then using quarternions representation in order to use convolution in the Gausssian Kernel,

- we then smooth surface normals in the manifold SO(3) with adequate splines,

- we finally integrate, solving Poisson's equation in order to constrain the mesh to be smooth and coherent.

- we apply surface reconstruction [3].

Example of reconstructed surface is in figure 2.

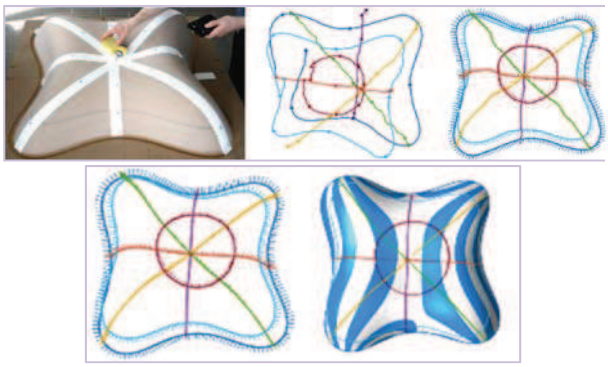

Figure 2: acquired surface and steps of reconstruction

Errors are about 1% for all simulated and real surfaces acquired with our device.

Perspectives

Perspectives concern several fields: hardware first with a new device to develop, allowing more freedom for acquisition; algorithms with incremental mesh definition [additional curves after first scanning], and even crowd sensing applications for instance to monitor a structure from collaborative measurements.

RELATED PUBLICATIONS:
[1] Tibor Stanko, Nathalie Saguin-Sprynski, Laurent Jouanet, Stefanie Hahmann and Georges-Pierre Bonneau, Morphorider: Acquisition and Reconstruction of 3D Curves with Mobile Sensors, IEEE Sensors, pp1170-1172, 10/2017.
[2] Tibor Stanko, Stefanie Hahmann, Georges-Pierre Bonneau and Nathalie Saguin-Sprynski, Shape from sensors: curve networks on surfaces from 3D orientations, Computers & Graphics (Proc. SMI, vol 66, pp74-84, 8/2017
[3] Tibor Stanko, Stefanie Hahmann, Georges-Pierre Bonneau and Nathalie Saguin-Sprynski, Smooth interpolation of curve networks with surface normals, in Proc. Eurographics -short papers, pp. 21-24, May 2016

REAL-TIME MONITORING OF TRAVELLER'S PSYCHOLOGICAL STRESS

RESEARCH TOPIC:
Wearables, stress observer, travel, ambulatory, model

AUTHORS:
G. Vila, C. Godin, O. Sakri, S. Ollander, E. Labyt, A. Vidal, S. Charbonnier (UGA, Gipas-Lab), A. Campagne (UGA, LPNC)

ABSTRACT:
The paper presents the main results of a pilot study, using accelerometer measures and several physiological signals during a travel from Grenoble to Bilbao for traveler's stress monitoring. The traveler identified three events of high stress and one period with low stress. Feature extraction and machine learning were performed to build a personalized model, with the user's stress levels as output. Based on this model, a smartphone application has been developed in order to record and visualize the estimated stress. This demonstrator has been tested and validated during another travel, from Grenoble to Brussels

SCIENTIFIC COLLABORATIONS: UGA Gipas-Lab, UGA, LPNC

Context and Challenges

Within the BonVoyage project, our goal was to develop a smartphone application for real time assessment of traveler stress using wearable sensors. Some previous results [1] were conducted using existing database [2] during driving using laboratory sensors. Stress evaluation was processed offline. Our contribution targets this estimation in real time using wearable sensors and in real life ambulatory condition.

Main Results

Empatica™ E4 wristband (https://www.empatica.com/e4-wristband) was used In order to collect physiological signals (Electro-dermal activity, skin temperature, accelerometer, photo-pletismogram). From raw data, feature were computed and a linear model was used to fit features to participant stress annotations during his journey. A smartphone application has been developed. The application embeds the Empatica E4 data collection, the feature computation the model and the real time logging and drawing of raw data and model output. Our smartphone application used the model to record and estimate the same participant's stress levels based on sensor data during another journey not used for training the model. During this journey the stress annotated by the traveler was used only for comparison with the model output and performances assessment. Those results are presented in table 1, for 3 distinct part of the travel where we can see a good correspondence between annotation and model output. Figure 1 shows two screenshots of algorithm's results on one-hour time durations, on a graphical user interface for two distinct periods of the journey. The first one on the left shows a particularly stressful event (server crash before the travel departure), while the second on the right is not particularly stressful. The model estimation correspond to what was experienced by the traveler.

Mode	No. Ex.	RMSE (raw output)	RMSE (clipped output)	Cr %
Shuttle	68	0.202 ±0.041	0.189 ±0.039	97.1 ±4,0
Train I	95	0.189 ±0.031	0.154 ±0.026	92.6 ±5,3
Train II	83	0.171 ±0.031	0.094 ±0.017	100 ±0
Mean	-	0.187 ±0.035	0.146 ±0.027	96.5 ±3.2

Table 1 : Performances for each transport mode during the test phase : transport mode, number of example, Root Mean Square Error and Classification rate (%).

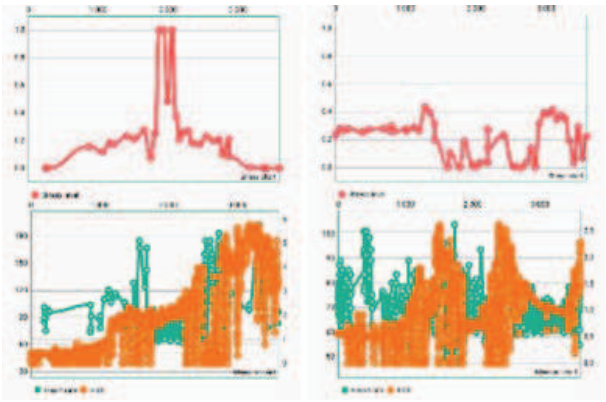

Figure 1:Smartphone Application screenshots: stress estimated (top) and raw signals (bottom) for Heart Rate [bpm] in green, and Skin Conductance [µS] in orange for server crash (left), airport leasure in train (right).

Perspectives

Our purpose was to present preliminary results and to highlight the potential of this kind of tools for the future of transportation. Obviously, there is a lot of improvements to be done. The feature set can be optimized and more complex models could be tested. First of all, a more extensive data collection with several das and several travelers should be conducted to be the basis of a model robust to inter and intra individual variabilities for a wide range of situations.

RELATED PUBLICATIONS:
[1] S. Ollander, C. Godin, S. Charbonnier, and A. Campagne, "Feature and Sensor Selection for Detection of Driver Stress," presented at the 3rd International Conference on Physiological Computing Systems, 2017, pp. 115–122.,
[2] J. A. Healey, "Wearable and automotive systems for affect recognition from physiology," Thesis, Massachusetts Institute of Technology, 2000.

FEASIBILITY OF WI-FI SITE SURVEYING USING CROWDSOURCED DATA

RESEARCH TOPIC:
Crowdsourcing, data fusion, indoor localization

AUTHORS:
Sylvain Leirens, Christophe Villien, Bruno Flament (Invensense)

ABSTRACT:
Efficient use of indoor positioning algorithms requires mapped information. Manual survey of Wi-Fi fingerprints is a costly process and needs to be updated on a regular basis. The feasibility of an automatic survey based on crowdsourced data is studied. Local noisy Wi-Fi measurements (RSSI levels) and estimated pedestrian trajectories are collected through user's devices (smartphones), in order to estimate the spatial distribution of RSSI levels.

SCIENTIFIC COLLABORATIONS:

Context and Challenges

Indoor positioning relies mainly on fusing pedestrian trajectories and map information, e.g. Wi-Fi fingerprinting, and blue prints with walls and accessibility information (entrances, doors, etc.). Pedestrian trajectories suffer from a significant amount of drift over time, especially when based on measurements from low-cost inertial sensors. Map information is used to correct for trajectory drifting during the fusion process.

Crowdsourced data consist typically of outdoor GNSS, pedestrian trajectories and RSSI measurements (Wi-Fi, Bluetooth). Coming from a large amount of users these data can be efficiently processed to automatically survey RSSI maps.

Main Results

One on the main difficulty is to deal with positioning uncertainty. Pedestrian trajectories are approximated using piecewise linear modeling. The pedestrian behavior is simulated as a random walk, exhibiting a growing uncertainty along the trajectory.

Admissible RSSI measurements are selected according to the accuracy in position estimates along trajectories. The availability of a previous map significantly improves the accuracy. The RSSI map is updated using Bayesian inference with probability law from previous map as prior probability density.

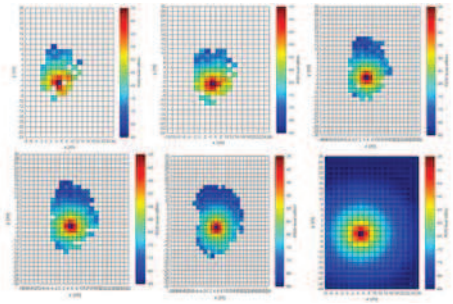

Figure 1 Fusion for growing number of users (ground truth at bottom-right).

Figure 1: illustrates the updating process of a RSSI map (xy-plane) when the number of users grows. The 2-dimensional space is partitioned into non-overlapping rectangular regions, so that any point in the space can be identified to lie in only one of these regions. For each Wi-Fi access point, a probability law is associated to every region in the map, which gives the probability of RSSI level when receiving Wi-Fi signals in a particular region of the space. RSSI levels are simulated using log-distance path loss models.

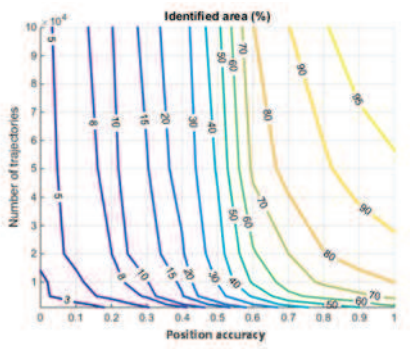

Figure 2 Crowdsourcing performance.

In practice, position estimates in pedestrian trajectories are refined using fingerprinting-based algorithms or particle filtering [2]. The map surveying capabilities are assessed in Figure 2 by looking at the identified area for a particular site. The position accuracy is rated from 1 (no uncertainty) down to 0 (unreliable). As expected, the reachable area increases with growing quantity of data. But the position uncertainty limits the performance which remains bounded even for large amounts of data.

Perspectives

Mapping using a crowdsensing approach can deal with other modalities as well, such as magnetic field for indoor localization. Another promising trend is source localization, e.g. high emitting vehicles in urban areas.

RELATED PUBLICATIONS:
[1] S. Leirens, C. Villien, and B. Flament, "Feasibility of WiFi Site-Surveying Using Crowdsourced Data", in Latent Variable Analysis and Signal Separation, 2017, pp. 479-488.
[2] F. Evennou and F. Marx, "Advanced Integration of WiFi and Inertial Navigation Systems", EURASIP Journal on Applied Signal Processing, 2006, pp. 1-11.

05 SECURITY

- On-Chip Techniques
- Deployment of IoT devices & systems
- Embedded cryptography
- Side-channel attacks
- Security Testing Tools
- Blockchains

METHODS AND TOOLS FOR TEE SECURITY TESTING: AN EXAMPLAR INDUSTRIAL PARTNERSHIP IN THE AWARD WINNING MOBITRUST PROJECT

RESEARCH TOPIC:
Model base test automation - vulnerability detection scanner

AUTHORS:
JC Fonbonne, J Guillot

ABSTRACT:
More than 1 billion TEE-enabled processors are shipped per quarter but only one industrial products is today certified. TEE security technology actually addresses the not-so-constrained resource environment having a rich operating system to cover multiple security requirements and use cases for industrial, consumer or medical devices. Understandably, TEE happens with particular needs in terms of testing. The award winning [4] MOBITRUST project promotes an efficient solution to perform vulnerability detection with the appropriate toolchain running an exhaustive test suite for any standardized TEE implementation.

SCIENTIFIC COLLABORATIONS: TRUSTONIC, Global Platform

Context and Challenges

The MOBITRUST project, started in 2015, aimed at developing a complete framework to enhance security and privacy of mobile platforms. The consortium included major industrial actors, a silicon vendor, security providers, SMEs and RTOs at European level. The CEA Leti contributed to the work package focusing on security and privacy evaluation methodology for product certification. The efforts focused on vulnerability analysis and penetration testing automation adapted to a product's environment and constraints.

Main Results

The founding building blocks on which relies a major part of the security and privacy functionalities of the platform are the secure boot and the Trusted Execution Environment (TEE) standardized by Global Platform (GP) association. By definition, TEE is an isolated execution environment that runs alongside the rich OS and hosts trusted services offered to that rich environment. GP also published a TEE protection profile as well as a security test suite to be exercised when assessing the security robustness. We experimented a testing tool that implements the security test suite on any TEE platform in a fully automated way and extended the test suite with test cases close to the platform hardware security functions.

The TEE security test suite is divided into three principal components:

- the test suite and scenario that defines all the test cases and lists the operations performed within. The test suite included, at the end of 2017, one thousands of abuse and misuse tests covering the cryptographic services, the isolated objects handling, the secure storage, the trusted functions commands and the protected memory manager,
- the test operation server agent sitting on the rich OS of the remote device that relays the invoked operation from the tester station and determines the test's verdict,
- the test trusted application (TTAs) that attempts to execute illegal or unexpected operations directly on the TEE core via the standardized function calls.

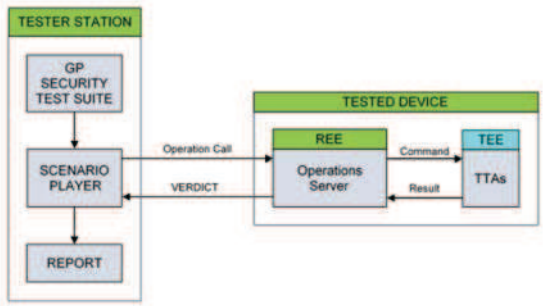

Figure 1: Block diagram of the TEE security test toolchain

Those results were achieved based on a close collaboration with the industrial partner TRUSTONIC who develops and provides the TEE core packaged in a software design kit. We did the development of the interface building blocks and the integration within a complete toolchain:

- the test suite player with integrated report generation,
- the remote operations agent
- the extension TTAs analyzing vulnerabilities of critical hardware features such as platform configuration, memory management unit or direct memory access controller.

The toolchain was successfully experimented on the TEE core designed by TRUSTONIC and the results exposed to GP devices security task force.

Perspectives

This new complete TEE security test framework could be multiple uses. The test case database is a starting point and could be enriched with new vulnerabilities or adapted for new combined hardware/firmware functionalities. Concurrently, the tool chain could ease the adoption of the TEE technology by new industrial fields like for medical or industrial systems. In any case, this know-how is a minimum requirement for an ITSEF to be selected as a Global Platform accredited laboratory for TEE security evaluation.

RELATED PUBLICATIONS:
[1] J. Bennett, "Devices with trustonic tee, 08 2015.
[2] Bernabeu, Gil, et al. "MBT for global platform compliance testing: Experience report and lessons learned." Software Reliability Engineering Workshops (ISSREW), 2014 IEEE International Symposium on. IEEE, 2014.
[3] Global Platform TEE Security Test Suite v1.0.2 - Official - 11 2016
[4] MOBITRUST was awarded the "Catrene Innovation Award 2017".

COMPARISON OF FINGERPRINT AUTHENTICATION ALGORITHMS FOR SMALL IMAGING SENSORS

RESEARCH TOPIC:
Fingerprint Biometric, Computer Vision and Pattern Recognition

AUTHORS:
M. Bourjot, R. Perrier, J-F. Mainguet

ABSTRACT:
The demand for biometric systems has been increasing with the growth of the smartphone market. Amongst them, fingerprint sensors are the most widespread because they seem to provide a good balance between reliability, cost and ease of use. According to smartphone manufacturers, the security level is guaranteed to be high. However, the small size of those sensors of few millimeters squared prevents the use of minutiae algorithms for authentication. So far, only few studies has focused on this problem, though many pattern recognition algorithms already exist together with commercial solutions which are supposedly robust. This work tries to provide insights on how to tackle this problem by analyzing the performance of three algorithms dedicated to pattern recognition.

Context and Challenges

Biometric systems get more and more integrated in our societies for authentication purposes. Amongst them, fingerprint has been used since many years because it achieves a good tradeoff between reliability, ease of use and technological cost. It is now conceivable to integrate fingerprint sensors in everyday life objects like door locks, cars or smartphones.

Yet to target such applications, especially for smartphones, the sensor which captures the fingerprint has to be cropped down to few millimeters squares; this greatly reduces the information available for authentication algorithms. Original minutiaes based algorithms were designed for sensors of few centimeters squares, and though they are an international standard for the fingerprint authentication task, they cannot be used anymore. Currently, there is no agreement on how to perform authentication with smaller fingerprint sensors.

In this work, we adapted and compared three methods from the pattern recognition literature to fit our needs: Zero mean Normalized Cross Correlation (ZNCC), Scale Invariance Feature Transform (SIFT) and Harris SSD (Sum of Square Differences). We showed that the latter approach, which is a simplified version of an algorithm suggested by microsoft for image mosaicing, is particularly suited for the authentication task with small imaging fingerprint sensors [1].

Main Results

The main output of this work is in the design of the Harris SSD method to extract as much information as possible on the fingerprint image. It is composed of two steps:

- Features extraction using the Harris corner detector; we observed experimentally that it has the ability to detect minutiaes, as well as sweat pores and width variations on fingerprint ridges.
- Descriptors computation around each extracted feature; we cropped several small patches of 15x15 pixels oriented with respect to the ridge to which it belongs. This gives us a collection of patches which characterizes the fingerprint.

Figure 1 summarizes those two steps. The authentication is then performed by comparing collections between fingerprint images using the SSD criterion. Figure 2 shows authentication results on a real database from internet.

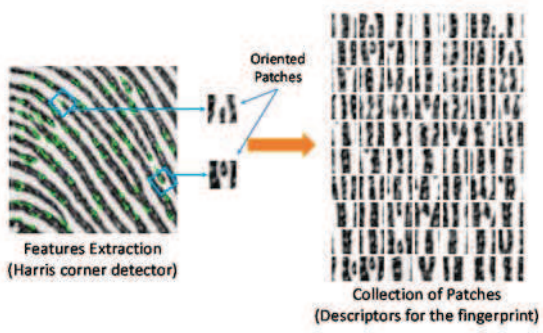

Figure1: Harris SSD method principle. The green arrows on the left figure show the extracted features with the Harris detector. The right figure is the collection of oriented patches which best characterizes the fingerprint and will be successively used for authentication.

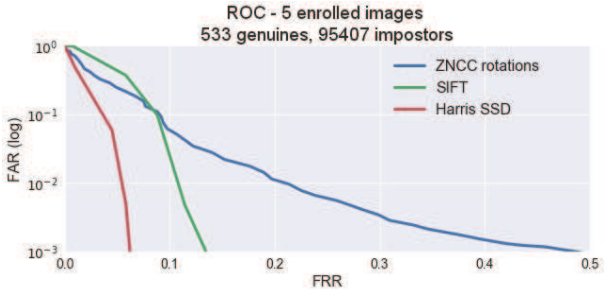

Figure 2: Authentication results for the three algorithms on an internet database; the lower the curve, the better.

Perspectives

Future work could focus on decreasing the matching process execution time to meet the requirements of the application.

RELATED PUBLICATIONS:
[1] M. Bourjot, R. Perrier, J. F. Mainguet, "Etude d'algorithmes d'authentification pour petits capteurs d'empreinte digitale", *CORESA 2017*, Nov 2017, Caen, France
English version: https://arxiv.org/pdf/1712.06882

METHODS AND TOOLS FOR TEE SECURITY TESTING: AN EXAMPLAR INDUSTRIAL PARTNERSHIP IN THE AWARD WINNING MOBITRUST PROJECT

RESEARCH TOPIC:
Model base test automation - vulnerability detection scanner

AUTHORS:
JC Fonbonne, J Guillot

ABSTRACT:
More than 1 billion TEE-enabled processors are shipped per quarter but only one industrial products is today certified. TEE security technology actually addresses the not-so-constrained resource environment having a rich operating system to cover multiple security requirements and use cases for industrial, consumer or medical devices. Understandably, TEE happens with particular needs in terms of testing. The award winning [4] MOBITRUST project promotes an efficient solution to perform vulnerability detection with the appropriate toolchain running an exhaustive test suite for any standardized TEE implementation.

SCIENTIFIC COLLABORATIONS: TRUSTONIC, Global Platform

Context and Challenges

The MOBITRUST project, started in 2015, aimed at developing a complete framework to enhance security and privacy of mobile platforms. The consortium included major industrial actors, a silicon vendor, security providers, SMEs and RTOs at European level. The CEA Leti contributed to the work package focusing on security and privacy evaluation methodology for product certification. The efforts focused on vulnerability analysis and penetration testing automation adapted to a product's environment and constraints.

Main Results

The founding building blocks on which relies a major part of the security and privacy functionalities of the platform are the secure boot and the Trusted Execution Environment (TEE) standardized by Global Platform (GP) association. By definition, TEE is an isolated execution environment that runs alongside the rich OS and hosts trusted services offered to that rich environment. GP also published a TEE protection profile as well as a security test suite to be exercised when assessing the security robustness. We experimented a testing tool that implements the security test suite on any TEE platform in a fully automated way and extended the test suite with test cases close to the platform hardware security functions.

The TEE security test suite is divided into three principal components:

- the test suite and scenario that defines all the test cases and lists the operations performed within. The test suite included, at the end of 2017, one thousands of abuse and misuse tests covering the cryptographic services, the isolated objects handling, the secure storage, the trusted functions commands and the protected memory manager,
- the test operation server agent sitting on the rich OS of the remote device that relays the invoked operation from the tester station and determines the test's verdict,
- the test trusted application (TTAs) that attempts to execute illegal or unexpected operations directly on the TEE core via the standardized function calls.

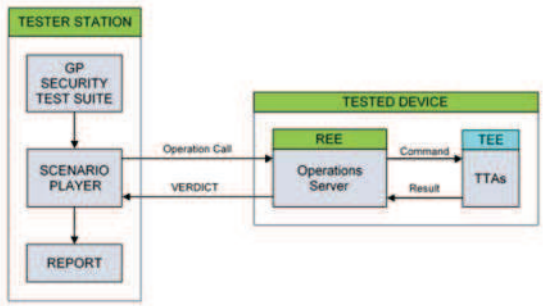

Figure 1: Block diagram of the TEE security test toolchain

Those results were achieved based on a close collaboration with the industrial partner TRUSTONIC who develops and provides the TEE core packaged in a software design kit. We did the development of the interface building blocks and the integration within a complete toolchain:

- the test suite player with integrated report generation,
- the remote operations agent
- the extension TTAs analyzing vulnerabilities of critical hardware features such as platform configuration, memory management unit or direct memory access controller.

The toolchain was successfully experimented on the TEE core designed by TRUSTONIC and the results exposed to GP devices security task force.

Perspectives

This new complete TEE security test framework could be multiple uses. The test case database is a starting point and could be enriched with new vulnerabilities or adapted for new combined hardware/firmware functionalities. Concurrently, the tool chain could ease the adoption of the TEE technology by new industrial fields like for medical or industrial systems. In any case, this know-how is a minimum requirement for an ITSEF to be selected as a Global Platform accredited laboratory for TEE security evaluation.

RELATED PUBLICATIONS:
[1] J. Bennett, "Devices with trustonic tee, 08 2015.
[2] Bernabeu, Gil, et al. "MBT for global platform compliance testing: Experience report and lessons learned." Software Reliability Engineering Workshops (ISSREW), 2014 IEEE International Symposium on. IEEE, 2014.
[3] Global Platform TEE Security Test Suite v1.0.2 - Official - 11 2016
[4] MOBITRUST was awarded the "Catrene Innovation Award 2017".

CONVOLUTIONAL NEURAL NETWORKS WITH DATA AUGMENTATION: A COMPREHENSIVE PROFILING SIDE-CHANNEL ATTACK STRATEGY, ROBUST TO TRACES MISALIGNMENT

RESEARCH TOPIC:
Side-Channel Attacks, Convolutional Neural Networks, Data Augmentation, Machine Learning, Trace Misalignment

AUTHORS:
Eleonora Cagli, Cécile Dumas, Emmanuel Prouff (Safran Identity and Security, ANSSI)

ABSTRACT:
In the context of the security evaluation of cryptographic implementations, profiling attacks (or Template attacks) may suffer from the traces misalignment. We propose a strategy based on the Convolutional Neural Networks (CNN) that avoids to perform critical preprocessing phases. To significantly increase the performances of the CNN, we moreover propose to use the data augmentation (DA) technique. The excellent results achieved in the presented experiments prove that this is a very efficient alternative to the state-of-the-art profiling attacks.

SCIENTIFIC COLLABORATIONS: None

Context and Challenges

In smartcard security, the profiling attack scenario allows to evaluate the worst-case, admitting the attacker is able to characterize the device leakages. First, a leakage model is estimated, then the profiled leakage model is exploited to extract key-dependent information. The classical Template Attack (TA) is today the most popular approach: it approximates the information leakage by a Gaussian distribution. To prevent Side-Channel Attacks (SCA), chip manufacturers commonly implement countermeasures that create misalignment in the measurements sets. Until now two approaches have been developed to deal with this problem. The first one simply consists in increasing the number of side-channel acquisitions. The second one, which is usually preferred, consists in applying alignment techniques in order to limit the desynchronization effects. Nevertheless, realignment techniques might compromise the attack, instead of improving performances.

Main Results

Basically, the particularity of CNN method is that it shares parameters across space, leading the network to learn shift-invariant features. This property makes the profiling attacks with CNNs efficient and easy to perform, since they do not require any critical preprocessing phase.

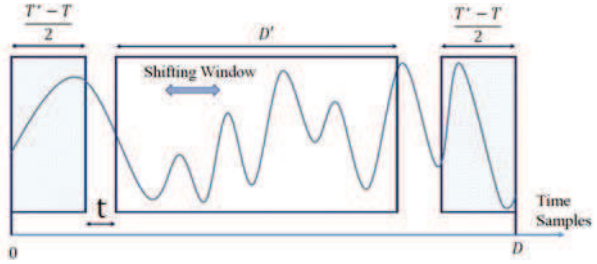

Figure 1.:Shifting technique for Data Augmentation.

Extracting information from misaligned traces requires anyway more acquisitions. In machine learning domain the DA technique [2, 3] is a widely accepted alternative: it consists in artificially enlarging the profiling set, generating new traces through well-chosen deformations of the acquired ones. We propose two kinds of deformations, which we denote by "Shifting" and "Add-Remove". Shifting deformation (SH_T) simulates a random delay effect of maximal amplitude T, by randomly selecting a shifting window of the acquired trace, as shown in Figure 1. The Add-Remove (AR_R) deformation simulates a level R clock jitter effect.

Paradoxically, instead of trying to realign the traces, we propose to further misalign them (a much easier task!), and we show that such a practice provides a great benefit to the CNN attack strategy.

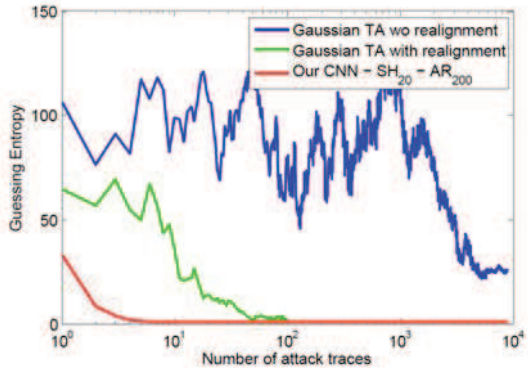

Figure 2: Comparison between a Gaussian template attack, with and without realignment, and our CNN strategy.

In Figure 2 the performances of our CNN approach are compared to the best ones we could obtain with the TA approach, among many preprocessing possibilities. CNN outperforms the TA either in case the preprocessing performed includes or not a realignment technique. This confirms that the CNNs are able to integrate an effective realignment in the training phase, confirming their robustness to the jitter effect.

Perspectives

Other DA techniques, emulating other kinds of random phenomena due to noise or to other countermeasures, should be developed and exploited to raise the performances of a wider range of attacks. Moreover DA could provide further benefits to attacks that target unbalanced data.

RELATED PUBLICATIONS:
[1] E. Cagli, C. Dumas, E. Prouff "Convolutional Neural Networks with Data Augmentation Against Jitter-Based Countermeasures." In Cryptographic Hardware and Embedded Systems (CHES), pp 45-68, 2017.
[2] P.Y. Simard, D. Steinkraus, and J.C. Platt, et al. "Best practices for convolutional neural networks applied to visual document analysis." In ICDAR, vol.3, pp 958-962. 2003.
[3] S.C. Wong, A. Gatt, V. Stamatescu, and M.D. McDonnell. "Understanding data augmentation for classification: when to warp?" In Digital Image Computing: Techniques and Applications (DICTA), pp 1-6. IEEE, 2016..

NANOFOCUSED X-RAY BEAMS TO REPROGRAM SECURE CIRCUITS

RESEARCH TOPIC:
Attack performed for the evaluation of the security of the information technologies devices

AUTHORS:
S. Anceau, P. Bleuet, J. Clediere, L. Maingault, J-L. Rainard, R. Toucoulou (ESRF)

ABSTRACT:
Experimentations on ESRF focalized beam line in Grenoble allowed to demonstrate that a focalized XRays perturbation changes the state of a single NMOS transistor and of a single memory cell of SRAM-EEPROM and Flash memories block in a semi-permanent manner. This proof of concept has been realized on a new CMOS technology device (45 nm). The 50 nm focalization allows to modify one single NMOS transistor. The most aggressive technologies (<20nm) can be addressed with this technique even with a 50nm focalization diameter.

SCIENTIFIC COLLABORATIONS: European Synchrotron Research Facility (ESRF, Grenoble, France)

Context and Challenges

Scientists in the domain of security evaluation investigate possible physical attacks hackers can use to threaten the security of integrated circuits. New perturbation attacks have to be developed for the evolution of the state of the art of integrated circuits' security. Thanks to these experimentations the future development of specific protections has to be obtained and the level of digital security standards has to be maintained.

Main Results

Despite the deployment of protections in smart card like devices, induced faulted results have been classically obtained with laser beam light for the last 20 years. In order to further investigate the new possibilities of electromagnetic perturbations with different wavelengths, the effects of ionizing radiations like the X-Ray beam represented a good challenging opportunity. The proximity of the ESRF in Grenoble and the possibility to focus the X-Ray beam down to few tens of nanometers allows us to change the information of single Flash, EEPROM and RAM memory cells [1]. This modification is semi-permanent because it is reversible with a simple annealing.

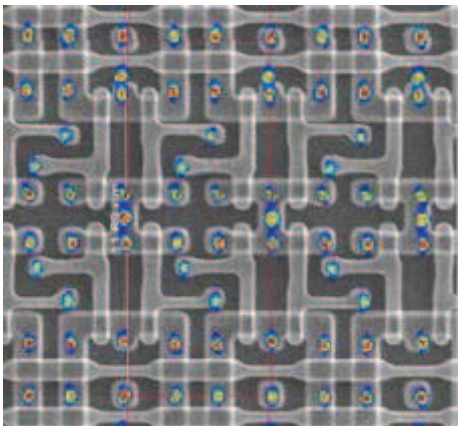

Figure 1: Precise localization of the transistors to attack with the help of fluorescence scan and deprocessing layout picture of the circuit.

Changing bit by bit the Non Volatile Memory's (NVM) content or modifying the state of the program stored in the memory constitute critical threats to a circuit's security. As it is possible to address single transistors in advanced technology nodes (45nm nodes) security countermeasures and detection mechanisms could be deactivated, faults in cryptographic algorithms can be obtained and memory block might be reprogrammed.

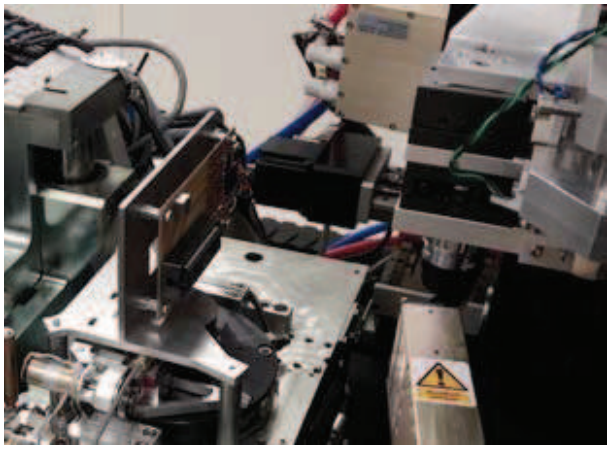

Figure 2: Experimental set up of the device sample in front of the XRays nanofocused beam in the ID16B beam line of ESRF in Grenoble.

This type of perturbation of individual memory cell and transistors with semi-permanent faulted results can be obtained without removing the package of the devices and without leaving any traces.

Perspectives

The next step is now to try to reproduce the same effect with more 'classical' lab equipment, i.e. but without the use of a synchrotron. With this step, this type of perturbation attack, like for laser attacks 20 years ago, might become a part of security certification process.

RELATED PUBLICATIONS:
[1] S. Anceau, P. Bleuet, J. Clédière, L. Maingault, J.L. Rainard, R. Tucoulou : “Nanofocused X-Ray Beam To Reprogram Secure Circuits”, CHESS 2017, Taiwan.

CELTIC: A FAULT ATTACK SIMULATOR FOR EVALUATING SECURE EMBEDDED SOFTWARE

RESEARCH TOPIC:
Cybersecurity, Fault attacks, Code analysis

AUTHORS:
L. Dureuil, **L.Maingault**, J. Clédière, P. De Choudens, M.-L. Potet (UGA)

ABSTRACT:
Embedded software, even without any bugs, can be attacked by injecting faults during code execution with a laser beam for instance. These attacks are very powerful and surprisingly no tools are dedicated to assess a code's security against fault attacks or to find potential vulnerabilities. We introduce CELTIC, a fault attack simulator on microcontrollers whose goal is to evaluate code security automatically based on a complete embedded software analysis. CELTIC has already been used for measuring efficiencies of a whole set of countermeasures against fault injections and constitutes a very good link between real and simulated attacks.

SCIENTIFIC COLLABORATIONS: VERIMAG, UGA

Context and Challenges

Injecting faults during code execution - for instance with a laser beam - is a very powerful attack on embedded software. However it is difficult to find out vulnerability in a code or assess a real protection against all kinds of attacks. To tackle this issue a simulator of fault injection on embedded software called CELTIC was developed. It automatically finds weak parts within the code that should be attacked (attacker's point of view) or protected (developer's point of view.

Main Results

CELTIC simulates an embedded microprocessor at the system level on a regular x86 computer. Its purpose is to evaluate code security against fault attacks. This tool is designed to be realistic with real-world attacks, not dependent on a specific processor architecture, and propose an automatic and comprehensive code review against faults attacks.

CELTIC uses binary code execution (to be realistic) with the help of a specific description file of the chip architecture. The user chooses a fault model that is integrated during the code execution and launches a fault injection simulation campaign. Every output is stored and can be analyzed for vulnerabilities' search.

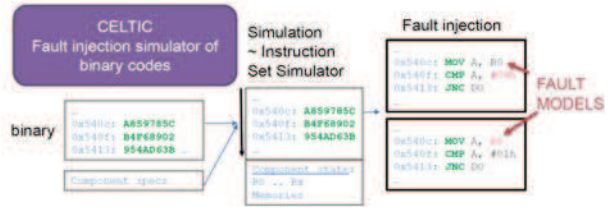

Figure 1: Workflow of a fault injection simulation campaign in CELTIC

The fault model describes which part of the chip is attacked (memory, registers, code), how it is modified (bit flip, bit set…), and when during the execution the fault occurs. It is very versatile and a method was developed to find out an effective model for each type of chip [1].

Results have already been obtained with CELTIC. First CELTIC has been efficiently used to evaluate the robustness of a full set of codes with different types of countermeasures against fault attacks [2].

It is also used for real life chip security evaluation. It helps an evaluator to automatically find vulnerabilities and/or get a better understanding of the fault that is injected into smartcards. In these evaluations, simulations are very close to actual laser attacks, which gives a confidence in CELTIC for vulnerability search (Figure 2).

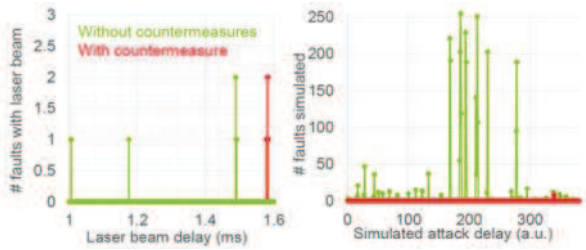

Figure 2: Comparison between laser attack and simulation.

Perspectives

The main objective of further development is to use the tools that exist for static code analysis (code flow graph, abstract interpretation) in order to accelerate long code simulations without giving up on accuracy of low-level simulations. Incorporating these tools at the binary level would open many ways to aim more precisely at potential vulnerabilities and quickly find multi-fault vulnerabilities

RELATED PUBLICATIONS:
1) Louis Dureuil, Marie-Laure Potet, Philippe de Choudens, Cécile Dumas, and Jessy Clédière. From Code Review to Fault Injection Attacks: Filling the Gap. In 14th Smart Card Research and Advanced Application Conference (CARDIS'15). Springer, 2015
[2] Louis Dureuil, Guillaume Petiot, Marie-Laure Potet, Thanh-Ha Le,Aude Crohen, and Philippe de Choudens. FISSC: a Fault Injection and Simulation Secure Collection. n Computer Safety, Reliability and Security – 35th International Conference SAFECOMP 2016,Lectures Notes in Computer Science. Springer, 2016

ACCESS RIGHTS MANAGEMENT FOR THE BLOCKCHAIN OF THINGS

RESEARCH TOPIC:
ISecurity, Privacy, Trust, Value, IoT, Blockchain, Data Protection

AUTHORS:
Christine Hennebert, Laurent-Frédéric Ducreux, Matthieu Volat

ABSTRACT:
One of the attributes of IoT systems consists in providing secure user access, via the internet, to mico-data collected from constrained and remote objects and stored in the cloud. While the IoT is "data-centric", its security is ensured by an authorization server located in the cloud. The blockchain or distributed ledger technology allows decentralization of the security and privacy services in distributed "user-centric" systems. The demonstrator developed by the CEA-LETI aims at proving the concept of such decentralized security and privacy services ensured by design through a Smart Contract that orchestrates the distributed application. In a first realization, the platform consists of a private instance of Ethereum, which in addition to intrinsically providing the notions of traceability, integrity and immutability of the information recorded in its shared register, allows to also take into account the distributed identity management, the data protection, the (micro)-monetization of the data exchanges, as well as the distributed trust in a low consumption system.

SCIENTIFIC COLLABORATIONS: None

Context and Challenges

The blockchain technology is emerging as a high-potential technology, which, combined with smart contracts, allows the automation of tasks and asset transfers in a decentralized system. Our research on the blockchain technology focuses on two aspects: the efficient management of privacy and enhancing the security of implementation of blockchains. The use case that we consider is the one based on smart energy management involving the collection and management of consumption data. We developed a Proof of Concept (PoC) of a blockchain platform where users have access to micro-data (sent over a wireless network) produced by IoT constrained sensors according to a B2C scheme. The blockchain ensures security, privacy and trust by design in order to orchestrate distributed applications using personal data and compliant with the European Global Data Protection Regulation (GDPR).

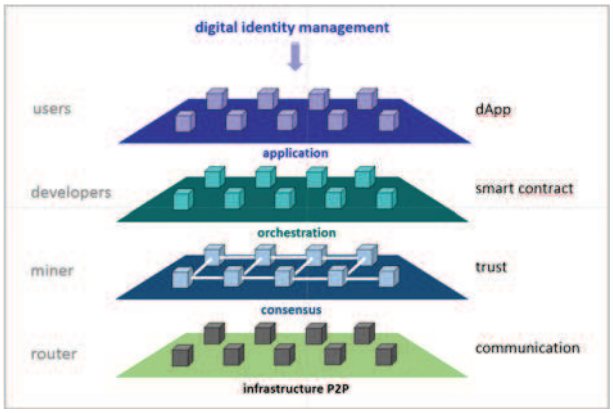

Figure 1: The layered architecture

Main Results

Our PoC, aiming at the use case a micro-grid with co-ownership, allows us to perform an in-depth study of how to securely exploit data measurements made in the context of energy consumption, considering things like the GDPR and for having secure implementations. Several policies have been implemented, including delegation of access rights to personal data then requiring the consent of the owner of those micro-data.

This first demonstrator is composed of the different sub-systems:

- the IoT chain that produces and collects the data,
- embedded GPU on NVIDIA Tegra for the mining,
- a set of smart contracts that orchestrate securely the access to the protected data,
- applications to manage and trace the access rights of the data in the blockchain,
- applications to treat and visualize the aggregated data.

The specificity of this platform lies in the control subsystem based on the blockchain and a set of smart contracts that manage the access in read and write to the databases.

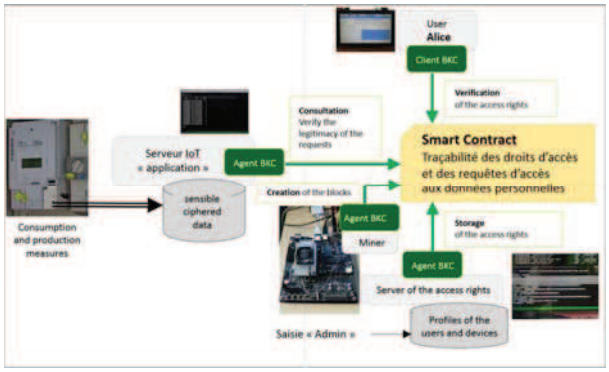

Figure 2: Operational view of the blockchain platform

Perspectives

Now that we have shown how to manage the privacy issue, we shall focus on how to harden the implementation of the blockchain using secure hardware and how to enhance the management of the blockchain using Artificial Intelligence.

RELATED PUBLICATIONS:
[1] Jorge Bernal Bernabe, Ignacio Elicegui, Etienne Gandrille, Nenad Gligoric, Alex Gluhak, Christine Hennebert, Jose L. Hernandez-Ramos, Carmen López, Andrea Manchinu, Klaus Möessner, Michele Nati, Colin O'Reilly, Niklas Palaghias, Antonio Pintus, Luis Sánchez, Alberto Serra, Rob van Kranenburg, "SocIoTal — The development and architecture of a social IoT framework", Global IoT summit 2017, Genève, 6-9 June 2017, DOI: 10.1109/GIOTS.2017.8016286
[2] Christine Hennebert, « Méthode d'échange de clés par contrat intelligent déployé sur une chaine de blocs », demande de brevet français, n°EN 17 63394, décembre 2017
[3] Christine Hennebert, « Méthode d'échange de clés authentifié par chaîne de blocs », demande de brevet français n°EN 17 63393, décembre 2017

USING HOMOMORPHIC ENCRYPTION FOR DATA CONFIDENTIALITY IN EMBEDDED PROCESSORS

RESEARCH TOPIC:
Processor Design, Hardware Security, Homomorphic Encryption.

AUTHORS:
T. Hiscock, O. Savry and L. Goubin (UVSQ).

ABSTRACT:
Gentry's breakthrough of Fully Homomorphic Encryption (FHE) in 2009 completely revolutionized the field of secure computation. The most studied use of FHE is to offload computations to a cloud provider while preserving the confidentiality of the input data. This work investigates a somewhat different application of homomorphic encryption. It shows how one can use homomorphic encryption to build a fully encrypted data path within a microprocessor. This approach prevents any sensitive data to leak through memory extraction techniques or side-channel leakages.

SCIENTIFIC COLLABORATIONS: Université de Versailles Saint Quentin en Yvelines.

Context and Challenges

Keeping sensitive data confidential is a challenging problem for embedded processors. The designer has to take into account a large number of attacks, ranging from software vulnerabilities to physical attacks. Memory encryption is a well-known and sound countermeasure against memory extraction. But at some point, data still needs to be decrypted in order to be processed, which may introduce side-channel leakages. In 2009, Gentry constructed the first fully homomorphic encryption (FHE) scheme, capable of evaluating arbitrary functions over encrypted data. FHE provides a convenient framework for securing computations. Modern FHE schemes (BGV, FV, GSW) are orders of magnitude faster than Gentry's first scheme, but they remain unaffordable for embedded implementations.

Main Results

The cost of FHE is mainly due to the so-called bootstrapping procedure. It requires the scheme to support the evaluation of its own decryption circuit homomorphically. This requirement generally imposes very large parameters and thus increases processing time. Our first contribution is a lightweight hardware-only bootstrapping. The idea introduced in [1,2] is to perform a decryption followed by a new encryption, which produces the same effect as a bootstrapping. The whole process is made secure by adding homomorphically a random mask. Provided that the noise generation and the decryption are made free from leakage, the overall flow is secure.

Figure 1: The proposed lightweight bootstrapping procedure

This bootstrapping-like procedure is lightweight in the sense that it does not require homomorphic computations. Thus, one can select parameters of the encryption scheme to support only a very small number of homomorphic operations. As a consequence, it drastically reduces the cost of homomorphic encryption.

This lightweight bootstrapping is then used to build a homomorphic arithmetic and logical unit (HE ALU) and inserted into a MIPS processor pipeline [1], as shown below. Slight modifications to the processor decoding logic is also required to provide additional instructions that operate over encrypted data.

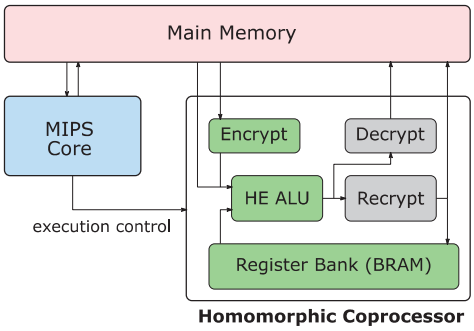

Figure 2: Global architecture of our homomorphic processor

The Brakerski Gentry and Vaikuntanathan scheme (BGV) is used to implement homomorphic operations. The complete design is fully synthetized at 100 MHz on an Altera Arria V GX FPGA. The homomorphic accelerator occupies 40% of the total area. The basic homomorphic operations (boolean exclusive-OR and AND) on encrypted bytes require roughly 300 µs. With this architecture one should be able to evaluate homomorphically an AES algorithm in 4 min and with 171 MB of storage. This compares well with the current BGV AES evaluation, which requires 62 min and 3.4 GB of storage on a desktop computer.

Perspectives

This work showed that under some hypothesis, a fairly efficient processor working over encrypted data can be built. The architectural design space of homomorphic encryption algorithms is huge. Several improvements remain to be done to reduce the latency of computations. Future work will also include the study of methods to secure homomorphic decryption, so that the cost of the lightweight bootstrapping can be fully evaluated. Another upcoming work is to identify interesting applications that would benefit from this processor architecture.

RELATED PUBLICATIONS:
[1] T. Hiscock, O. Savry, and L. Goubin, Chiffrement homomorphe pour la protection de calculs sur processeur embarqué, RESSI 2017, https://ressi2017.sciencesconf.org/133764/document
[2] T. Hiscock and O. Savry. Method for confidential execution of a program operating on data encrypted by a homomorphic encryption. U.S. Patent Application No 15/440,157.

BREAKTHROUGHS IN PRACTICAL SIDE CHANNEL ATTACKS AGAINST PAIRING BASED CRYPTOGRAPHY

RESEARCH TOPIC:
Pairing Based Cryptography (PBC), side channel attacks, ElectroMagnetic (EM) measurements

AUTHORS:
Damien Jauvart, Nadia El M-rabet (EMSE), Louis Goubin (UVSQ) and Jacques J.A. Fourniert

ABSTRACT:
Pairing Based Cryptography (PBC) is an emerging cryptographic used in innovative protocols like Identity Based Encryption. However, implementations of PBC can be vulnerable to side channel attacks (SCA). We demonstrate how such attacks against PBC can be improved by drastically reducing the number of curves. We even show that by having a "horizontal approach", only one curve is needed for the full recovery of the secret key. Finally we show that SCA are also feasible even in presence of countermeasures like point randomization, prompting the need to look for new and more efficient countermeasures.

SCIENTIFIC COLLABORATIONS: Université de Versailles St Quentin en Yvelines and Mines St Etienne.

Context and Challenges

Pairing Based Cryptography (PBC) is an emerging cryptographic tool that allows innovative security protocols like Boneh & Franklin's Identity Based Encryption (IBE) or Joux's multi-party Diffie-Hellman key exchanges. When used in a scheme like IBE, a pairing $e(P,Q)$ is calculated between two points of an elliptic curve where one of the two points (P or Q) is the secret decryption key. The objectives of this research work are to evaluate to what extent physical attacks (side channel attacks or fault injections) can be used to find this secret key and to devise efficient countermeasures against such attacks.

In the past, the CEA Leti has been pioneering practical research breakthroughs in the feasibility and exploitation of fault attacks to break PBC despite the complexity of the underlying mathematics [1]. Now the focus is on another family of physical attacks, namely side channel attacks. Unlike for fault attacks, theoretical schemes for breaking PBC using side channel attacks have been proposed in the literature. The objectives from there were to evaluate the practical feasibility of such attacks and to study the efficiency of the countermeasures proposed so far in the literature.

Our practical experiments targeted a software implementation of a Tate pairing, implemented in Assembly & C languages, and running on a COTS device embedding an ARM Cortex M3 processor. Note that the device did not integrate any hardware countermeasure against physical attacks. The side channel used is based on measurements of the ElectroMagnetic (EM) waves emitted by the device during the execution of the Pairing algorithm.

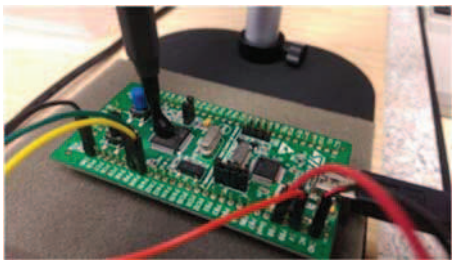

Figure 1: EM probe over targeted device.

Main Results

We first investigated about the practical feasibility and efficiency of side channel attacks against the Tate pairing. By doing a fine-grained characterization of the EM leakages of the 32-bit platform running the device, we managed to achieve a 10 times gain [2] in terms of number of side channel traces needed to carry out an entire attack, based on Correlation Power Analysis (CPA), compared to the best results reported in the literature so far.

We then investigated about the feasibility of a new side channel approach, called a "horizontal attack", against a PBC implementation. The principal of this attack is to exploit the fact that the secret key (actually the coordinates of the secret point) is being used at different instants during one same execution: hence by doing the right sampling of the signal, statistical analyses can be carried on the different chunks to retrieve the value of the secret used. With this approach, only one side channel curve is needed to perform the attack, as compared to the "classical" CPA (above) where we needed 200 traces [3].

One of the countermeasures proposed in the literature against the above attacks is based on *point randomization*: at each execution of a pairing calculation, the public point is combined with a new random value in such a way that the attacker has no straight forward way of determining the real values used during the pairing calculation, and hence circumventing her ability of doing statistical analyses leading to the recovery of the secret key. However, by finely analyzing the way this countermeasure is implemented, we devised an attack, based on a chosen message approach, where, despite the presence of the randomization, we can look for collisions in the EM traces measured and derive from these collisions the secret value used. We implemented this countermeasure in our Tate pairing implementation and validated the feasibility of this new attack in practice [4].

Perspectives

Now that we have demonstrated that a side channel attack against PBC is possible even on one single side channel trace and that point randomization is not an efficient countermeasure against side channel attacks, new countermeasures have to be sought and validated.

RELATED PUBLICATIONS:

[1] "On the security of pairing implementations", Ronan Lashermes, PhD thesis, Université de Versailles Saint Quentin en Yvelines, September 2014.
[2] "Improving Side-Channel Attacks against Pairing-Based Cryptography" by Damien Jauvart, Jacques Fournier, Nadia El Mrabet and Louis Goubin, in the proceedings of the 11th International Conference on Risks and Security of Internet and Systems (CRISIS 2016), Springer-Verlag, Roscoff, September 2016.
[3] "Protecting Pairing algorithms against physical attacks", Damien Jauvart, PhD thesis, Université de Versailles Saint Quentin en Yvelines, September 2017.
[4] "First Practical Side-Channel Attack to Defeat Point Randomization in Secure Implementations of Pairing-Based Cryptography" by Damien Jauvart, Jacques J.A. Fournier and Louis Goubin, in the proceedings of SECRYPT 2017, Springer-Verlag, Madrid, July 2017.

IOT COMPONENTS LIFECYCLE BASED SECURITY ANALYSIS

RESEARCH TOPIC:
IoT device lifecycle, risk analysis, threat scenario, medical devices

AUTHORS:
J. Marconot, F. Pebay-Peyroula, D. Hely (Univ. Grenoble Alpes, LCIS)

ABSTRACT:
Security flaws in connected objects may cause dramatic system failures. We investigate how the management of the lifecycle of connected devices can impact the security of a system's assets. First we define a generic model for a device lifecycle, which shows the complexity of the problem with the different actors and their respective roles. Then we dig further into the problem with a risk analysis of a case study: a connected Insulin pump. Based on the EBIOS methodology, we detail the threat scenarios and identify the criticality of lifecycle management on a connected object's security. One of the solutions to address such requirements is based on innovative PUF technologies, which can be integrated in the early stages of lifecycle and could secure the access to the device's assets.

SCIENTIFIC COLLABORATIONS: Univ. Grenoble Alpes, LCIS

Context and Challenges

The IoT ecosystem is growing exponentially, involving different actors and novel technologies: it leads to more complex architectures, with longer production process and new technical operations. During these interactions we need to ensure the security of critical functionalities, sensitive data and proprietary assets. At the same time we have to respect the constraints of IoT devices: low cost fabrication, energy consumption, flexibility etc. Such devices hence have complex lifecycles which, when not properly managed, may have severe security impacts on those devices' assets.

Main Results

We first realize a state of art of the characteristics of a device lifecycle, which is complex and unstandardized [1]. We present the roles' distribution, the required technical intervention and what kind of interactions expose the assets. For instance, the device producer may contact these third parties: suppliers of system-on-chips, suppliers of software modules, subcontractors for assembly and tests, technical operators for deployment and maintenance.

There is a need to ensure a trust during these interactions. The lack of access control and security may be exploited through internal or external threats. The diverse of nature of these vulnerabilities is complex. Moreover attacks can be performed at precise phases and impact the device later in its lifecycle.

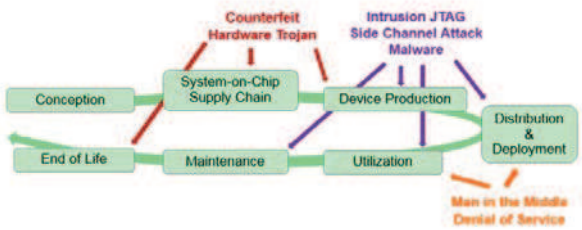

Figure1: Threats across the LifeCycle

These lifecycle characteristics vary as well as security requirements. It depends on the constraints induced by regulatory laws, the intended use of the device and the needs of companies.

Based on this theoretical work, we demonstrate the pertinence of introducing the holistic view of lifecycle in order to correctly evaluate the security requirements. We consider the case of a medical device, namely the embedded system for insulin regulation.

With the risk analysis methodology EBIOS we detail precisely the targeted critical assets, which properties (confidentiality, integrity) have to be ensured and what the consequences can be in case of failures.

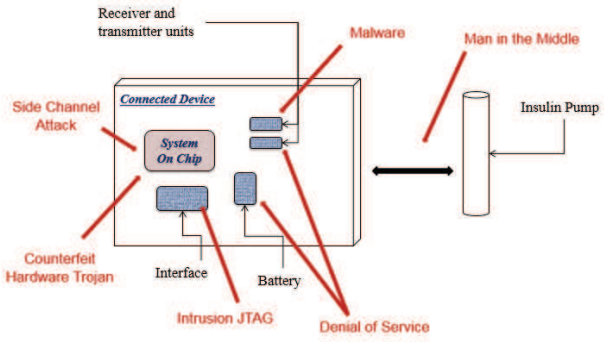

Figure 2: Threats against medical devices

The results show that the identified vulnerabilities concern different components of the device and may compromise the entire system.

This analysis points to the need of integrating by design features to manage securely the device's lifecycle.

Perspectives

The next phase of this research work is now to investigate about technologies that might mitigate the identified threats during a device's lifecycle. One such technology identified so far is the PUF (Physically Unclonable Function). A PUF provides authentication properties and can be used to build security protocol. Integrated in the first stage of a device's lifecycle. Such a technology would allow legitimate users to have access to critical assets and services while keeping intruders and hackers at bay.

RELATED PUBLICATIONS:
[1] J. Marconot, F. Pebay-Peyroula, D. Hely, "IoT Components Lifecycle based Security Analysis," 2017 Euromicro Conference on Digital System Design (DSD)

PRACTICAL PHYSICAL ATTACKS AGAINST LIGHT WEIGHT CRYPTOGRAPHY

RESEARCH TOPIC:
Light Weight Cryptography (LWC), side channel attacks, fault attacks

AUTHORS:
Alexandre Adomnicai (TO), Benjamin Lac, Anne Canteaut (Inria), Renaud Sirdey, Laurent Masson (TO) & Jacques J.A. Fournier

ABSTRACT:
The advent of the IoT brings along new security requirements and constraints linked to the ubiquity and pervasiveness of connected objects, namely regarding on the light-weightness of the cryptographic algorithms used to ensure data confidentiality (among other things). We look at the security of those light weight ciphers from a physical attacks' perspective. We focus on two major families of such ciphers, namely LS-Designs and ARX structures for which we identified and tested new physical attack paths, prompting the need to investigate about new countermeasures against physical attacks for such light weight ciphers.

SCIENTIFIC COLLABORATIONS: CEA DPACA, CEA List, Inria & Trusted Objects (TO)

Context and Challenges

The advent of the Internet of Things (IoT) brings along new security requirements and constraints linked to the ubiquity and pervasiveness of the objects on one side and to the performance and connectivity of the servers on the other side. On one side, low power and high performance cryptographic algorithms (using so-called Light Weight Cryptography - LWC) have to be implemented to resist physical attacks (side channel and fault attacks). On the other side, the servers need to be empowered to perform calculations and analytics on secure data, in a homomorphic manner with which the LWC deployed on the objects' side have to be compatible [1].

Up to now, the light weight cryptographic algorithms proposed and standardized have been studied to resist cryptanalytic attacks. We have been exploring the physical attack space regarding LWC: with respect to the existing literature, we have not only been proposing new attack schemes but also been demonstrating the practical feasibility of those attacks. Our work has been focusing on fault attacks against one family of light weight ciphers called LS-Designs and on side channel attacks against another family called ARX structures.

Main Results

LS-Designs are a family of SPN-based block ciphers whose linear layer is based on the so-called interleaved construction. They are often used in connected objects with high performance and low-resource constraints. We first proposed a general method for Differential Fault Analysis (DFA) on any block cipher based on LS-designs and other families of SPN with similar structures. This generalization has allowed us to successfully perform such an attack against a hardware implementation of SCREAM, using the TLS-Design Scream with a fixed tweak [2]. Our target of evaluation was an implementation of SCREAM on a Xilinx FPGA. The faults were injected using electromagnetic pulses. The synchronization between the SCREAM execution and the injection means was based on a preliminary simple electromagnetic analysis of the running algorithm.

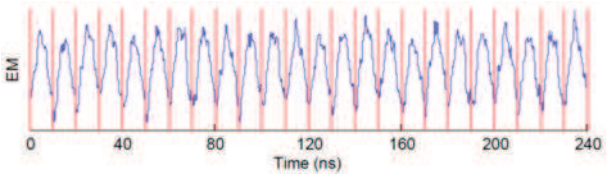

Figure 2: EM trace with the 24 rounds of SCREAM

ChaCha is an exemplar light weight stream cipher having an ARX structure, with interesting light weight and high performance properties for IoT devices. It has been recently included into the cryptography portfolio of the TLS standard. We studied the resistance of two software implementations of ChaCha against electromagnetic side channel analyses: both implementations were software ones for a 32-bit platform, one implemented in C language and one implemented in Assembly language with a maximum use of the CPU's registers. The first one could be attacked rather straight-forwardly using "classical" Correlation Power Analysis (CPA) targeting specific data-dependent memory accesses. In the second implementation, where all calculations were done within the processor's register files, the straight-forward CPA did not work: instead we had to come up with a new attack, which we called the *Bricklayer attack*, targeting the entire quarter round of the ChaCha [3].

Perspectives

Our latest results illustrate to what extent side channel and fault attacks are real threats to the security of light weight ciphers. Efficient countermeasures have to be sought in order to protect such ciphers against both kinds of physical attacks. We are currently investigating about a "general" approach for having secure software implementations of such ciphers while preserving as much as possible their small footprint and their performances.

RELATED PUBLICATIONS:
[1] Anne Canteaut, Sergiu Carpov, Caroline Fontaine, Jacques Fournier, Benjamin Lac, Maria Naya-Plasencia, Renaud Sirdey and Assia Tria, “End-to-end data security for IoT: from a cloud of encryptions to encryption in the cloud”, presented at the C&ESAR 2017 Conference, Rennes, France, November 2017.
[2] Benjamin Lac, Anne Canteaut, Jacques Fournier and Renaud Sirdey , “DFA on LS-Designs with a Practical Implementation on SCREAM”, in the proceedings of COSADE 2017, Springer-Verlag, Paris, April 2017.
[3] Alexandre Adomnicai, Laurent Masson & Jacques Fournier, “Bricklayer Attack: A Side-Channel Analysis on the ChaCha Quarter Round”, in the proceedings of the INDOCRYPT 2017, Springer-Verlag, Chennai, November 2017.

GHANDILEO: DEVELOPING AN INDOOR GUIDANCE SYSTEM FOR THE VISUALLY IMPAIRED USING A USER-CENTRIC DESIGN

RESEARCH TOPIC:
Indoor navigation, user centric design approach, inertial motor unit

AUTHORS:
C. Villemazet, F. Coulon-Lauture, I. Chartier, N. Vuillerme (UGA)

ABSTRACT:
The major aim of the GHANDILEO project is to assist people with visual or motor disabilities to move into business areas and therefore improve their employability. The proposed technology is a real time accurate indoor guidance solution essentially based on signals from the infrastructure. The major roadblocks are the precision of the guidance system and the ergonomics of the solution. The guidance solution has been deployed in a CEA building to validate its performance and robustness before experimentation in one building of the regional prefecture to assess usage with visually impaired employees.

SCIENTIFIC COLLABORATIONS: Université Grenoble Alpes

Context and Challenges

Indoor navigation is still a challenging task for people with disabilities, in particular for those who are blind or have a visual impairment. Although indoor navigation and wayfinding tools already exist, they have some major drawbacks that hamper their use in real-life. The GHANDILEO project has specifically been conceived to address this crucial issue.

The aim of the GHANDILEO project was to design, implement, assess and deploy an innovative indoor guidance system specifically designed to enhance the safety and independence of people with any kind of disabilities navigating within their workplace.

Main Results

We used a user centered design approach (i) to understand and define the needs and expectations of people who are blind or visually impaired in terms of mobility in their workplace, then (ii) to draw up technical specifications of their desired indoor navigation solution including functional and usability requirements among others, and finally (iii) to assess the effectiveness and suitability of this solution in real situations (Fig. 1).

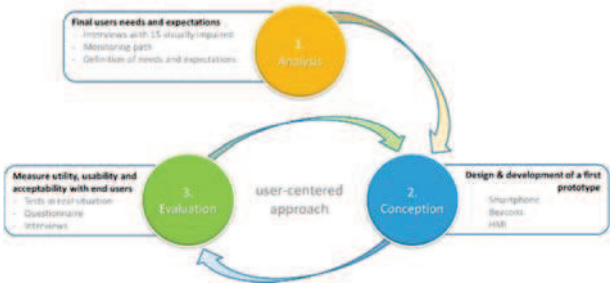

Figure 1: User Centered Design of GHANDILEO project

We first conducted interviews of 15 persons who are blind or visually impaired. Although these interviews covered numerous issues, the main conclusions concerned the usefulness of such a solution if a vocal communication interface system is implemented on their smartphone. Then, based on these inputs, we have developed a smartphone-based indoor guidance system that uses internal inertial sensors and Bluetooth beacons deployed in the building for accurate navigation and a vocal guidance module (Fig. 2). Pedestrian Dead-Reckoning (PDR) tracks the movements based on embedded sensors into the smartphone. The major drawback of IMU sensors is signals drift. To synchronize virtual model and physical reality, information from beacons are then merged. A particle filter based on point mass representations of probability densities is lastly used to improve accuracy. This newly-developed solution deployed in the IRT Nanoelec testbed has been assessed by 5 blind or visually impaired persons who consider it usable and useful. Finally, a validation study has been performed within the buildings of the Prefecture of the Auvergne-Rhône-Alpes region (France) with visually impaired employees.

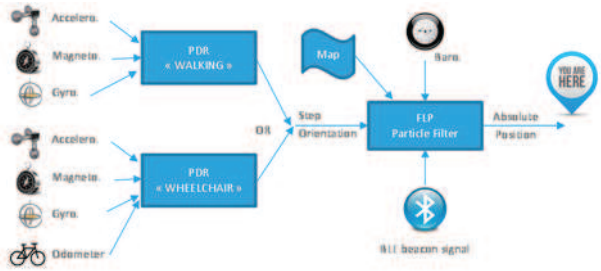

Figure 2: Principle of the geolocation system

We have implemented a user-centered design to support the entire development of an indoor guidance system for blind and visually impaired people. This smartphone based system has been demonstrated to be useful and easy to use, and hence, seems of added value to the intended users.

Perspectives

However, although promising, these results have to be confirmed using a larger sample for longer periods. Algorithms have to be improved especially related to the number of beacons that have to be deployed to ensure a precise indoor guidance for disabled people..

RELATED PUBLICATIONS:
[1] Villemazet, C., Passot, M., Chartier, I., Coulon-Lauture, F., Vuillerme, N. "GHANDILEO: developing an indoor guidance system for visually impaired people using a user-centered design", 16th International Mobility Conference (IMC16), Dublin (Ireland), 25-26 June 2017.

06 PHD DEGREES AWARDED IN 2017

- **Matthias GEISLER**
- **Tibor STANKO**
- **Thomas HISCOCK**
- **Jessye DOS SANTOS**
- **Jimmy MACERAUDI**
- **Amine EL KACIMI**
- **Yoann ROTH**
- **Andrès-Felipe OSPINA TRIVIÑO**

MATTHIAS GEISLER

MECHANICAL ENERGY HARVESTING SYSTEMS FOR SMART CLOTHES

Université Grenoble Alpes (France)

The functionalization of ordinary objects with embedded electronic systems is a fast-growing trend, commonly referred to as the Internet of Things. The growth of this domain has triggered an interest for energy harvesting solutions to reduce the need to recharge batteries, or even to replace them.

This thesis has explored different energy harvesters structures to efficiently convert the user's mechanical energy into electricity to supply smart wearables. Based on power requirement considerations for a typical "smart shirt", three concepts have been investigated: (i) an inertial electromagnetic generator, the size of an AA-battery, designed to convert footsteps impacts. A thoroughly modelled and optimized device has been able to generate power densities over 800µW/cm^3 while attached on the arm during a run;

(ii) a "looped" inertial structure adapted to exploit the swing-type motions of the user's limbs. This system is able to produce milliwatts-level powers from the motion of a small magnetic ball inside the device;

(iii) a generator relying on electrostatic induction and exploiting variable capacitance structures to turn clothes deformations into electricity.

The comparison of those three energy harvesters provides an interesting basis for the future developments of energy harvesters converting one's mechanical energy.

TIBOR STANKO

SHAPE RECONSTRUCTION OF MESHED SMOOTH SURFACES EQUIPPED WITH INERTIAL SENSORS

Université Grenoble Alpes (France)

We introduce a new kind of monitoring device, allowing the shape acquisition of a structure via a single mobile node of inertial sensors and an odometer. Here, we present a complete framework for 3D shape reconstruction. The challenges are threefold: sensor measurements are noisy and inconsistent; the acquired curve network has to be reconstructed from orientations; the smooth surface needs to be inferred from a collection of curves with normals. To compute the shape, we formulate the reconstruction as a set of optimization problems. Using discrete representations, these problems are resolved efficiently. We present two main contributions. First, we introduce a novel method for creating well-connected networks with cell-complex topology using only orientation and distance measurements and a set of user-defined constraints. By working directly with orientations, our method robustly resolves problems arising from data inconsistency and sensor noise. Second, we address the problem of surfacing a closed 3D curve network with given surface normals. The patch-finding problem can be solved unambiguously and an initial piecewise smooth triangle mesh is computed. We then compute the final mesh by combining the standard Laplacian-based variational methods with the curvature information. The normal input increases shape fidelity, global smooth and visual pleasing shapes. The proposed framework was tested on real-world data acquired using our device and the mean error remains around 1%.

THOMAS HISCOCK

DESIGN AND IMPLEMENTATION OF A MICROPROCESSOR WORKING WITH ENCRYPTED INSTRUCTIONS AND DATA

Universités Versailles Saint Quentin

Embedded processors are today ubiquitous, dozen of them compose and orchestrate every technology surrounding us, from tablets to smartphones and a large amount of invisible ones. At the core of these systems, processors collect data, process it and interact with the outside world. As such, they are expected to meet very strict safety and security requirements. From a security perspective, the task is even more difficult, since the user has a physical access to the device, allowing a wide range of specifically tailored attacks. Confidentiality, both in terms of software code and data is one of the fundamental properties expected for such systems. The first contribution of this work is a software encryption method based on the control flow graph of the program. It allows the use of stream ciphers to provide lightweight and efficient encryption, suitable for constrained processors. The second contribution is a data encryption mechanism based on homomorphic encryption. With this scheme, sensible data remain encrypted not only in memory, but also during computations. Then, the integration and evaluation of these solutions on Field Programmable Gate Array (FPGA) with some example programs will be discussed.

JESSYE DOS SANTOS

PRIVACY IN CONSTRAINED WIRELESS SENSOR NETWORKS

Université Grenoble Alpes (France)

In the context of this thesis, privacy is extended to the objects identifier. Nowadays, the wireless communication standards provide security mechanisms whatever the communication protocols used including the low power ones designed to run on constrained environment. However, the frame header that comprises necessary information for routing and for the proper functioning of the network is always sent in clear text. Collecting and gathering these metadata by eavesdropping is dangerous for the environments and applications based on these networks. The work carried out in this thesis aims to explore how simple passive attacks on meshed networks based on IEEE 802.15.4 used to collect and exploit metadata allow to infer critical information about the network, the environment where the network is deployed and the behavior of users. Two kinds of solutions to hide the node addresses are studied. The first one provides anonymity for the devices. In the second kind of solutions, pseudonyms are used by nodes enabling the capability to audit the traffic within the network. To evaluate the characteristics and the performances of the solutions, a simulator has been used to reproduce the behavior of a meshed wireless sensor network embedding Contiki OS. Thus we introduce a solution, Ephemeral, that allows hiding device addresses included in the sent frames by using pseudonyms without overhead on the control frames. Ephemeral provides a tunneling solution

JIMMY MACERAUDI

RADIOLOCATION AND SIGNAL PROCESSING ALORITHMS ADAPTED TO AN INTEGRATED IMPULSE RADIO - ULTRA WIDEBAND RECEIVER ARCHITECTURE

Université Rennes 1 (France)

The impulse radio - ultra wideband (IR-UWB) radiolocation technology theoretically enables to estimate the time of flight of transmitted pulses at the nanosecond scale and hence, the relative distance between a transmitter and a receiver within a few tens of centimeters. However, despite these intrinsic properties, radio link obstructions (carrying body, obstacles…) degrade positioning performance in practice.

In the frame of this PhD research, one imposed constraint was to rely on a low –complexity integrated IR-UWB receiver, capable of finely resolving the entire multipath profile. An in-depth study of the estimated channel was conducted first. Semi-deterministic models (i.e., according to geometry) were proposed to account for the relative temporal evolution of multipath components, as well as for their mutual interference.

Based on these studies, adapted multipath detection, association and tracking algorithms were subsequently combined (e.g., parallel multi-hypothesis Kalman filters). The latter capture the space-time correlation of multipath components under mobility, while mitigating their collision effects in dense channels. For each non-line-of-sight link independently (i.e., with respect to a given anchor), the arrival time of the missing direct path is thus corrected out of tracked secondary paths, before feeding a conventional mobile tracking filter. These developments were validated by means of both simulations and indoor experiments.

AMINE EL KACIMI

FLEXIBLE PIEZOELECTRIC SENSORS BASED ON GaN MICROWIRES IN CAPACTIVIE STRUCTURES

Université Grenoble Alpes (France)

GaN wire-based flexible piezoelectric sensors were developed into vertical and horizontal architectures. This study ranges from the device design using finite element (FE) modeling, to the device fabrication including wire growth by MOVPE (metal organic vapor phase epitaxy) and a patented assembly process of the flexible membranes, and to the electrical charaterizations of the sensors in traction and compression. FE models explore the working principles of both types of architectures, in order to understand in depth the potential generation mechanicams occurring at the wire level. For the first time, these models take into account the screening effects induced by doping through a strong coupling of the piezoelectric and semiconductor physics. This method was also used to establish the main design rules which provide guidance for the fabrication at the device level. Indeed, the effects of (i) the wire geometrical parameters, (ii) the materials, and (ii) the overall device structure on the piezoelectric performances of the sensor were studied from a theoretical point of view and translated in terms of optimal process parameters to be targeted and tuned accordingly. Electrical characterizations were carried out in order to corroborate these design rules experimentally. An appropriate automated mechanical bench was used and a proper readout circuit developed. 2 inch flexible piezoelectric sensors were reproducibly obtained which generated several volt peak output

YOANN ROTH

THE PHYSICAL LAYER FOR LOW POWER WIDE AREA NETWORKS: A STUDY OF COMBINED MODULATION AND CODING ASSOCIATED WITH AN ITERATIVE RECEIVER

Université Grenoble Alpes (France)

More than 10% of the Internet-of-Things (IoT) connections are expected to be realized through Low Power Wide Area (LPWA) networks, representing several billions of connected devices. Several industrial solutions have been developed and a standardization process is ongoing. The low levels of sensitivity and low data rate required for the long range communication are achieved by the means of two strategies: a narrow-band strategy and a low spectral efficiency strategy. Considering the limits of the information theory, additional gains in the communication's energy efficiency can be achieved. Nonetheless, a trade-off between spectral efficiency and energy efficiency should always be made. Reliable transmission with high energy efficiency will necessarily result in poor spectral efficiency, and in comparison, a system with a higher spectral efficiency has to consume more energy to transmit the same amount of bits with the same arbitrary level of error.

This work considers the low spectral efficiency strategy. The combination of orthogonal modulations and a powerful channel code is studied. The scheme, so-called Turbo-FSK, associates the low spectral efficiency of Frequency Shift Keying (FSK) with the energy efficiency gain of a turbo receiver. Low levels of spectral efficiency can be achieved while optimizing the use of the available resource. We demonstrates the potential of the proposed solution to achieve low levels of sensitivity and to outperform existing schemes.

Andrés Felipe OSPINA TRIVIÑO

TACTILE SENSING SYSTEM FOR ROBOTICS DEXTEROUS MANIPULATION

Université Pierre et Marie Curie (France)

During these 3 years, Andres Ospina worked on an application aimed at enhancing the MEMS-type 3D force sensor developed within LETI. His work has focused on the realization of a tactile sensor adapted to the dextrous manipulation of objects as well as the implementation of a real time algorithm of slip detection based on the measurements coming from the system.

Before carrying out the system, a first step of conditioning the MEMS sensor has been performed. A characterization of the coated sensor shows that the linearity and bandwidth characteristics of the sensor are almost unchanged while increasing the resistance of the sensor to the major forces (from 1.5N to 10N of maximum normal force)

Once the sensor is ready for the application, he realized two tactile systems to measure the position of the center of the forces applied, the 3 coordinates of the applied force and the normal moment applied on the surface.

In the third and final part of the work, a viscoelastic model was developed to link object slippage to force / cut measurements performed by the touch system

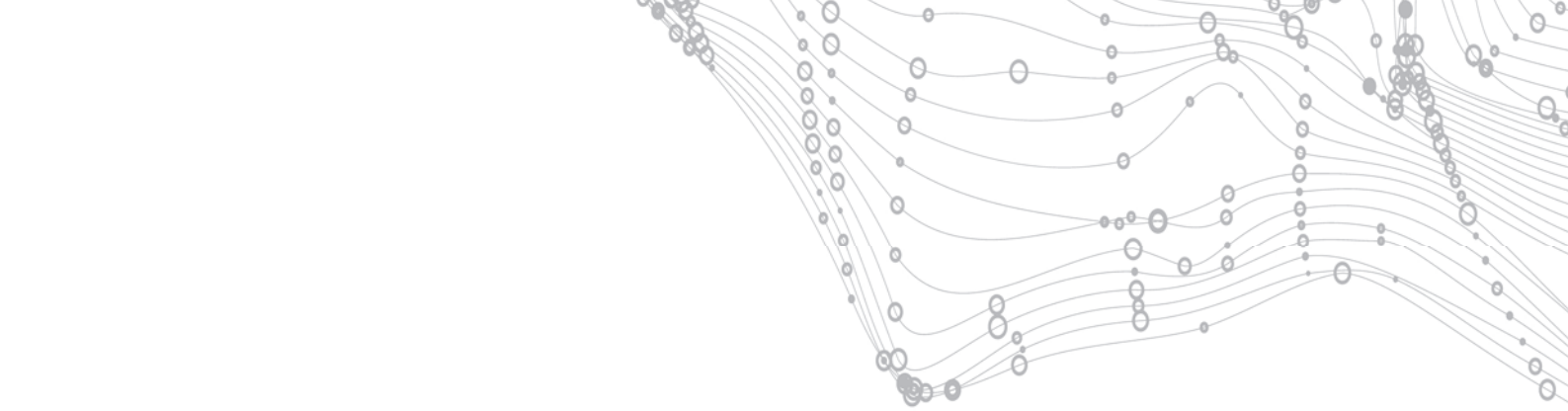

2017

Annual research report

SYSTEMS

2017

Annual research report

SYSTEMS

Contacts

Sébastien DAUVÉ
Head of Systems Division
sebastien.dauve@cea.fr

Jean-Louis AMANS
Deputy Head of Systems Division
jean-louis.amans@cea.fr

Emilio CALVANESE-STRINATI
Scientific Manager
emilio.calvanese-strinati@cea.fr

Jean-Michel LÉGER
Program Manager
jean-michel.leger@cea.fr

Dimitri KTENAS
Head of Telecom Department
dimitri.ktenas@cea.fr

Thierry BOUDET
Head of Energy Electronics & Sensor Systems Department
thierry.boudet@cea.fr

Bruno CHARRAT
Head of Electronics and components Department
bruno.charrat@cea.fr

leti cea tech | TECHNOLOGY RESEARCH INSTITUTE

Commissariat à l'énergie atomique et aux énergies alternatives
Minatec Campus | 17 rue des Martyrs | 38054 Grenoble Cedex 9 | France
www.leti.fr/en

INSTITUT CARNOT Leti